

Florida Institute of Technology

Scholarship Repository @ Florida Tech

Theses and Dissertations

5-2024

Development of Chiral Lewis Base Catalysts for Chlorosilane-Mediated Asymmetric C-C Bond Formations

Changgong Xu

Florida Institute of Technology, cxu2013@my.fit.edu

Follow this and additional works at: <https://repository.fit.edu/etd>

 Part of the [Organic Chemistry Commons](#)

Recommended Citation

Xu, Changgong, "Development of Chiral Lewis Base Catalysts for Chlorosilane-Mediated Asymmetric C-C Bond Formations" (2024). *Theses and Dissertations*. 1450.
<https://repository.fit.edu/etd/1450>

This Dissertation is brought to you for free and open access by Scholarship Repository @ Florida Tech. It has been accepted for inclusion in Theses and Dissertations by an authorized administrator of Scholarship Repository @ Florida Tech. For more information, please contact kheifner@fit.edu.

Development of Chiral Lewis Base Catalysts for Chlorosilane-Mediated
Asymmetric C-C Bond Formations

by

Changgong Xu

A dissertation submitted to the College of Engineering and Science of
Florida Institute of Technology
in partial fulfillment of the requirements
for the degree of

Doctor of Philosophy
in
Chemistry

Melbourne, Florida
May, 2024

We the undersigned committee hereby approve the attached dissertation,
“Development of Chiral Lewis Base Catalysts for Chlorosilane-Mediated
Asymmetric C-C Bond Formations”
by
Changgong Xu

Norito Takenaka, Ph.D.
Associate Professor
Chemistry and Chemical Engineering
Major Advisor

Yi Liao, Ph.D.
Professor
Chemistry and Chemical Engineering

Nasri Nesnas, Ph.D.
Professor
Chemistry and Chemical Engineering

James R. Brenner, Ph.D.
Associate Professor
Chemistry and Chemical Engineering

Jessica Smeltz, Ph.D.
Associate Professor and Interim Department Head
Chemistry and Chemical Engineering

Abstract

Title: Development of Chiral Lewis Base Catalysts for Chlorosilane-Mediated Asymmetric C-C Bond Formations

Author: Changgong Xu

Advisor: Norito Takenaka, Ph.D.

The chiral hydrazine is a crucial structural motif that serves as pivotal structural elements in numerous natural products and biologically significant molecules. We are particularly interested in the catalytic asymmetric reduction of hydrazones, as well as the catalytic asymmetric propargylation and allenylation of hydrazones, because they provide direct pathways to these enantio-enriched chiral building blocks. In this work, we will explore the potential of two different categories of chiral Lewis base catalysts in the said transformations.

Developed by another student in our group, axial-chiral 3,3'-triazolyl biisoquinoline *N,N'*-dioxides derived catalysts are tested and demonstrated its capability in activating various hydrazone substrates in asymmetric hydrosilylation reactions. Another catalyst evaluated is a helicene-based 2,2'-bipyridine *N*-monoxide. It has shown great potential in asymmetrically catalyzing the propargylation of acylhydrazones with allenyltrichlorosilane, as well as in the

allenylation of acylhydrazones with propargyltrichlorosilane. It showcased its capability of inducing enantioselectivity while maintaining great regioselectivity under an optimized catalytic system.

These classes of catalysts have been found to complement each other quite well. Their modular synthesis approach also facilitated the creation of diverse catalyst variants with different steric and electronic properties.

Table of Contents

| | |
|---|------|
| Abstract | iii |
| List of Figures | viii |
| List of Schemes | ix |
| List of Tables..... | xi |
| Acknowledgement..... | xii |
| Dedication | xiii |
| Chapter 1 Evaluation of 3,3'-Triazolyl Biisoquinoline <i>N,N'</i> -Dioxide Catalysts for Asymmetric Transfer Hydrogenation of Hydrazones with Trichlorosilane | 1 |
| 1.1 Introduction | 1 |
| 1.1.1 Chiral Hydrazine | 1 |
| 1.1.2 Catalysis in Hydrazone Reduction | 2 |
| 1.1.3 Trichlorosilane | 6 |
| 1.1.4 Lewis-Base Catalysis | 7 |
| 1.2 Reaction Condition Optimization | 13 |
| 1.2.1 3,3'-Triazolyl Biisoquinoline <i>N, N'</i> -dioxide | 13 |
| 1.2.2 Preliminary Experiment and Solvents..... | 15 |
| 1.2.3 Hydrazone Protecting Groups | 18 |
| 1.2.4 Triazolyl Groups of the Biisoquinoline..... | 19 |
| 1.3 Hydrosilylation of Benzoyl Hydrazones | 22 |

| | |
|---|----|
| 1.3.1 Hydrazone Substrate Scope | 22 |
| 1.3.2 Attempt with Higher Scale..... | 26 |
| 1.3.3 Structural Analysis of the Reducing Species | 27 |
| 1.4 Conclusion | 30 |
| 1.5 Experimental Section | 31 |
| 1.5.1 General Information | 31 |
| 1.5.2 Experimental Procedures | 33 |
| 1.5.3 Computational Procedures | 53 |
| Chapter 2 Evaluation of Helicene-Derived 2,2'-Bipyridine <i>N</i> -Monoxide Catalyst for the Enantioselective Propargylation of <i>N</i> -Acylhydrazones with Allenyltrichlorosilane..... | 54 |
| 2.1 Introduction | 54 |
| 2.1.1 Helicene-Derived Catalysts..... | 54 |
| 2.1.2 Enantioselective Propargylation of Imines | 58 |
| 2.2 Reaction Condition Optimization | 63 |
| 2.2.1 Synthesis of Optically Pure Helicene Catalyst..... | 63 |
| 2.2.2 Basic Reaction Parameters | 65 |
| 2.2.3 Evaluation of Biisoquinoline-Based Catalysts..... | 68 |
| 2.3 Propargylation of <i>N</i> -Acylhydrazones..... | 70 |
| 2.4 Conclusion | 74 |
| 2.5 Experimental Section | 75 |
| 2.5.1 General Information | 75 |

| | |
|---|-----|
| 2.5.2 Experimental Procedures | 77 |
| Chapter 3 Asymmetric Allenylation of <i>N</i> -Acylhydrazones with Propargyltrichlorosilane Catalyzed by Helical Chiral 2,2'-Bipyridine <i>N</i> - Monoxide | 99 |
| 3.1 Introduction | 99 |
| 3.1.1 Allenes and α -allenylamines | 99 |
| 3.1.2 Enantioselective Allenylation of Imines | 100 |
| 3.2 Reaction Condition Optimization | 103 |
| 3.2.1 Synthesis of Propargyltrichlorosilane | 103 |
| 3.2.2 Evaluation of Lewis Base Catalysts | 107 |
| 3.3 Allenylation of <i>N</i> -Acylhydrazones | 110 |
| 3.4 Conclusion | 114 |
| 3.5 Experimental Section | 115 |
| 3.5.1 General Information | 115 |
| 3.5.2 Experimental Procedure | 117 |
| References | 138 |

List of Figures

| | |
|--|----|
| Figure 1. Examples of biologically active molecules and organocatalysts that possess chiral hydrazines.. | 2 |
| Figure 2. Development of Malkov's Sigamide catalyst..... | 8 |
| Figure 3. Malkov's analysis of catalyst functionalization for their diamides catalyst in trichlorosilane-mediated aromatic ketimine reduction. | 9 |
| Figure 4. Presumable competition on the binding trichlorosilane silicon center between the Lewis-base catalyst and the acyl substituent of hydrazone. | 12 |
| Figure 5. Design principles for the 3, 3' substituted biisoquinoline <i>N, N'</i> -dioxides catalysts. | 14 |
| Figure 6. Computed structures of the two lowest energy minima for 2a-HSiCl ₃ complex. | 29 |
| Figure 7. 3-D demonstration of helicene's unique shape with hexahelicene and how helical structure's mirror images embody chiral characteristics..... | 55 |
| Figure 8. Important examples in the history of helicene chemistry..... | 56 |
| Figure 9. Structure of (<i>p</i>)-1-aza[6]helicene in 3-D with its nitrogen atom screened by its surroundings. | 57 |
| Figure 10. The solid-state structure of helicene-derived 2,2'-bipyridine <i>N</i> -monoxide catalyst and its expected complex with allenyltrichlorosilane..... | 58 |

List of Schemes

| | |
|--|-----|
| Scheme 1. The first example of asymmetric catalytic hydrogenation using a rhodium-based catalyst..... | 3 |
| Scheme 2. General scheme of transition metal-catalyzed enantioselective hydrogenation of hydrazones. | 4 |
| Scheme 3. Direct reductive hydrazination using trichlorosilane and organic chiral Lewis-base catalyst. | 5 |
| Scheme 4. Catalytic cycle for trichlorosilane mediated Lewis-base catalysis..... | 7 |
| Scheme 5. Catalytic asymmetric reduction of acyl hydrazones with trichlorosilane and chiral bisoquinoline <i>N, N'</i> -dioxides catalyst. | 12 |
| Scheme 6. The 1.0 mmol scale reaction with the model substrate under optimized reaction conditions. | 27 |
| Scheme 7. Selectivity issue with a mixture of propargyl and allenic reagents. | 59 |
| Scheme 8. Demonstration of chiral transition metal-catalyzed enantioselective propargylation of imines. | 60 |
| Scheme 9. Organocatalyst catalyzed propargylation of glyoxylate-derived acylhydrazone with allenylboronic acids. | 61 |
| Scheme 10. Preliminary experiment of chiral Lewis base-catalyzed propargylation of <i>N</i> -acylhydrazones with allenyltrichlorosilane. | 61 |
| Scheme 11. Purposed enantioselective intermediate complexes of the investigating catalysis. | 62 |
| Scheme 12. Improved optical resolution process of helicene 5 with salt-mediated crystallization, with 2 more steps to get helicene catalyst (<i>p</i>)-4. | 64 |
| Scheme 13. Examples of diverse heterocycles synthesized from allenic amines. . | 100 |
| Scheme 14. Regioselectivity of propargylation and allenylation addition reactions. | 101 |

| | |
|--|-----|
| Scheme 15. Catalytic enantioselective allenylation of imines. | 102 |
| Scheme 16. Lewis base catalyzed allenylation of acylhydrazones with propargyltrichlorosilane. | 102 |
| Scheme 17. Hoveyda's catalytic approaches for allenylation of aldimines..... | 104 |
| Scheme 18. Regioselective synthesis of allenic alcohol from aldehyde and propargyltrichlorosilane. | 105 |
| Scheme 19. Regioselective synthesis of propargyltrichlorosilane..... | 106 |

List of Tables

| | |
|--|-----|
| Table 1. Selected entries from Malkov's organocatalytic enantioselective reduction of aromatic ketimines with trichlorosilane..... | 11 |
| Table 2. Solvent screening for model reaction..... | 16 |
| Table 3. Hydrazone protecting group screening. | 19 |
| Table 4. Evaluation of 3,3'-substituted biisoquinoline catalysts. | 20 |
| Table 5. Hydrosilylation of benzoyl hydrazones with optimized reaction parameters. | 26 |
| Table 6. Evaluation of the basic reaction parameters.. | 66 |
| Table 7. Evaluation of biisoquinoline based catalysts with allenyltrichlorosilane added as a CH ₂ Cl ₂ solution at -78°C..... | 69 |
| Table 8. Propargylation of various acylhydrazones in 0.1 mmol scale with allenyltrichlorosilane and catalyst (<i>P</i>)-4 under optimized reaction parameters..... | 74 |
| Table 9. Evaluation of the Lewis base catalysts in allenylation of <i>N</i> -acylhydrazones with propargyltrichlorosilane. | 109 |
| Table 10. Allenylation of various acylhydrazones in 0.1 mmol scale with propargyltrichlorosilane and catalyst (<i>M</i>)-4 under optimized reaction parameters | 113 |

Acknowledgement

I would like to express my sincere gratitude to my advisor, Dr. Norito Takenaka, for his continuous guidance and support throughout my PhD training. Not only is he an excellent chemist with great knowledge, but also a good teacher who is always willing to educate us and provide insight on the projects. I would also like to thank my dissertation committee members, Dr. James Brenner, Dr. Yi Liao, and Dr. Nasri Nesnas, for their invaluable support, encouragement, and time.

I would like to thank the Chemistry Program for financial support through teaching assistantships and the National Institute of Health for financial support in the form of research assistantships.

I would also like to thank Dr. Joel Olson, who was my advisor during my Master's training, for encouraging me to pursue the PhD degree. I also want to express my appreciation to my colleagues Franklin Thornburgh and Megan Sterling from Dr. Olson's research group, as well as ShiYu Sun, Carlyn Reep, and Noble Blako from Dr. Takenaka's research group. They were good friends and helped me so much during my hardest time.

Dedication

For my family

Chapter 1

Evaluation of 3,3'-Triazolyl Biisoquinoline *N,N'*-Dioxide Catalysts for Asymmetric Transfer Hydrogenation of Hydrazones with Trichlorosilane

1.1 Introduction

1.1.1 Chiral Hydrazine

The chiral hydrazine is a motif that exists in many useful pharmaceutical compounds, natural products, chiral organocatalysts, etc. [1–6]. As shown in Figure 1, hydrazine **A** *D*-(+)-JB-516 is an inhibitor of monoamine oxidase [1]. Cyclic hydrazine **B** azacastanospermine was found to be effective as an inhibitor of almond β -glucosidase and rice α -glucosidase [6]. In catalysis chemistry, *N*-acyl hydrazines **C** and **D** were identified as efficient organocatalysts in asymmetric Diels-Alder reactions [3]. Hydrazine **E**, categorized as LY288513, is a promising preclinical candidate because of its cholecystokinin inhibition capability [6]. Due to its wide applications in plentiful fields, chiral hydrazine has been extensively investigated, and many synthetic pathways of reaching such motif enantio-selectively and reliably have been developed over the past few decades. Among these, catalytic asymmetric reduction of readily available acyl hydrazones can provide direct access to enantio-enriched chiral hydrazines [7–9].

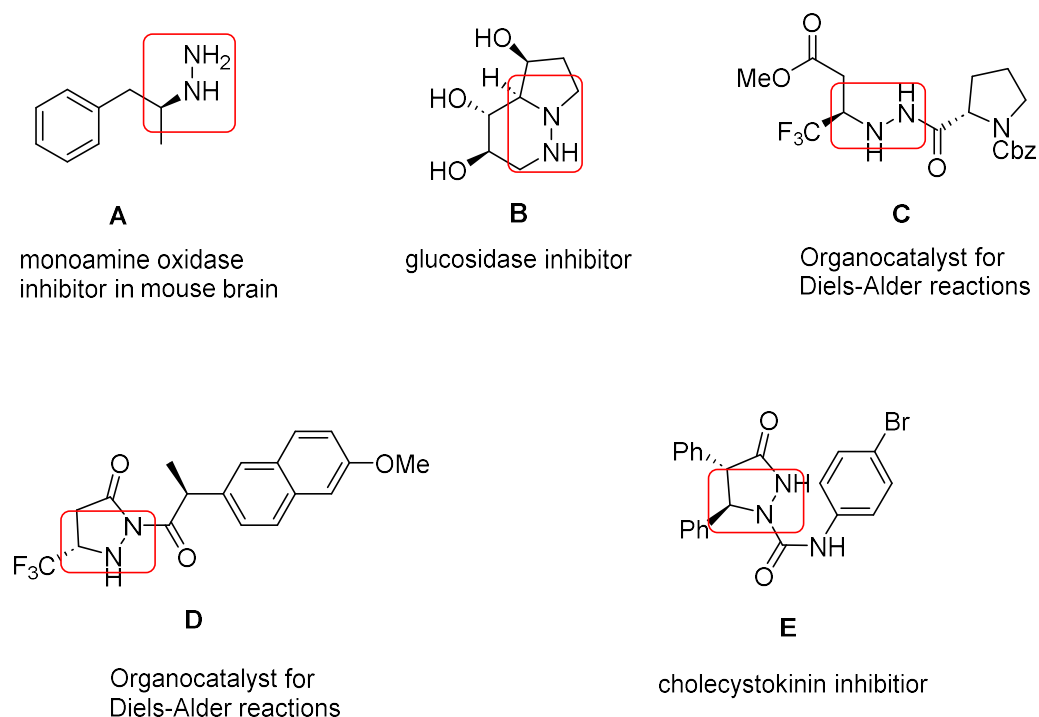
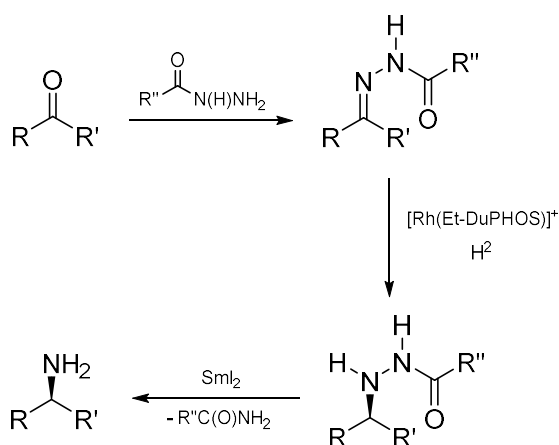


Figure 1. Examples of biologically active molecules and organocatalysts that possess chiral hydrazines. A: inhibitor for monoamine oxidase; B: azacastanospermine, a potent inhibitor of almond β -glucosidase and rice α -glucosidase; C and D: organocatalysts identified for Diels-Alder reactions; E: preclinical candidate for its cholecystokinin inhibition capability.

1.1.2 Catalysis in Hydrazone Reduction

One traditional method of making chiral hydrazines is by utilizing transition metal-based chiral catalysts. The first transition metal catalyzed enantioselective

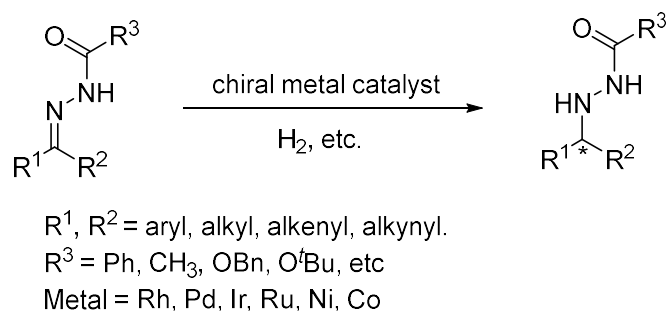
hydrogenation of acyl hydrazones was reported in 1992 (Scheme 1; [10]). In this first example, Burk and Feaster used rhodium-based catalysts for the asymmetric hydrogenation of *N*-acylhydrazones and were able to achieve up to 97% ee [10]. In their study, they also found out important factors that influenced the catalytic efficiency of their system: 1) the electron-rich nature of the DuPHOS ligand of the catalyst, and 2) the existence of substrate chelation from the secondary donor carbonyl oxygen to the catalyst's metal center [11].



Scheme 1. The first example of asymmetric catalytic hydrogenation using a rhodium-based catalyst [10].

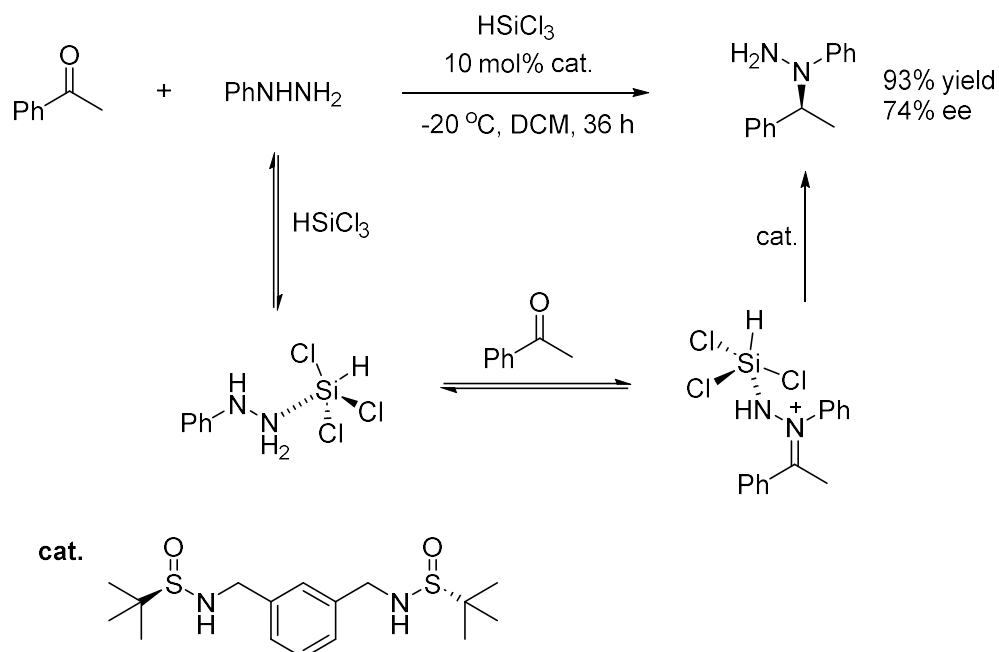
After seeing the potential of metal-based catalysts in asymmetric catalytic reactions, especially on hydrazone reductions, it had become one of the most important fundamentals for developing this type of reaction.

Besides the latter widely used rhodium-based catalysts, other metals like palladium, iridium, ruthenium, nickel, and cobalt were also being investigated (Scheme 2).



Scheme 2. General scheme of transition metal-catalyzed enantioselective hydrogenation of hydrazones.

Most of these metal catalysts enabled enantioselective reactions and gave impressive scopes and results [5,6,12–21]. However, they also come with their own disadvantages, such as being very expensive or being harmful to the human body and/or environment. Therefore, metal-free procedures for reaching chiral hydrazine are still needed and are currently relatively limited. In this case, organocatalytic pathways can be a potent way for this purpose, but not many examples were around by the time of our investigation.



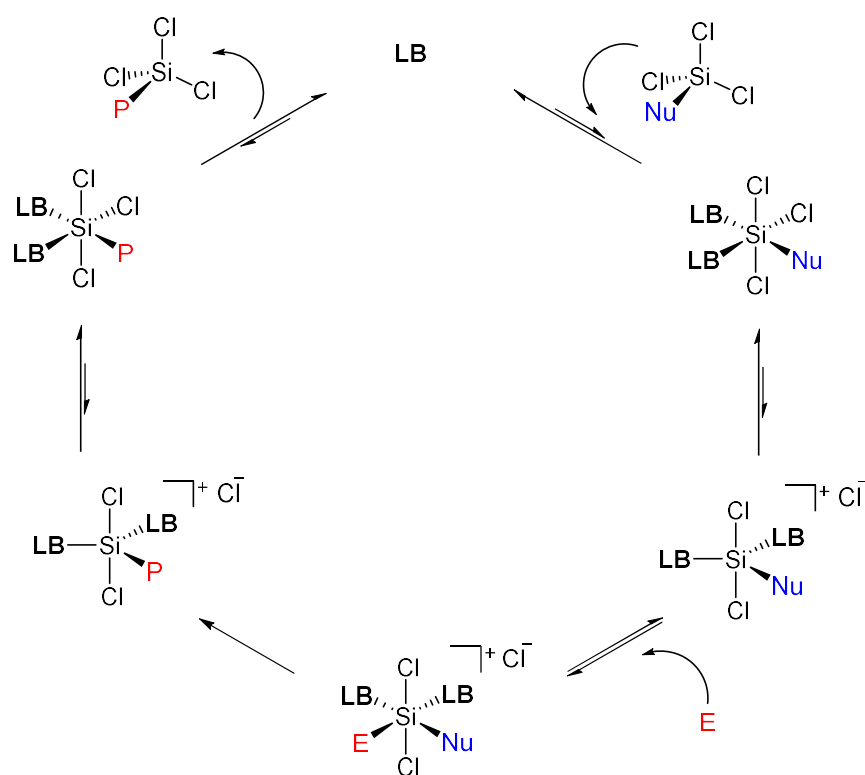
Scheme 3. Direct reductive hydrazination using trichlorosilane and organic chiral Lewis-base catalyst [22].

One patent from Japan in 2001 described an example of a hydrazone reduction from a tosylhydrazone undergoing asymmetric hydrosilylation catalyzed by a non-metal catalyst [23]. Aside from that, we found another study in 2016 that focuses on direct reductive amination using organic Lewis-base and trichlorosilane [22]. In their work, they used trichlorosilane to produce the iminium intermediate from acetophenone in dichloromethane (DCM) and completed the reductive hydrazination with a chiral bis-sulfonamide catalyst (an organic Lewis-base catalyst), which they were able to achieve the corresponding hydrazine in 93% yield and 74% ee (Scheme 3).

1.1.3 Trichlorosilane

From the aforementioned examples and in the search for a viable reducing agent for organocatalysis, we found trichlorosilane as a good option for our purpose.

Compared to other options, such as organo- samarium or chromium and dibutylchlorotin hydride, trichlorosilane is very inexpensive as its commercial supply is well-established by the silicon industry. It is also relatively easy to handle, and its related reactions mostly form non-hazardous silicon by-products that are environmentally friendly, like NaCl and SiO₂, upon quenching. When being used as a reducing agent for C=N reductions, trichlorosilane will need to be activated by a Lewis-base catalyst through coordination to generate a hypervalent Lewis acid intermediate, in the form of hexa-coordinated silicon structures, which will then undergo a catalytic cycle as shown in Scheme 4. In this type of reduction, applying an appropriate chiral Lewis base can control the stereochemistry of the corresponding product. This made both trichlorosilane-mediated reductive reactions and Lewis-base catalysis attractive topics and led to the development of many efficient catalysts [24–26].



Scheme 4. Catalytic cycle for trichlorosilane mediated Lewis-base catalysis.

1.1.4 Lewis-Base Catalysis

One important example of the chiral Lewis bases in the asymmetric reduction reaction is from Malkov's group. They took inspiration from Matsumura's L -proline-derived formamide based catalysts and had its proline framework replaced with *N*-methyl valine, a more versatile choice that led to their diamides catalysts

(Figure 2; [27]) [26–29]. They later further optimized their catalyst to what they called Sigamide for the purpose of trichlorosilane-mediated enantioselective reduction of ketimines and were able to achieve impressive results up to 97% ee [27].

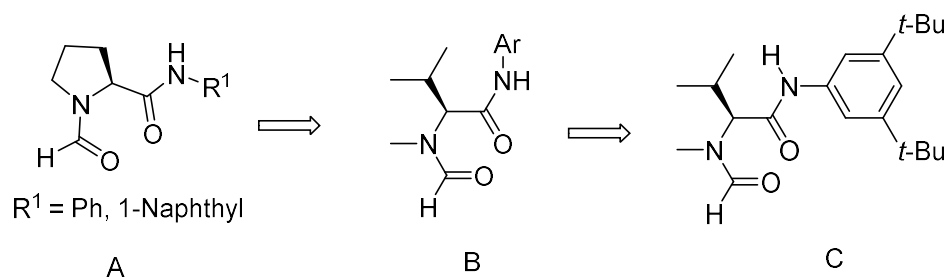


Figure 2. Development of Malkov's Sigamide catalyst. A: Matsumura's L-proline-derived catalysts. B: Malkov's N-methyl valine derived bisamides catalysts. C: optimized Sigamide catalyst [27].

During the optimization of their diamides catalyst, Malkov also analyzed many important aspects related to the development of the chiral Lewis-base catalyst for imine reduction. These aspects were found to greatly affect the catalyst's electronic and steric properties. First, the structure of the catalyst should be designed considering the activation of trichlorosilane. As shown in Figure 3, their chiral Lewis-base has two strategically positioned amide carbonyl oxygens that are sufficiently Lewis-basic [29]. Their Lewis basicity can make them good electron donors and enable the coordination with the silicon center of the trichlorosilane, thus playing an important role in the catalyst's catalytic efficiency.

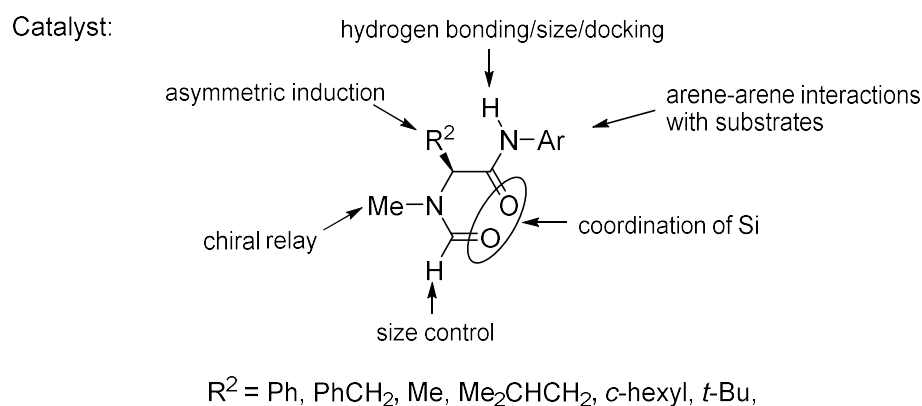
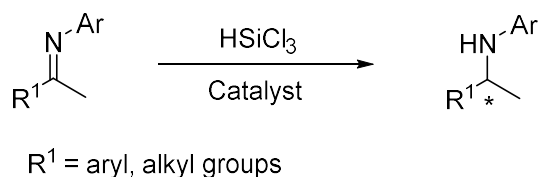
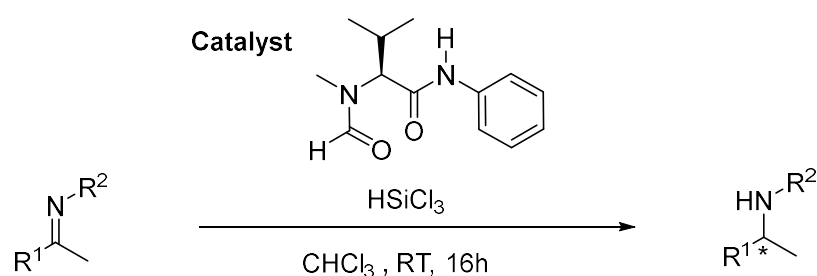


Figure 3. Malkov's analysis of catalyst functionalization for their diamides catalyst in trichlorosilane-mediated aromatic ketimine reduction [29].

Aside from that, the enantioselectivity and reactivity of this reduction are also heavily affected by the catalyst-imine interactions. Hence, the structure of the imine should also be considered. In the case of ketimines, one of the carbon center's substituents is preferably aromatic while the other one is preferably alkyl. This creates a bigger difference between two substituents sterically and electronically for the silicon-catalyst complex's approach and can often lead to better enantioselectivity.

The *N*-substituent (ketimine's protecting group) also plays a crucial role in the enantiodifferentiating process. This is realized by putting specific substituents onto

Lewis-base catalysts that promote desired interaction with ketimine's *N*-substituent that leads to significantly better enantioselectivity of reduction. This mechanistic behavior is shown in Malkov's work, where the arene-arene interaction between the *N*-aryl substituent of ketimine and the amide aromatic group heavily dictates the enantioselectivity of the product. The absence of this conjugation by replacing the aromatic ketimine protecting group with non-aromatic ones like cyclohexyl, butyl or benzyl (entries 7-9) did not shut down the reaction but almost seized the enantioselectivity completely, as can be observed from Table 1. This indeed showcased how important imine protecting groups are to their corresponding reduction reactions and the importance of exploring reduction pathways for imines having different protecting groups [29].



| Entry | R^1, R^2 | Yield (%) | ee (%) |
|-------|--|-----------|--------|
| 1 | Ph, Ph | 79 | 86 |
| 2 | 4-MeOC ₆ H ₄ , Ph | 57 | 80 |
| 3 | 4-CF ₃ C ₆ H ₄ , Ph | 43 | 87 |
| 4 | 2-Naphth, Ph | 60 | 87 |
| 5 | <i>c</i> -C ₆ H ₁₁ , Ph | 80 | 37 |

| | | | |
|---|--|----|----|
| 6 | Ph, 4-MeOC ₆ H ₄ | 96 | 85 |
| 7 | Ph, <i>c</i> -C ₆ H ₁₁ | 50 | <5 |
| 8 | Ph, <i>n</i> -Bu | 60 | <5 |
| 9 | Ph, CH ₂ Ph | 46 | 8 |

Table 1. Selected entries from Malkov's organocatalytic enantioselective reduction of aromatic ketimines with trichlorosilane[29]. Reactions were carried out at 0.5 mmol scale with 1.5 equivalent of HSiCl₃, 10 mol% of catalyst and CHCl₃ as solvent at room temperature for 16 hours.

While the milestones of the development of Lewis-base organocatalyst and many related examples involved amide-based derivatives [30–32], there were also other motifs being looked at, such as pyridine *N*-oxides [33–38], phosphine oxides [39–41] and sulfinamides [42,43]. They have been extensively tested on trichlorosilane-mediated asymmetric hydrosilylation of ketimines in numerous studies, but most of them were limited to specific types of ketimine with aryl and alkyl groups as the nitrogen protecting group. The reason for the lack of acyl hydrazone examples is likely because the carbonyl oxygen of the acyl hydrazone group can possibly compete with the Lewis basic donors on the catalyst on forming hypervalent silicon complexes. This scenario is very likely to be the reason for the diminishing catalytic effect of the catalyst in asymmetric ketimine reductions (Figure 4).

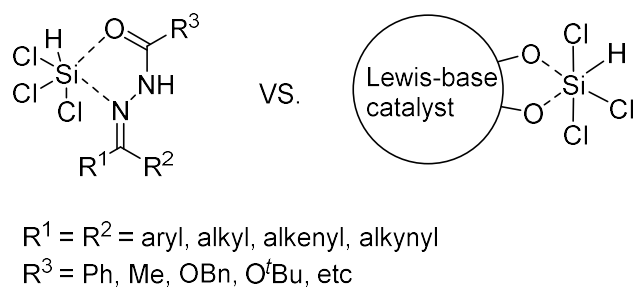
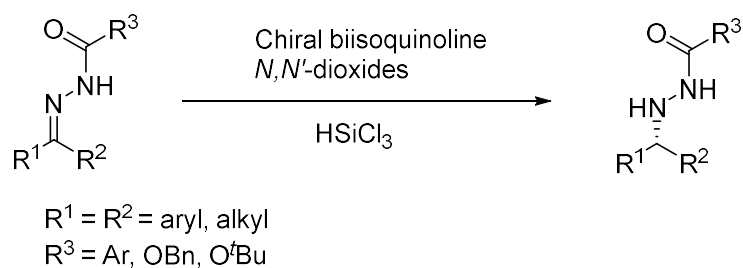


Figure 4. Presumable competition on the binding trichlorosilane silicon center between Lewis-base catalyst and the acyl substituent of hydrazone.

Due to this difficulty of handling acyl hydrazone, the only examples we could find that faced similar challenges were the ones mentioned earlier, in which *N*-tosyl and *N*-phenyl substituted hydrazones were reduced using Lewis-base catalysts with trichlorosilane [23]. With that being said, we were interested in exploring the effectiveness of our newly developed axial-chiral 3,3'-triazolyl biisoquinoline *N*, *N'*-dioxide catalysts in this type of hydrosilylation (Scheme 5) [44].



Scheme 5. Catalytic asymmetric reduction of acyl hydrazones with trichlorosilane and chiral biisoquinoline *N*, *N'*-dioxides catalyst.

1.2 Reaction Condition Optimization

1.2.1 3,3'-Triazolyl Biisoquinoline *N, N'*-dioxide

The biisoquinoline *N, N'*-dioxide is an axial-chiral structure heavily investigated by our group for many years inspired by 1,1'-Binaphth-2-ol (BINOL), one of the most successful and prominent class of scaffolds in asymmetric catalysis [45]. The synthetic method of making 3,3'-triazolyl biisoquinoline *N, N'*-dioxide was published by my colleague Shiyu and Carlyn in 2021. The design principle for this catalyst is to create a chiral pocket from the 3, 3' positions of the biisoquinoline to increase its enantioselective capability (Figure 5, **A** and **B**; [44]).

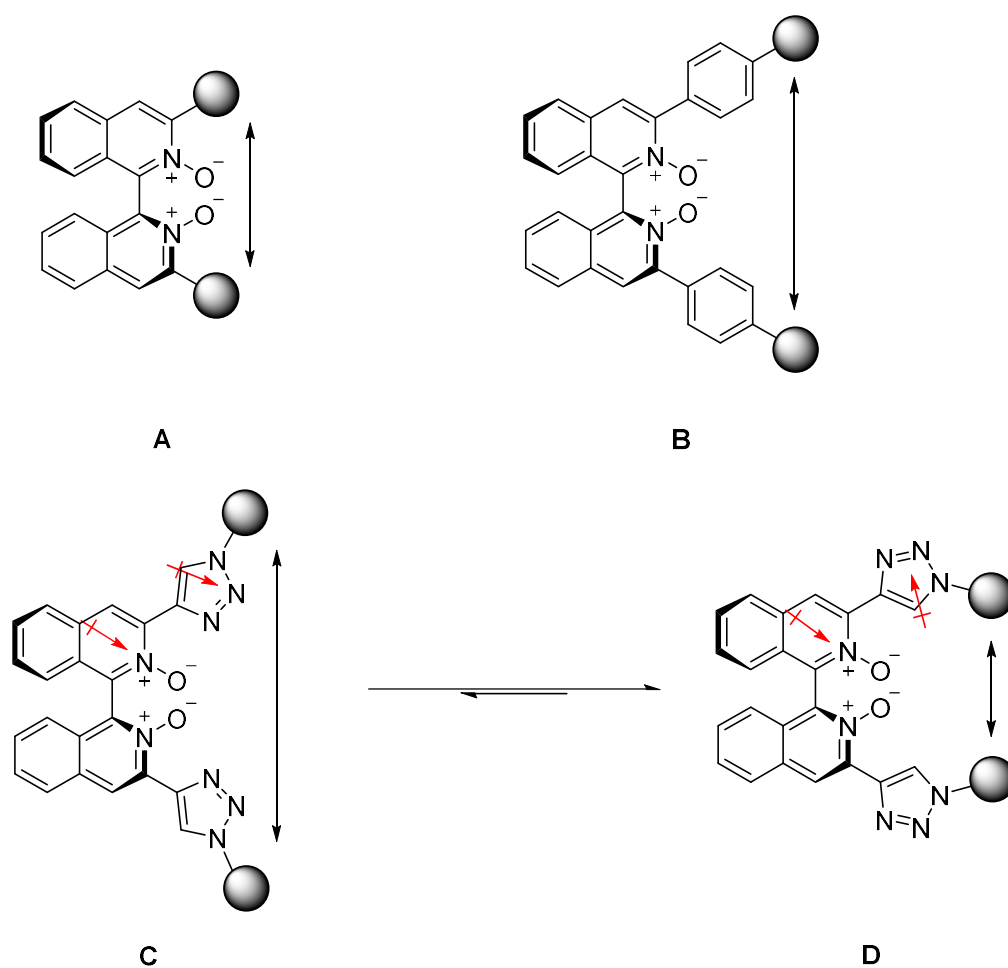


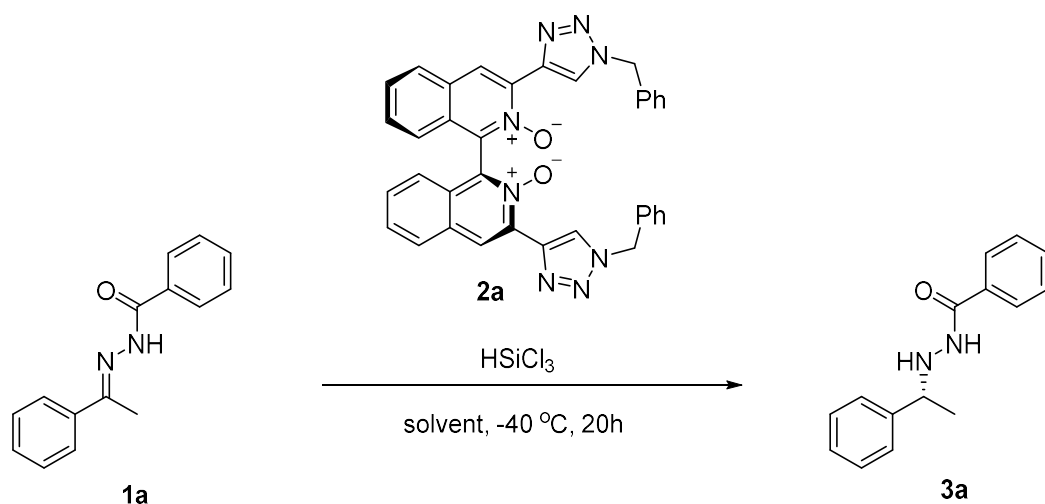
Figure 5. Design principles for the 3, 3' substituted biisoquinoline *N, N'*-dioxides catalysts [44]. A and B: chiral pocket size comparison of 3,3'-substituted biisoquinolines. C and D: dipole moments affecting the chiral pocket size of triazolyl-biisoquinolines.

Modifying a biisoquinoline *N, N'*-dioxides' 3, 3' positions can drastically change its catalytic behavior and by substituting it with a phenyl linker can extend the pocket's reach. However, further modifications will mostly end up with a wider

pocket (Figure 5B; [44]) making the “arms” further away from the reaction site. To create a bigger chiral cavity on the catalyst, they utilized the dipole moments of the pyridine *N*-oxide and 1,2,3-triazole ring in the formation of D (Figure 5, C and D; [44]). The resulting catalyst catalog, 3,3'-triazolyl biisoquinoline *N*, *N'*-dioxide, was found to be particularly effective when activating trichlorosilane at low temperatures. Hence, we hypothesized that they could also activate the reduction of acyl hydrazone in low temperatures, which should therefore limit background reactions.

1.2.2 Preliminary Experiment and Solvents

Once the type of Lewis-base catalyst was decided, we then moved on to the optimization of the other reaction parameters. For the hydrazone substrate, we began with the most basic acyl protracting group as shown in Table 2 with one of the more efficient triazolyl catalysts in its development. Based on the selected catalyst's capability of challenging low temperature asymmetric catalytic reactions, our preliminary study started with -40°C for 20 hours. This is to prevent possible background reactions as much as possible, which turned out to be successful.



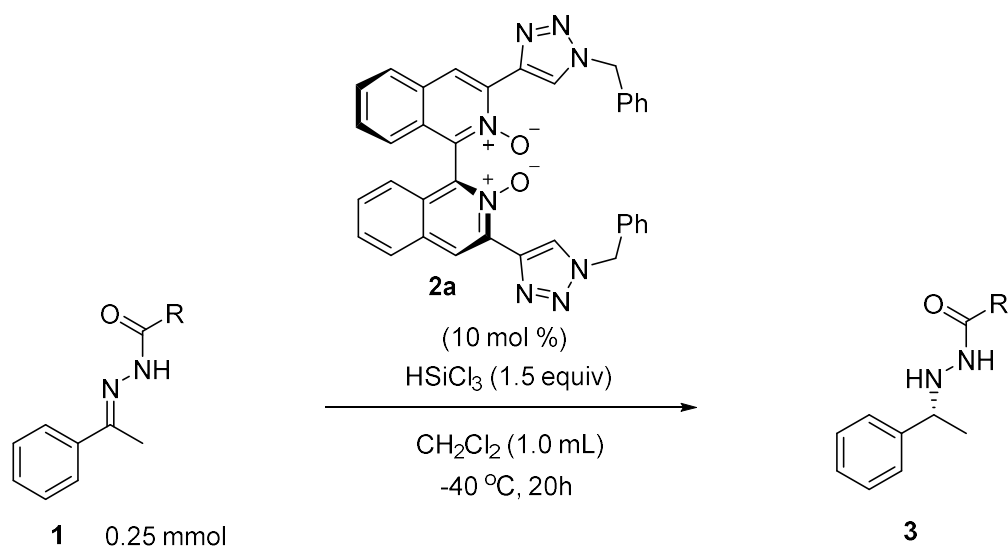
| Entry | Solvent | Yield (%) ^a | ee (%) |
|----------------|---------------------------------|------------------------|--------|
| 1 ^b | CH ₂ Cl ₂ | trace | - |
| 2 | CH ₂ Cl ₂ | 48 | 53 |
| 3 | CHCl ₃ | 34 | 66 |
| 4 | CH ₃ CN | 50 | 32 |
| 5 ^c | THF | 26 | 14 |
| 6 ^d | CH ₂ Cl ₂ | 44 | 58 |
| 7 ^e | CH ₂ Cl ₂ | 40 | 58 |
| 8 ^f | CH ₂ Cl ₂ | 42 | 58 |

Table 2. Solvent screening for model reaction. Unless otherwise noted, all reactions were carried out with 0.25 mmol hydrazone, 1.5 equiv HSiCl₃, 10 mol % catalyst, and 1.0 mL solvent. a) NMR yield was determined using 1,1,2,2-tetrachloroethane as standard. b) Without catalyst. c) Product stereochemistry was (*S*) configuration. d) 2.0 mL solvent was used. e) 250 mg of 4 Å molecular sieve was used. f) 3.0 equiv of HSiCl₃ was used.

The background reaction that ran without any catalyst gave trace amount of yield (entry 1). The preliminary experiment with the selected catalyst and dichloromethane was able to achieve 48% yield and 53% ee, which looked promising (entry 2). Other solvents that are commonly used for trichlorosilane-mediated reactions were also looked at. One solvent we looked at was chloroform and it resulted in higher enantioselectivity with 66% ee but yield went down to 34% (entry 3). Acetonitrile, on the other hand, gave a slightly higher yield of 50% but resulted in a much lower ee of 32% (entry 4). The last solvent we used was tetrahydrofuran (entry 5). It not only offered the lowest yield and % ee (26% yield, 14% ee), but also produced the product as the opposite (*S*) enantiomer. Through these results we found that dichloromethane is the optimal choice of solvent. It is worth noting that dichloromethane did not completely dissolve the hydrazone in this scale. Therefore, we decided to try using twice as much solvent, but it did not show much of a difference (entry 6). It is well known that trichlorosilane may produce a small amount of HCl during storage or mishandling. To avoid the potential influence from this strong acid, we used 4 Å molecular sieve for the acid scavenging, which had proven to be effective in our previous research [46]. However, this did not lead to either better yield or higher % ee in this study (entry 7). We also tried doubling the trichlorosilane's amount, but also did not see better results (entry 8).

1.2.3 Hydrazone Protecting Groups

Next, we tested a few different acyl protecting groups on hydrazone under the model reaction condition (Table 3). Hydrazone's protecting groups have shown great impact on both reactivity and enantioselectivity in their catalytic asymmetric reductions. One study by Schuster in recent years using ruthenium-based catalyst were able to achieve up to 97% yield and 97% ee when having Cbz or Boc as hydrazone's protecting group [16]. However, other protecting groups they tried gave significantly lower ee with one (N, N-dimethyl-substituted) even having 0% conversion rate. With that in mind, we also tried Boc and Cbz (entry 1 and 2, respectively) and were able to get decent ee, but at the cost of low conversion rate. We noticed both Boc and Cbz groups have more Lewis basic C=O units compared to a benzoyl group due to the more electron donating ^tBu and ether unit in Boc and Cbz, respectively. Hence, we also tried a less Lewis basic hydrazone (entry 3). The enantioselectivity of this product was slightly higher than entry 2, but the yield went all the way down to 14%. These trials demonstrated that the current method is notably sensitive to hydrazone protecting groups.



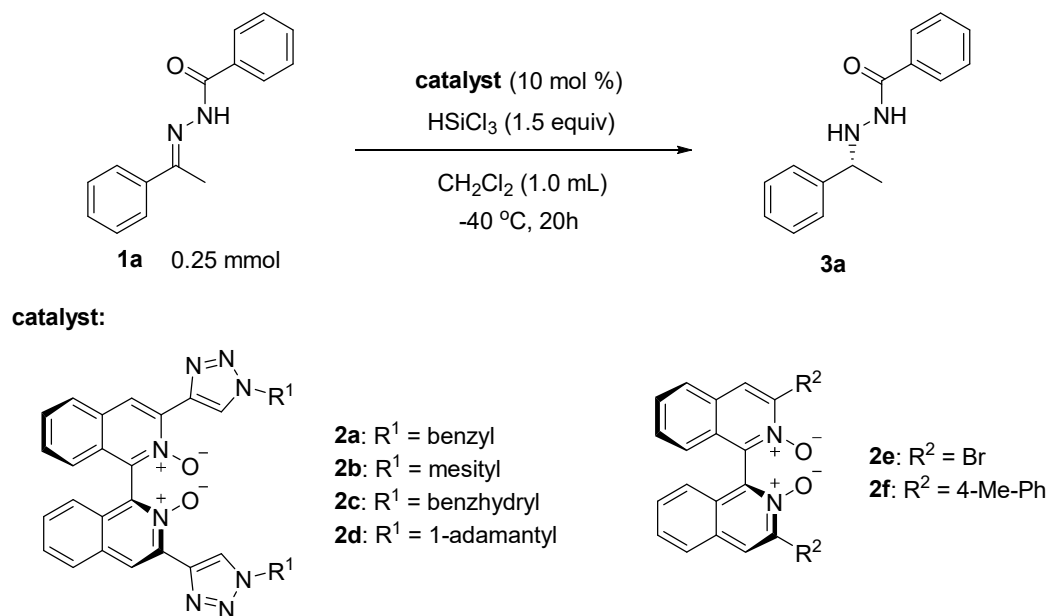
| Entry | R | Yield (%) ^a | ee (%) |
|-------|-------------------------------------|------------------------|-----------------|
| 1 | O ^t Bu (1b) | 36 | 71 ^b |
| 2 | OBn (1c) | 21 | 64 |
| 3 | 4-NO ₂ -Ph (1d) | 14 | 69 |

Table 3. Hydrazone protecting group screening. a) NMR yield was determined using 1,1,2,2-tetrachloroethane as standard. b) Value is estimated because chiral HPLC did not show a clear separation between two enantiomers.

1.2.4 Triazolyl Groups of the Biisoquinoline

The last step of the reaction condition optimization is the evaluation of 3, 3'-substituted biisoquinoline N, N'-dioxides catalysts (Table 4). Beside the catalyst **2a**

that was used in consolidating model reaction, we also tested three other 3, 3'-
 triazolyl substituted biisoquinolines (Table 4, 1b-d).



| Entry | Catalyst | Yield (%) ^a | ee (%) |
|-------|----------|------------------------|--------|
| 1 | 2a | 48 | 53 |
| 2 | 2b | 8 | 18 |
| 3 | 2c | 19 | 74 |
| 4 | 2d | 14 | 54 |
| 5 | 2e | trace | - |
| 6 | 2f | trace | - |

Table 4. Evaluation of 3,3'-substituted biisoquinoline catalysts. a) NMR yield was determined using 1,1,2,2-tetrachloroethane as standard.

Catalyst **2b** did not perform to our expectation, giving only 18 % ee with almost no conversion yield. Catalysts **2c** and **2d**, however, were able to produce products in decently high ee, especially **2c**, reaching 74% ee. This was so far the highest ee we could reach for the model reaction. Overall, all three catalysts gave very low yield compared to catalyst **2a**, making **2a** our choice of catalyst for this reaction. These results suggested that tuning the triazolyl groups on this set of catalysts can effectively change their reactivity and enantioselectivity.

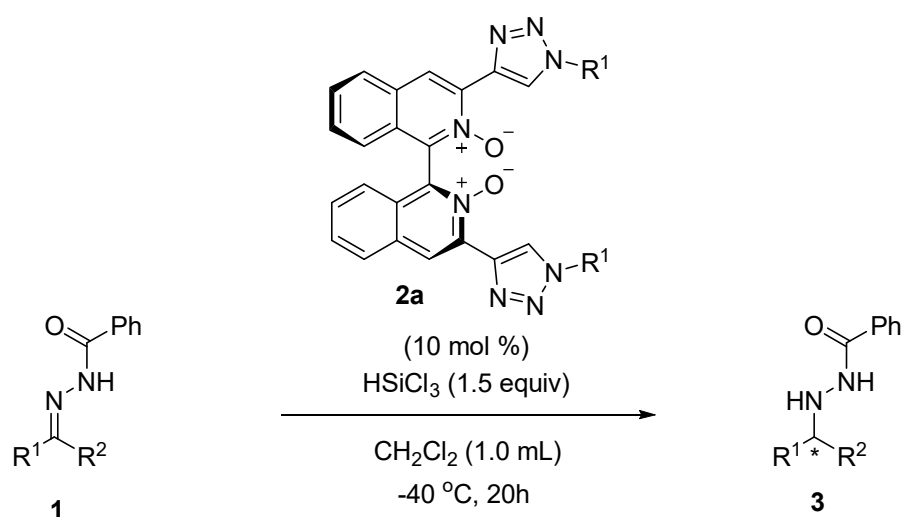
Besides the triazolyl catalyst, we also tested two conventional 3,3'-substituted biisoquinoline *N,N'*-dioxides catalysts (entry 5, 6). Surprisingly, despite **2f** exhibiting reactivity comparable to **2b–d** in the hydrosilylation of an N-phenyl ketimine with trichlorosilane, neither **2e** nor **2f** catalyzed the reaction at all [44]. However, these findings illustrated that the novel axial-chiral biisoquinolines represent a valuable addition to the current array of Lewis-base catalysts, promising advancements in their practical applications.

1.3 Hydrosilylation of Benzoyl Hydrazones

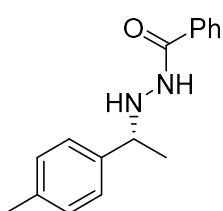
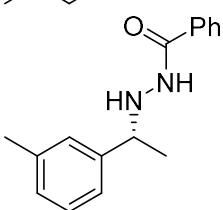
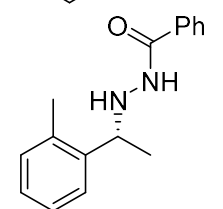
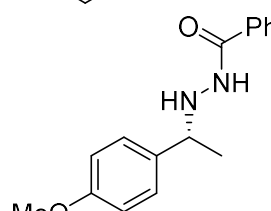
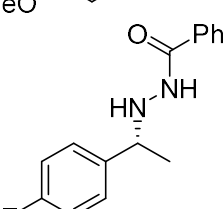
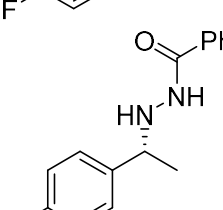
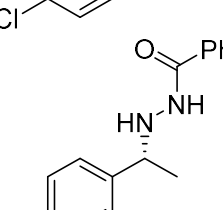
1.3.1 Hydrazone Substrate Scope

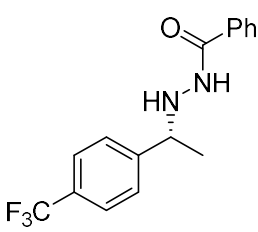
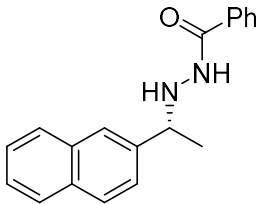
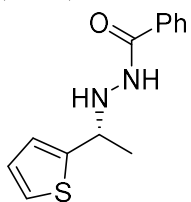
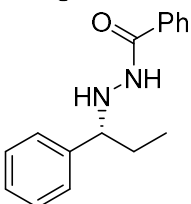
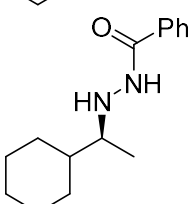
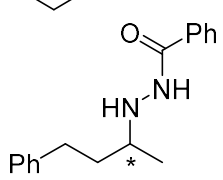
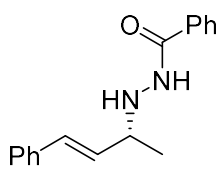
Once the reaction parameters were optimized, we moved on to assess how effectively the current catalytic system could selectively catalyze the hydrogenation of different benzoyl hydrazones with trichlorosilane (Table 5). We first tested how a simple methyl substitution on *para*, *meta* or *ortho* positions of R¹ phenyl (entries 2, 3 and 4, respectively) could affect the reactivity and selectivity of the reactions. To our surprise, this small change did cause a significant reactivity difference as compared to model substrate **3a**. First, the *ortho*-methyl substituted hydrazone (**1g**) did not promote the reaction at all. Although the *meta*-methyl substituted hydrazone (**1f**) behaved only slightly worse than **1a**, *para*-methyl substituted hydrazone (**1e**) reduced the yield to 27%, almost half of **1a**, while maintaining similar ee. Considering both **3e** and **3f** are structurally like **3a**, it was interesting to see how differently they affect this reaction. Entry 5-10 (**3h-m**) focus on changing the electronic nature of the aryl group with either electron withdrawing substitution (**3i-3l**) or electron donating ones (**3h, 3m**). Overall, the results showed that the enantioselectivity was mostly unaffected by tuning the phenyl ring's electron density, but reactivity may be negatively affected. Neither heteroaromatic **3n** nor **3o** (expected to have less yield for having longer alkyl group that increases steric

hindrance near C=N) made noticeable change in reactivity or selectivity. Replacing phenyl with a cyclohexyl group produced the opposite enantiomer with decent yield and ee (**3p**). For **3q**, having two alkyl C=N substitution that made structural differentiation harder and indeed reduced the selectivity drastically. An α,β -unsaturated hydrazone **3r** did not suit this study because reduction can take place producing **3q** as a side product.



| Entry | Hydrazine | Yield (%) | ee (%) |
|-------|--|-----------|--------|
| 1 | <div> <div> $\text{O}=\text{C}-\text{Ph}$ $\text{HN}-\text{NH}$ $\text{HN}-\text{CH}(\text{Ph})-\text{CH}_3$ </div> <div>3a</div> </div> | 48 | 53 |

| | | | | |
|---|-----------|---|----|----|
| 2 | 3e |  | 27 | 57 |
| 3 | 3f |  | 49 | 41 |
| 4 | 3g |  | 0 | - |
| 5 | 3h |  | 12 | 58 |
| 6 | 3i |  | 28 | 37 |
| 7 | 3j |  | 22 | 43 |
| 8 | 3k |  | 27 | 44 |

| | | | | |
|----|-----------|---|-----------------|----|
| 9 | 3l |  | 37 | 35 |
| 10 | 3m |  | 38 | 43 |
| 11 | 3n |  | 33 | 38 |
| 12 | 3o |  | 44 ^a | 36 |
| 13 | 3p |  | 33 | 46 |
| 14 | 3q |  | 48 ^a | 14 |
| 15 | 3r |  | 4 | 15 |

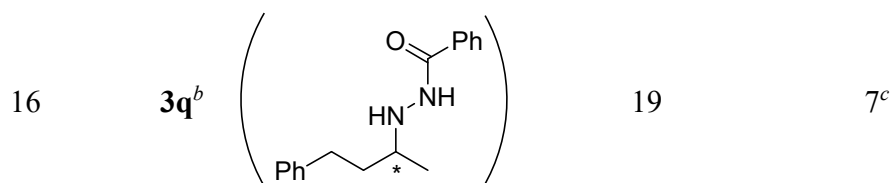
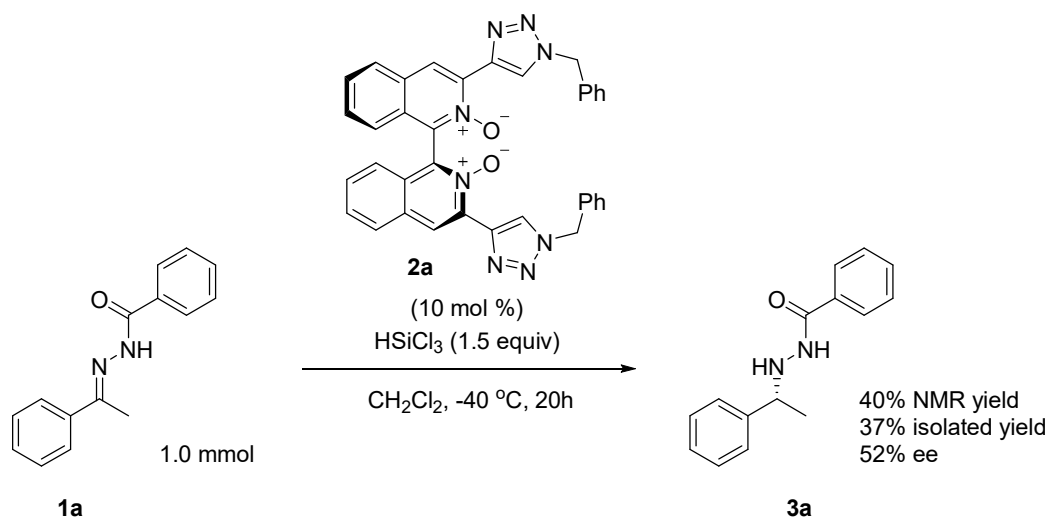


Table 5. Hydrosilylation of benzoyl hydrazones with optimized reaction parameters. All entries were carried out with 0.25 mmol hydrazones. Unless otherwise noted, yields were determined by ¹H NMR using 1,1,2,2-tetrachloroethane as standard. a) isolated yields. b) produced along with **3r in entry 15. c) estimated value based on HPLC; see experimental section for details.**

1.3.2 Attempt with Higher Scale

Considering all the testing above, hydrazone **1a** was determined to be the model substrate. We then went ahead tested to see if this reaction has the potential to be scaled up. With 1.0 mmol (scaled up from 0.25 mmol earlier) of **1a** under optimized reaction conditions, we were glad to see that the reactivity and selectivity of the outcome remained mostly unaffected (Scheme 6). After the reaction was completed, we were able to recover catalyst **2a** with a simple silica gel column chromatography, and the recovered catalyst was able retain its catalytic performance in the same reactions.



Scheme 6. The 1.0 mmol scale reaction with model substrate under optimized reaction condition.

1.3.3 Structural Analysis of the Reducing Species

It is believed that the actual active reducing species that controls the enantioselectivity in asymmetric catalytic hydrosilylation is the intermediate structure generated from the chiral catalyst and HSiCl_3 . There are two possible diastereomeric complexes that can be formed from C_2 -symmetric **2a** and HSiCl_3 if **2a** acts as a bidentate Lewis base. These two possible structures were investigated computationally using the PBEh-3c//C-PCM(DCM) method. First, the bidentate nature of **2a** was confirmed as its two oxygen atoms were able to bind to the silicon

center of HSiCl_3 . Also, this calculation showed that complex 1 has its energy 1.91 kcal/mol lower than complex 2. Through their space-filling models (Figure 6, right side), we were able to identify the anion- π -type interaction of HSiCl_3 's chlorine and hydrogen atoms with the two phenyls on catalyst's triazolyl groups for complex 1. For complex 2, HSiCl_3 has its two chlorine atoms being a part of these interactions. Although complex 1 is generated more due to lower energy, the hydrogen atom of HSiCl_3 is not very accessible by hydrazone, making us believe that complex 2 is more likely the major reducing agent [47,48].

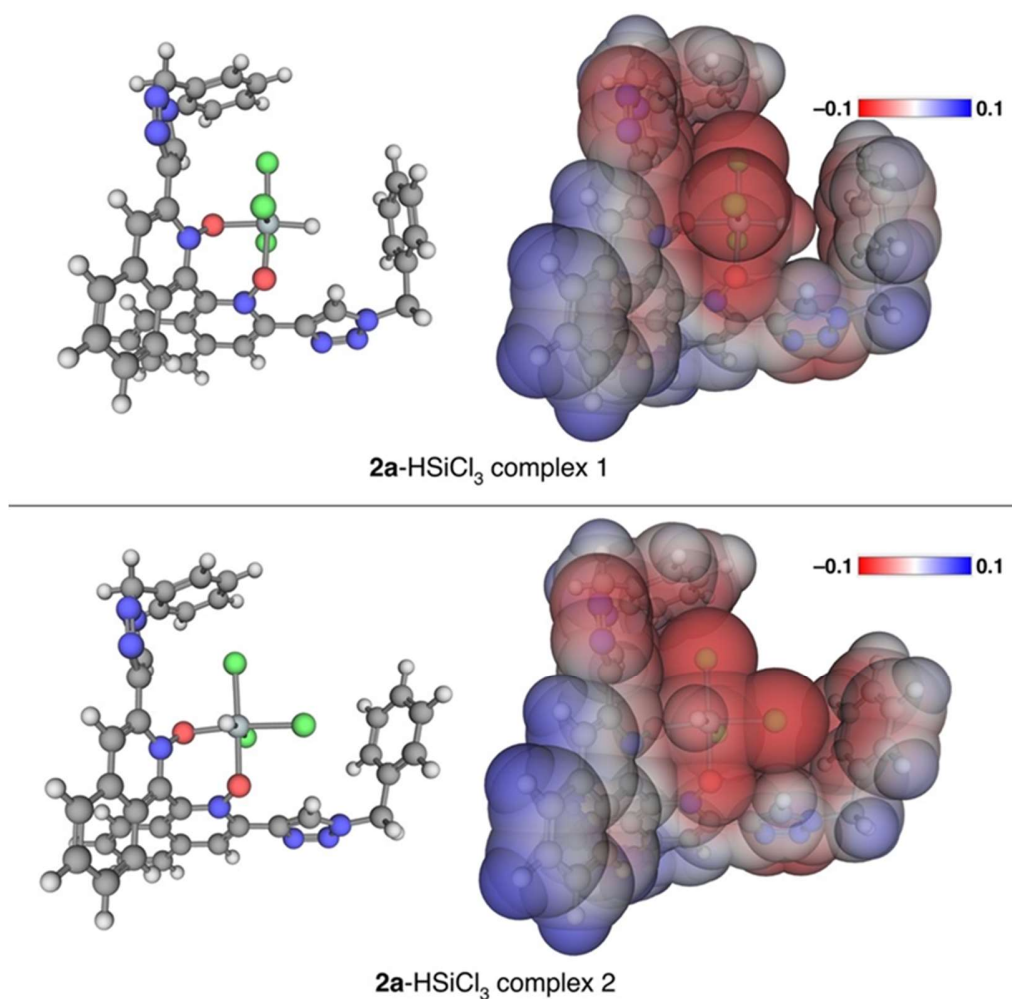


Figure 6. Computed structures of the two lowest energy minima for 2a-HSiCl₃ complex (i.e., two diastereomeric complexes) calculated with PBEh-3c//C-PCM(DCM). Both are shown with balls-and-sticks (left) and space filling (right) models. Molecular electrostatic potentials are also shown in the space filling models. The complex 1 (top) is 1.91 kcal/mol lower in energy than the complex 2 (bottom).

1.4 Conclusion

Based on our study, axial-chiral 3,3'-triazolyl biisoquinoline *N,N'*-dioxides have great potential to be a set of efficient catalysts for asymmetric transfer hydrogenation of acyl hydrazones with trichlorosilane. In this work, we showcased its capability of activating various hydrazone substrates in asymmetric hydrosilylation reactions. From the reaction condition optimization process, it was clear that the reactivity and enantioselectivity of the reactions are influenced by the catalyst's triazolyl units, which our modular synthesis enables easy access to diverse 3,3'-triazolyl biisoquinoline *N,N'*-dioxides.

1.5 Experimental Section

1.5.1 General Information

All reactions were carried out in oven- or flame-dried glassware under an atmosphere of dry argon or nitrogen unless otherwise noted. Except as otherwise indicated, all reactions were magnetically stirred and monitored by analytical thin-layer chromatography using SiliCycle[®] Inc. and EMD Millipore pre-coated silica gel plates with F₂₅₄ indicator. Visualization was accomplished by UV light (254 nm) with combination of potassium permanganate. Flash column chromatography was performed according to the method of Still [49] using silica gel 60 (mesh 230-400) supplied by SiliCycle[®] Inc. Yields refer to chromatographically and spectroscopically pure compounds, unless otherwise stated.

Commercial grade reagents and solvents were purchased from Sigma-Aldrich, Alfa-Aesar, Acros, Fisher, TCI, and VWR, and were used as received without further purification except as indicated below. Trichlorosilane was distilled over calcium hydride under an atmosphere of dry nitrogen prior to use.

Dichloromethane, chloroform, and acetonitrile were freshly distilled over calcium hydride under an atmosphere of dry nitrogen prior to use. Tetrahydrofuran was

freshly distilled over sodium and benzophenone under an atmosphere of dry nitrogen prior to use.

All ^1H NMR and ^{13}C NMR spectra were obtained using a Bruker 400 Ultrashield or an Oxford AS400 Spectrometer (^1H 400 MHz, ^{13}C 100 MHz) at ambient temperature in CDCl_3 purchased from Cambridge Isotope Laboratories, Inc. Chemical shifts in ^1H NMR spectra are reported in parts per million (ppm) relative to tetramethylsilane (δ 0.00 ppm) unless otherwise noted. The proton spectra are reported as follows δ (multiplicity, coupling constant J , number of protons). Multiplicities are indicated by s (singlet), d (doublet), t (triplet), q (quartet), m (multiplet), and br (broad). Chemical shifts in ^{13}C NMR spectra are reported in ppm relative to CDCl_3 (δ 77.0 ppm). All ^{13}C NMR spectra were recorded with complete proton decoupling. Infrared (IR) spectra were recorded using a Nicolet iS5 FT-IR instrument. MS data were obtained using an Agilent 6100 Quadrupole LC/MS. HRMS data were obtained at USF Mass Spec and Peptide Core Facility in the Department of Chemistry at the University of South Florida. Optical rotations were measured using a Jasco P2000 Polarimeter at 589 nm and were reported as $[\alpha]_{\text{D}}^{T\text{ }^\circ\text{C}}$, where C is reported in g/mL.

1.5.2 Experimental Procedures

Preparation of Hydrazones:

All hydrazones were prepared accordingly to the reported procedure [21].

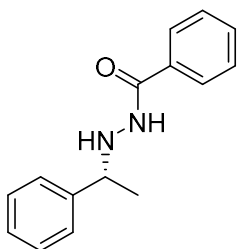
Preparation of Catalysts:

Catalysts **2a-d** were prepared according to our published procedure [44].

Catalysts **2e, f** were prepared according to our published procedure [50].

Representative Procedure for Catalytic Asymmetric Transfer Hydrogenation with Trichlorosilane:

(*R*)-*N'*-(1-Phenylethyl)benzohydrazide (**3a**):



A flame-dried test tube with a magnetic stir bar was charged with hydrazone **1a** (60 mg, 0.25 mmol), catalyst **2a** (15 mg, 0.025 mmol) and CH₂Cl₂ (1.0 mL), cooled to –50 °C, and then treated slowly with a solution of HSiCl₃ in CH₂Cl₂ (250 µL, 1.5 M). The reaction mixture was stirred at –40 °C for 20 hours, and then quenched by pouring it into 30 mL of saturated aqueous NaHCO₃ solution cooled to 0 °C. The resulting mixture was vigorously stirred for 30 min at room temperature and extracted twice with 15 mL of CH₂Cl₂. The combined organic layers were dried over Na₂SO₄, filtered, and condensed *in vacuo*. A ¹H NMR spectrum of the crude reaction mixture was taken with 1,1,2,2-tetrachloroethane as an internal standard (48% NMR yield). A fraction of the crude mixture was purified by prep TLC using 20% EtOAc in CH₂Cl₂ as an eluent for characterization purposes.

All spectral data were consistent with the literature values [21].

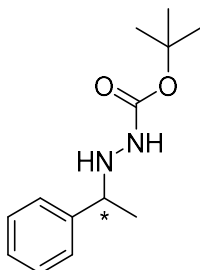
¹H NMR (400 MHz, CDCl₃) δ 7.63-7.60 (m, 2H), 7.50-7.46 (m, 1H), 7.42-7.34 (m, 7H), 7.32-7.27 (m, 1H), 5.10 (br d, *J* = 4.8 Hz, 1H), 4.26 (q, *J* = 6.8 Hz, 1H), 1.44 (d, *J* = 6.8 Hz, 3H).

ee = 53 %; [α]_D²² = +7.4 (*c* = 0.00067, CH₂Cl₂); The enantiomeric excess and the absolute stereochemistry were determined by HPLC analysis [21]: *t_R* (major) = 19.95 min; *t_R* (minor) = 29.01 min (Daicel Chiralcel[®] OJ-H with an OJ-H guard column, hexane/2-propanol = 90:10, 0.5mL/min).

The 1.0 mmol scale reaction:

A flame-dried Schlenk tube with a magnetic stir bar was charged with hydrazone **1a** (238 mg, 1.00 mmol), catalyst **2a** (60 mg, 0.10 mmol) and CH₂Cl₂ (4.0 mL), cooled to –50 °C, and then treated slowly with a solution of HSiCl₃ in CH₂Cl₂ (1.0 mL, 1.5 M). The reaction mixture was stirred at –40 °C for 20 hours, and then quenched by pouring it into 120 mL of saturated aqueous NaHCO₃ solution cooled to 0 °C. The resulting mixture was vigorously stirred for 30 min. at room temperature and extracted twice with 60 mL of CH₂Cl₂. The combined organic layers were dried over Na₂SO₄, filtered, and condensed *in vacuo*. A ¹H NMR spectrum of the crude reaction mixture was taken with 1,1,2,2-tetrachloroethane as an internal standard (40% NMR yield). The crude material was purified by flash column chromatography on silica gel with 2% Et₂O in CH₂Cl₂ to afford the title compound as a white solid (90 mg, 37%), followed by 50% EtOAc in CH₂Cl₂ to recover catalyst **2a** (60 mg, >99%).

(+)-*tert*-Butyl 2-(1-phenylethyl)hydrazinecarboxylate (3b):



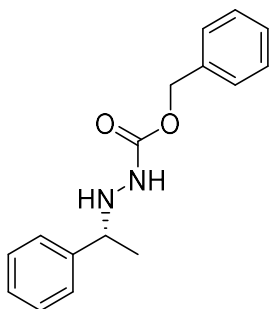
A ^1H NMR spectrum of the crude reaction mixture was taken with 1,1,2,2-tetrachloroethane as an internal standard (36% NMR yield). A fraction of the crude mixture was purified by prep TLC using 5% EtOAc in CH_2Cl_2 as an eluent for characterization purposes.

All spectral data were consistent with the literature values [9].

^1H NMR (400 MHz, CDCl_3) δ 7.35-7.26 (m, 5H), 5.97 (br s, 1H), 4.18 (br s, 2H), 1.44 (s, 9H), 1.33 (d, $J = 6.8$ Hz, 3H).

ee = approximately 71 %; $[\alpha]^{23}_{\text{D}} = +39.3$ ($c = 0.00067$, CH_2Cl_2); The enantiomeric excess was estimated by HPLC analysis as both enantiomers were not fully separated at the base line: t_R (major) = 20.63 min; t_R (minor) = 17.25 min (Daicel Chiralcel[®] OJ-H with an OJ-H guard column, hexane/2-propanol = 99:1, 0.5mL/min).

(*R*)-Benzyl-2-(1-phenylethyl)hydrazine-1-carboxylate (3c):



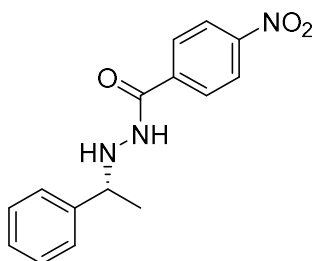
A ^1H NMR spectrum of the crude reaction mixture was taken with 1,1,2,2-tetrachloroethane as an internal standard (21% NMR yield). A fraction of the crude mixture was purified by prep TLC using 5% EtOAc in CH_2Cl_2 as an eluent for characterization purposes.

All spectral data were consistent with the literature values [18].

^1H NMR (400 MHz, CDCl_3) δ 7.35-7.27 (m, 10H), 6.13 (br s, 1H), 5.12 (s, 2H), 4.21 (br s, 2H), 1.34 (d, $J = 6.4$ Hz, 3H).

ee = 64 %; $[\alpha]_D^{23} = +60.4$ ($c = 0.00067$, CH_2Cl_2); The enantiomeric excess and the absolute stereochemistry were determined by HPLC analysis [18]: t_R (major) = 43.57 min; t_R (minor) = 33.45 min (Daicel Chiralcel[®] OJ-H with an OJ-H guard column, hexane/2-propanol = 90:10, 0.5 mL/min).

(*R*)-1-Phenyl-1-(2-*p*-nitrobenzoylhydrazino)ethane (3d):



A ^1H NMR spectrum of the crude reaction mixture was taken with 1,1,2,2-tetrachloroethane as an internal standard (14% NMR yield). A fraction of the crude mixture was purified by prep TLC using 20% EtOAc in CH_2Cl_2 as an eluent for characterization purposes.

^1H NMR (400 MHz, CDCl_3) δ 8.24 (d, J = 8.8 Hz, 2H), 7.77 (d, J = 8.8 Hz, 2H), 7.54 (d, J = 5.6 Hz, 1H), 7.41-7.29 (m, 5H), 5.11 (br d, J = 4.8 Hz, 1H), 4.26 (q, J = 6.4 Hz, 1H), 1.45 (d, J = 6.4 Hz, 3H).

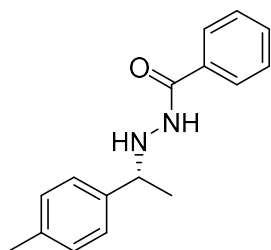
^{13}C NMR (100 MHz, CDCl_3) δ 165.2, 149.8, 142.7, 138.5, 128.7, 128.1, 127.8, 127.2, 123.9, 60.1, 21.3.

IR (thin film): 3276, 2973, 1642, 1522, 1343, 867, 848, 760, 715, 699 cm^{-1}

HRMS (ESI): Exact mass calculated for $\text{C}_{15}\text{H}_{16}\text{N}_3\text{O}_3^+$ $[\text{M}+\text{H}]^+$ expected: 286.1186, found: 286.1188.

ee = 69 %; $[\alpha]_D^{23} = +84.9$ (c = 0.00067, CH₂Cl₂); The enantiomeric excess and the absolute stereochemistry were determined by HPLC analysis [11]: t_R (major) = 57.56 min; t_R (minor) = 51.44 min (Daicel Chiralcel® OJ-H with an OJ-H guard column, hexane/2-propanol = 90:10, 0.5 mL/min).

(*R*)-*N'*-(1-(*p*-Tolyl)ethyl)benzohydrazide (3e):



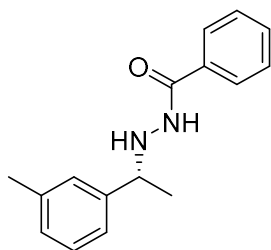
A ¹H NMR spectrum of the crude reaction mixture was taken with 1,1,2,2-tetrachloroethane as an internal standard (27% NMR yield). A fraction of the crude mixture was purified by prep TLC using 20% EtOAc in CH₂Cl₂ as an eluent for characterization purposes.

All spectral data were consistent with the literature values [21].

¹H NMR (400 MHz, CDCl₃) δ 7.64-7.61 (m, 2H), 7.51-7.47 (m, 1H), 7.41-7.38 (m, 3H), 7.30 (d, *J* = 8.0 Hz, 2H), 7.17 (d, *J* = 8.0 Hz, 2H), 5.09 (b rs, 1H), 4.23 (q, *J* = 6.8 Hz, 1H), 2.36 (s, 3H), 1.42 (d, *J* = 6.8 Hz, 3H).

ee = 57 %; $[\alpha]_D^{23} = +8.5$ (c = 0.00067, CH₂Cl₂); The enantiomeric excess and the absolute stereochemistry were determined by HPLC analysis [21]: t_R (major) = 17.27 min; t_R (minor) = 31.13 min (Daicel Chiralcel® OJ-H with an OJ-H guard column, hexane/2-propanol = 90:10, 0.5 mL/min).

(*R*)-*N'*-(1-(*m*-Tolyl)ethyl)benzohydrazide (3f):



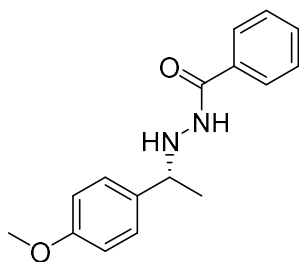
A ¹H NMR spectrum of the crude reaction mixture was taken with 1,1,2,2-tetrachloroethane as an internal standard (49% NMR yield). A fraction of the crude mixture was purified by prep TLC using 20% EtOAc in CH₂Cl₂ as an eluent for characterization purposes.

All spectral data were consistent with the literature values [21].

¹H NMR (400 MHz, CDCl₃) δ 7.63 (d, *J* = 7.2 Hz, 2H), 7.51-7.38 (m, 4H), 7.26-7.19 (m, 3H), 7.11 (d, *J* = 7.2 Hz, 1H), 5.10 (br s, 1H), 4.22 (q, *J* = 6.8 Hz, 1H), 2.36 (s, 3H), 1.43 (d, *J* = 6.8 Hz, 3H).

ee = 41 %; $[\alpha]_D^{22} = +29.0$ (c = 0.0013, CH₂Cl₂); The enantiomeric excess and the absolute stereochemistry were determined by HPLC analysis [21]: t_R (major) = 25.65 min; t_R (minor) = 29.36 min (Daicel Chiralcel® OJ-H with an OJ-H guard column, hexane/2-propanol = 95:5, 0.5 mL/min).

(*R*)-*N'*-(1-(4-Methoxyphenyl)ethyl)benzohydrazide (3h):



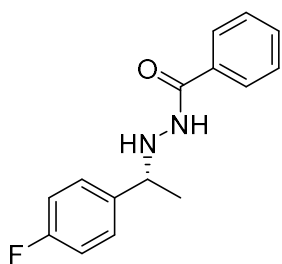
A ¹H NMR spectrum of the crude reaction mixture was taken with 1,1,2,2-tetrachloroethane as an internal standard (12% NMR yield). A fraction of the crude mixture was purified by prep TLC using 20% EtOAc in CH₂Cl₂ as an eluent for characterization purposes.

All spectral data were consistent with the literature values [21].

¹H NMR (400 MHz, CDCl₃) δ 7.64-7.61 (m, 2H), 7.51-7.47 (m, 1H), 7.42-7.38 (m, 3H), 7.34-7.31 (m, 2H), 6.91-6.88 (m, 2H), 5.08 (br s, 1H), 4.22 (q, *J* = 6.8 Hz, 1H), 3.82 (s, 3H), 1.42 (d, *J* = 6.8 Hz, 3H).

ee = 58 %; $[\alpha]_D^{22} = +23.8$ (c = 0.0013, CH₂Cl₂); The enantiomeric excess and the absolute stereochemistry were determined by HPLC analysis [21]: t_R (major) = 35.59 min; t_R (minor) = 59.24 min (Daicel Chiralcel® OJ-H with an OJ-H guard column, hexane/2-propanol = 90:10, 0.5 mL/min).

(*R*)-*N'*-(1-(4-Fluorophenyl)ethyl)benzohydrazide (3i):



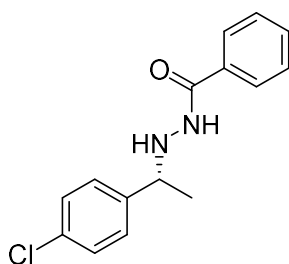
A ¹H NMR spectrum of the crude reaction mixture was taken with 1,1,2,2-tetrachloroethane as an internal standard (28% NMR yield). A fraction of the crude mixture was purified by prep TLC using 20% EtOAc in CH₂Cl₂ as an eluent for characterization purposes.

All spectral data were consistent with the literature values [21].

¹H NMR (400 MHz, CDCl₃) δ 7.63-7.61 (m, 2H), 7.52-7.35 (m, 6H), 7.04 (dd, J = 8.4, 8.4 Hz, 2H), 5.06 (br s, 1H), 4.26 (q, J = 6.8 Hz, 1H), 1.41 (d, J = 6.8 Hz, 3H).

ee = 37 %; $[\alpha]_D^{23} = +3.4$ (c = 0.00067, CH₂Cl₂); The enantiomeric excess and the absolute stereochemistry were determined by HPLC analysis [21]: t_R (major) = 21.37 min; t_R (minor) = 27.53 min (Daicel Chiralcel® OJ-H with an OJ-H guard column, hexane/2-propanol = 90:10, 0.5 mL/min).

(*R*)-*N'*-(1-(4-Chlorophenyl)ethyl)benzohydrazide (3j):



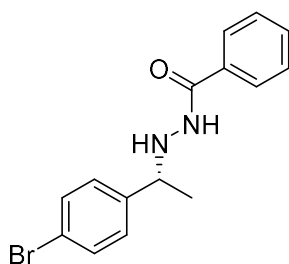
A ¹H NMR spectrum of the crude reaction mixture was taken with 1,1,2,2-tetrachloroethane as an internal standard (22% NMR yield). A fraction of the crude mixture was purified by prep TLC using 20% EtOAc in CH₂Cl₂ as an eluent for characterization purposes.

All spectral data were consistent with the literature values [21].

¹H NMR (400 MHz, CDCl₃) δ 7.62 (d, *J* = 7.2 Hz, 2H), 7.52-7.48 (m, 1H), 7.42-7.29 (m, 7H), 5.05 (br d, *J* = 4.8 Hz, 1H), 4.27-4.23 (m, 1H), 1.41 (d, *J* = 6.4 Hz, 3H).

ee = 43 %; $[\alpha]_D^{23} = +50.4$ (c = 0.00067, CH₂Cl₂); The enantiomeric excess and the absolute stereochemistry were determined by HPLC analysis [21]: t_R (major) = 20.97 min; t_R (minor) = 26.49 min (Daicel Chiralcel® OJ-H with an OJ-H guard column, hexane/2-propanol = 90:10, 0.5 mL/min).

(*R*)-*N'*-(1-(4-Bromophenyl)ethyl)benzohydrazide (3k):



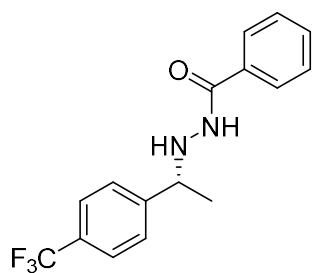
A ¹H NMR spectrum of the crude reaction mixture was taken with 1,1,2,2-tetrachloroethane as an internal standard (27% NMR yield). A fraction of the crude mixture was purified by prep TLC using 20% EtOAc in CH₂Cl₂ as an eluent for characterization purposes.

All spectral data were consistent with the literature values [21].

¹H NMR (400 MHz, CDCl₃) δ 7.62 (d, *J* = 7.6 Hz, 2H), 7.52-7.39 (m, 6H), 7.29 (d, *J* = 8.4 Hz, 2H), 5.06 (br s, 1H), 4.24 (q, *J* = 6.4 Hz, 1H), 1.40 (d, *J* = 6.4 Hz, 3H).

ee = 44 %; $[\alpha]_D^{23} = +50.7$ (c = 0.002, CH₂Cl₂); The enantiomeric excess and the absolute stereochemistry were determined by HPLC analysis [21]: t_R (major) = 23.36 min; t_R (minor) = 29.21 min (Daicel Chiralcel® OJ-H with an OJ-H guard column, hexane/2-propanol = 90:10, 0.5 mL/min).

(*R*)-*N'*-(1-(4-(Trifluoromethyl)phenyl)ethyl)benzohydrazide (3l):



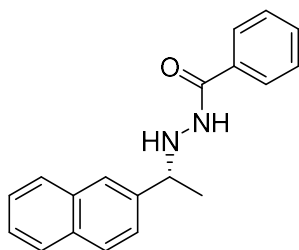
A ¹H NMR spectrum of the crude reaction mixture was taken with 1,1,2,2-tetrachloroethane as an internal standard (37% NMR yield). A fraction of the crude mixture was purified by prep TLC using 20% EtOAc in CH₂Cl₂ as an eluent for characterization purposes.

All spectral data were consistent with the literature values [21].

¹H NMR (400 MHz, CDCl₃) δ 7.63-7.61 (m, 4H), 7.53 (d, *J* = 8.0 Hz, 2H), 7.51-7.48 (m, 1H), 7.42-7.38 (m, 3H), 5.07 (br d, *J* = 6.8 Hz, 1H), 4.37-4.32 (m, 1H), 1.44 (d, *J* = 6.8 Hz, 3H).

ee = 35 %; $[\alpha]_D^{23} = +56.1$ (c = 0.00067, CH₂Cl₂); The enantiomeric excess and the absolute stereochemistry were determined by HPLC analysis [18]: t_R (major) = 28.48 min; t_R (minor) = 25.77 min (Daicel Chiralcel® AS-H with an AS-H guard column, hexane/2-propanol = 80:20, 0.5 mL/min).

(*R*)-*N'*-(1-(Naphthalen-2-yl)ethyl)benzohydrazide (3m):



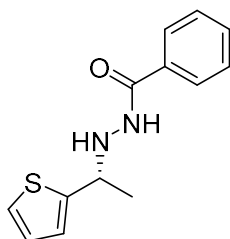
A ¹H NMR spectrum of the crude reaction mixture was taken with 1,1,2,2-tetrachloroethane as an internal standard (38% NMR yield). A fraction of the crude mixture was purified by prep TLC using 20% EtOAc in CH₂Cl₂ as an eluent for characterization purposes.

All spectral data were consistent with the literature values [15].

¹H NMR (400 MHz, CDCl₃) δ 7.87-7.81 (m, 4H), 7.61-7.56 (m, 3H), 7.50-7.44 (m, 4H), 7.37-7.34 (m, 2H), 5.19 (br d, *J* = 5.2 Hz, 1H), 4.43 (q, *J* = 6.8 Hz, 1H), 1.51 (d, *J* = 6.8 Hz, 3H).

ee = 43 %; $[\alpha]^{23}_D = +82.4$ (c = 0.00067, CH₂Cl₂); The enantiomeric excess and the absolute stereochemistry were determined by HPLC analysis [15]: t_R (major) = 36.05 min; t_R (minor) = 43.91 min (Daicel Chiralcel® OJ-H with an OJ-H guard column, hexane/2-propanol = 85:15, 0.5 mL/min).

(*R*)-*N'*-(1-(Thiophen-2-yl)ethyl)benzohydrazide (3n):



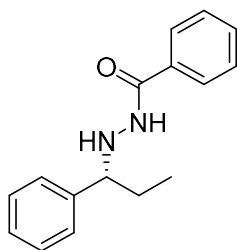
A ¹H NMR spectrum of the crude reaction mixture was taken with 1,1,2,2-tetrachloroethane as an internal standard (33% NMR yield). A fraction of the crude mixture was purified by prep TLC using 20% EtOAc in CH₂Cl₂ as an eluent for characterization purposes.

All spectral data were consistent with the literature values [21].

¹H NMR (400 MHz, CDCl₃) δ 7.67 (d, *J* = 7.2 Hz, 2H), 7.53-7.49 (m, 2H), 7.44-7.40 (m, 2H), 7.28-7.26 (m, 1H), 7.00-6.97 (m, 2H), 5.14 (br d, *J* = 4.8 Hz, 1H), 4.60-4.56 (m, 1H), 1.53 (d, *J* = 6.8 Hz, 3H).

ee = 38 %; $[\alpha]_D^{23} = +32.5$ (c = 0.001, CH₂Cl₂); The enantiomeric excess and the absolute stereochemistry were determined by HPLC analysis [21]: t_R (major) = 26.72 min; t_R (minor) = 32.39 min (Daicel Chiralcel® OJ-H with an OJ-H guard column, hexane/2-propanol = 90:10, 0.5 mL/min).

(*R*)-*N'*-(1-Phenylpropyl)benzohydrazide (3o):



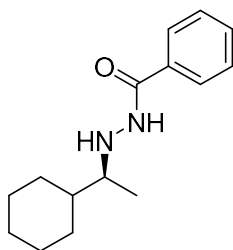
A ¹H NMR spectrum of the crude reaction mixture was taken with 1,1,2,2-tetrachloroethane as an internal standard (44% NMR yield). A fraction of the crude mixture was purified by prep TLC using 20% EtOAc in CH₂Cl₂ as an eluent for characterization purposes.

All spectral data were consistent with the literature values [18].

¹H NMR (400 MHz, CDCl₃) δ 7.60-7.58 (m, 2H), 7.49-7.46 (m, 1H), 7.40-7.33 (m, 7H), 7.32-7.27 (m, 1H), 5.18 (br d, *J* = 5.6 Hz, 1H), 4.00 (br dd, *J* = 6.8, 7.2 Hz, 1H), 1.94-1.83 (m, 1H), 1.77-1.66 (m, 1H), 0.87 (t, *J* = 7.6 Hz, 3H).

ee = 34 %; $[\alpha]_D^{23} = +37.2$ (c = 0.0013, CH₂Cl₂); The enantiomeric excess and the absolute stereochemistry were determined by HPLC analysis [18]: t_R (major) = 16.28 min; t_R (minor) = 19.15 min (Daicel Chiralcel® OJ-H with an OJ-H guard column, hexane/2-propanol = 90:10, 0.5 mL/min).

(*S*)-*N'*-(1-Cyclohexylethyl)benzohydrazide (3p):



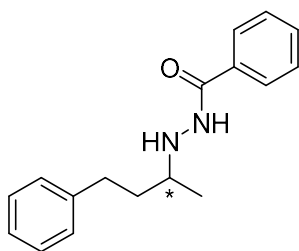
A ¹H NMR spectrum of the crude reaction mixture was taken with 1,1,2,2-tetrachloroethane as an internal standard (33% NMR yield). A fraction of the crude mixture was purified by prep TLC using 20% EtOAc in CH₂Cl₂ as an eluent for characterization purposes.

All spectral data were consistent with the literature values [19].

¹H NMR (400 MHz, CDCl₃) δ 7.76-7.74 (m, 2H), 7.54-7.43 (m, 4H), 4.89 (br s, 1H), 2.94-2.88 (m, 1H), 1.78-1.67 (m, 6H), 1.47-1.40 (m, 1H), 1.31-1.09 (m, 4H), 1.06 (d, *J* = 6.4 Hz, 3H).

ee = approximately 52 %; $[\alpha]^{21}_{\text{D}} = +4.1$ ($c = 0.001$, CH_2Cl_2); The enantiomeric excess was estimated by HPLC analysis as both enantiomers were not fully separated at the baseline. The absolute stereochemistry was determined by HPLC analysis[19]: t_R (major) = 41.11 min; t_R (minor) = 46.12 min (Daicel Chiralcel[®] OJ-H with an OJ-H guard column, hexane/2-propanol = 99:1, 0.5 mL/min).

(+)-*N'*-(4-Phenylbutan-2-yl)benzohydrazide (3q):



A ^1H NMR spectrum of the crude reaction mixture was taken with 1,1,2,2-tetrachloroethane as an internal standard (48% NMR yield). A fraction of the crude mixture was purified by prep TLC using 20% EtOAc in CH_2Cl_2 as an eluent for characterization purposes.

^1H NMR (400 MHz, CDCl_3) δ 7.74-7.72 (m, 2H), 7.55-7.43 (m, 4H), 7.31-7.17 (m, 5H), 4.91 (br s, 1H), 3.17-3.12 (m, 1H), 2.80-2.65 (m, 2H), 1.94-1.85 (m, 1H), 1.73-1.61 (m, 1H), 1.18 (d, $J = 6.4$ Hz, 3H).

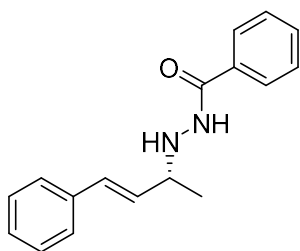
^{13}C NMR (100 MHz, CDCl_3) δ 167.5, 142.1, 132.9, 131.8, 128.7, 128.4, 128.3, 126.8, 125.8, 55.6, 36.7, 32.1, 18.6.

IR (thin film): 3315, 1640, 1539, 1472, 1456, 1377, 905, 894, 854, 729, 696 cm^{-1}

HRMS (ESI): Exact mass calculated for $\text{C}_{17}\text{H}_{21}\text{N}_2\text{O}^+$ $[\text{M}+\text{H}]^+$ expected: 269.1648, found: 269.1652.

ee = 14 %; $[\alpha]_D^{21} = +4.7$ ($c = 0.002$, CH_2Cl_2); The enantiomeric excess was determined by HPLC analysis: t_R (major) = 37.17 min; t_R (minor) = 30.40 min (Daicel Chiralcel[®] OD-H with an OD-H guard column, hexane/2-propanol = 90:10, 0.5 mL/min).

(*R*)-*N'*-(4-Phenyl-3-buten-2-yl)benzohydrazide (3r**):**



A ^1H NMR spectrum of the crude reaction mixture was taken with 1,1,2,2-tetrachloroethane as an internal standard (**3r**: 4% NMR yield; **3q**: 19% NMR yield). A fraction of the crude mixture was purified by prep TLC using 20% EtOAc

in CH₂Cl₂ as an eluent for characterization purposes. Compounds **3r** and **3q** were isolated as an inseparable mixture.

The mixture of **3r** and **3q** was analyzed by LC/MS (ES-APCI): t_R (**3r**) = 31.567 min, calculated for C₁₇H₁₉N₂O⁺ [M+H]⁺ expected: 267.1, found: 267.2; t_R (**3q**) = 31.344 min, calculated for C₁₇H₂₁N₂O⁺ [M+H]⁺ expected: 269.2, found: 269.2 (LC column: Poroshell120-EC-C18 43.0*50 mm, 2.7 μm; 24 °C; H₂O/Methanol=90:10; 0.5 ml/min).

3r : ee = 15 %; The enantiomeric excess and the absolute stereochemistry were determined by HPLC analysis [51]: t_R (major) = 40.47 min; t_R (minor) = 36.56 min (Daicel Chiralcel[®] AD-H with an AD-H guard column, hexane/2-propanol = 92:8, 0.5 mL/min)

3q : ee = 7 %; The enantiomeric excess was determined by HPLC analysis: t_R (major) = 45.25 min; t_R (minor) = 48.99 min (Daicel Chiralcel[®] AD-H with an AD-H guard column, hexane/2-propanol = 92:8, 0.5 mL/min).

1.5.3 Computational Procedures

All calculations have been performed with the Q-Chem 4 quantum chemistry code [52], using the PBEh-3c density functional theory composite procedure [53]. Solvent effects have been included using the C-PCM method with the dielectric constant of DCM ($\epsilon = 9.08$). Minima are converged within a threshold of 10^{-8} E_h, and have been confirmed minima using frequency calculations [54,55]. Molecular symmetry was not used because of the necessity of the C-PCM method. The C_2 symmetry expected for the two main minima (complex 1 and complex 2) is respected in an approximate manner. The initial structures for the geometry optimizations have been obtained via a molecular mechanics based conformational search algorithm, developed in-house. Given the fact that the molecules in this project and the nature of their interaction are well within the limits of recent validation studies of the method that we used, we expect geometries to be converged within 0.05 Å accuracy [56], and energies to be converged within 2 kcal/mol accuracy [57].

Chapter 2

Evaluation of Helicene-Derived 2,2'-Bipyridine *N*-Monoxide Catalyst for the Enantioselective Propargylation of *N*-Acylhydrazones with Allenyltrichlorosilane

2.1 Introduction

2.1.1 Helicene-Derived Catalysts

As asymmetric catalysis has become a powerful approach for synthetic organic chemistry, it is essential to create innovative chiral ligands and catalysts capable of efficiently inducing asymmetry in reactions [58–61]. In recent years, there has been significant advancement in the creation of innovative chiral ligands and catalysts. Among these, helicenes went under the spotlight due to their unique properties, such as the highly distorted screw-shaped structures that can enable multidimensional intermolecular interactions (Figure 7) [62,63].

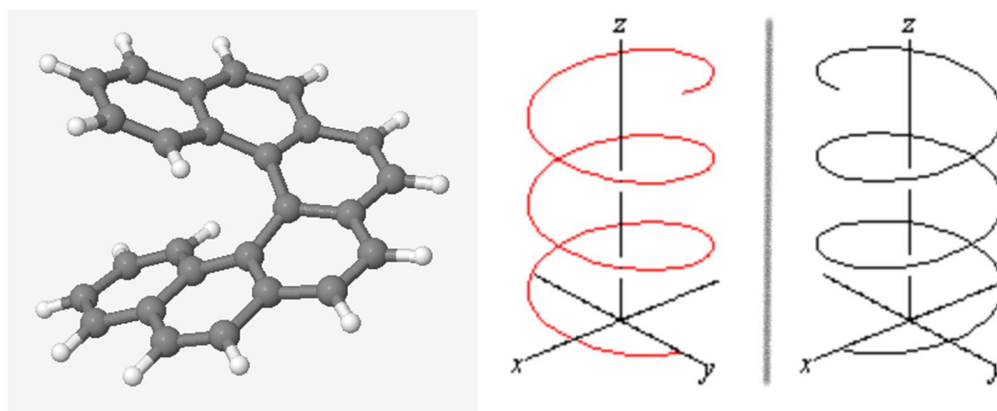


Figure 7. 3-D demonstration of helicene's unique shape with hexahelicene and how helical structure's mirror images embody chiral characteristics.

Despite not having any stereo-genic center, the steric repulsive interaction that exists between the two terminal aromatic rings can still induce chirality. This makes helicene a good candidate for building an enantioselective catalyst.

The history of helicene can be traced all the way back to the beginning of the 20th century when Meisenheimer and Witte synthesized the first two azahelicenes in 1903 (Figure 8, **A** and **B**; [64]). After that, the advancement of helicene chemistry was slowed down for many years until the work of Newman and Lednicer, who reported the first synthesis and resolution of hexahelicene (Figure 8, **C** and **D**; [65]). In 1968, Wynberg successfully synthesized the first enantioenriched heterohelicene when he used an oxidative photocyclization reaction to make the corresponding hexa- and heptahelicenes [66]. These milestones sparked great

interest in making various enantioenriched helicenes and their potential applications[67,68].

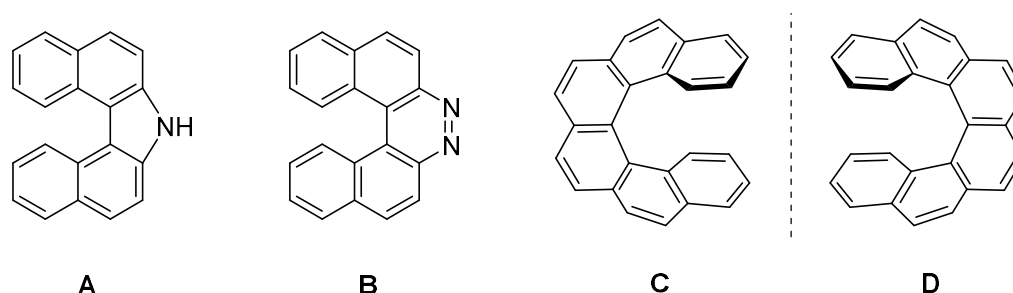


Figure 8. Important examples in the history of helicene chemistry. A and B: first aza[5]helicenes [64]. C and D: first enantioenriched (*M*)- and (*P*)-carbo[6]helicene, respectively [65].

Since the boom of helicene chemistry, many kinds of helicene molecules have been developed since the 1950s, with their functionality heavily investigated. With helicene's intriguing properties, it has already seen many applications in the organocatalysis field as chiral ligands or organocatalysts [69–73]. Among the plethora of examples of helicenes, 1-aza[6]helicene was particularly interesting to our group. As shown in Figure 9, the nitrogen atom in blue is sterically and stereo-electronically hard to access due to its surrounding conjugated π -system. Because this crowded space is formed by a continuously chiral framework, it is an ideal choice to implement the “chiral pocket” design principle for developing chiral

Lewis base catalysts [70,74–76]. With that in mind, our group has been working on crafting a range of chiral catalysts utilizing this azahelicene framework [46,74,76–80].

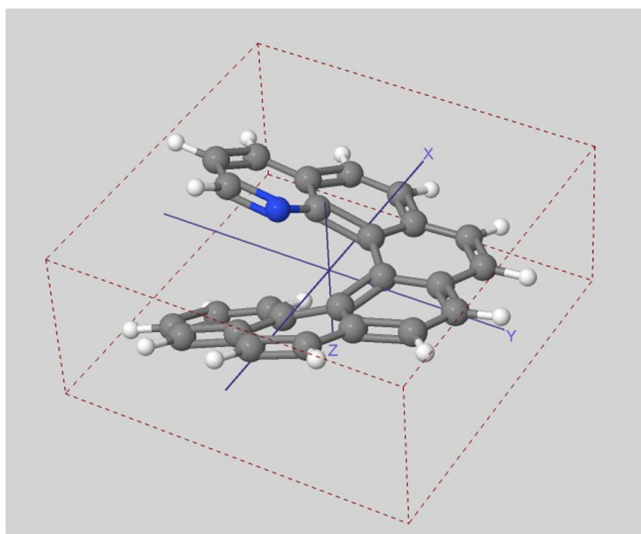


Figure 9. Structure of (*p*)-1-aza[6]helicene in 3-D with its nitrogen atom(blue) screened by its surroundings.

One feasible method to provide enantioselectivity to the reaction using this concept is to entrap reacting substrates near the continuously chiral region with a bidentate motif. By designing catalysts that have two electron donating sites spatially not too far away from each other (Figure 10, left side), it is possible to form the hexa-coordinated silicon complex (Figure 10, right side) that dictates the enantioselective process. We have demonstrated this approach in our earlier studies (including

Chapter 1) with two catalyst classes with different binding mechanisms: the Lewis base catalysts [46,77] and the hydrogen-bond donor catalysts [78,79].

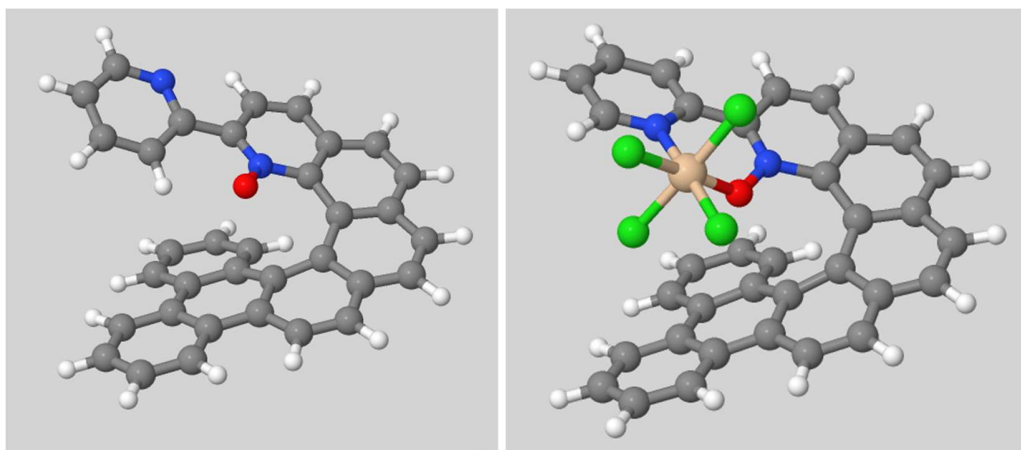
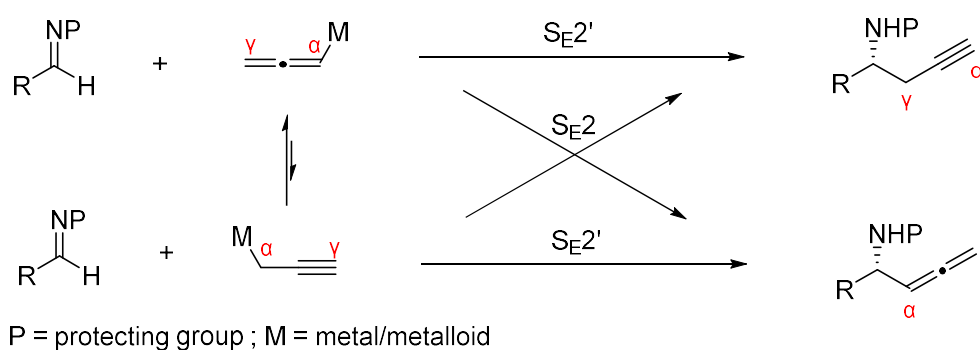


Figure 10. The solid-state structure of helicene-derived 2,2'-bipyridine *N*-monoxide catalyst (left) [77] and its expected complex with allenyltrichlorosilane (right). Blue: nitrogen; red: oxygen; yellow: silicon; green: chlorine or allene.

2.1.2 Enantioselective Propargylation of Imines

Asymmetric propargylation of imines allows for direct access to chiral homopropargylic amines, which are important building blocks used in the synthesis of natural products and medically relevant compounds. Therefore, the development of enantioselective catalytic variants of such motif has been an important goal in

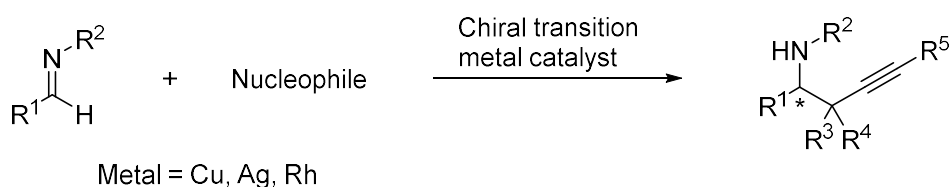
synthetic chemistry. Since the first report of propargylation reaction of carbonyl compounds utilizing organometallic reagents back in 1950s, there have been a plethora of examples of reagents derived from all different kinds of metals. However, due to the nature of propargyl organometallic reagents, they are very likely to rearrange to their corresponding allenic counterpart before the reactions take part, which resulting in a mixture of propargylic and allenic products undergoing either S_E2 or S_E2' mechanism (Scheme 7). Along with other factors such as steric hindrance on the reaction site, nature of the different metals and electrophilicity of the electrophile, the selectivity of propargylation reaction is a difficult challenge [81–89].



Scheme 7. Selectivity issue with a mixture of propargyl and allenic reagents.

With the advancement of asymmetric catalysis nowadays, many recent studies started to use catalytic approaches on asymmetric propargylation for its efficiency

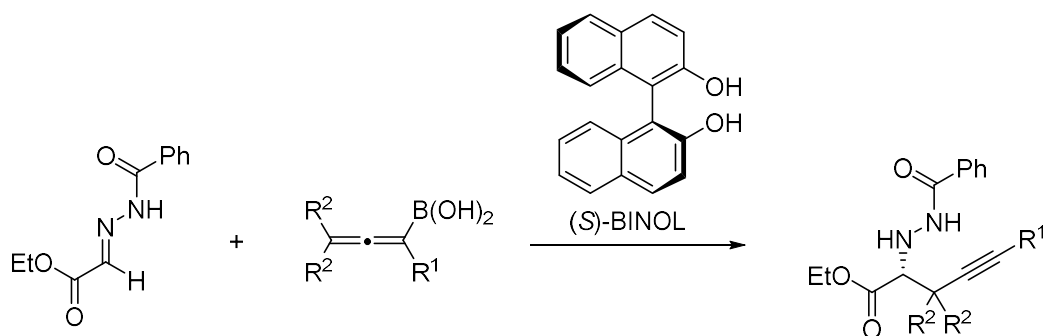
and economic potential. Several notable transition metal-catalyzed methods for the enantioselective catalytic propargylation of imines have been reported (Scheme 8).



Scheme 8. Demonstration of chiral transition metal-catalyzed enantioselective propargylation of imines.

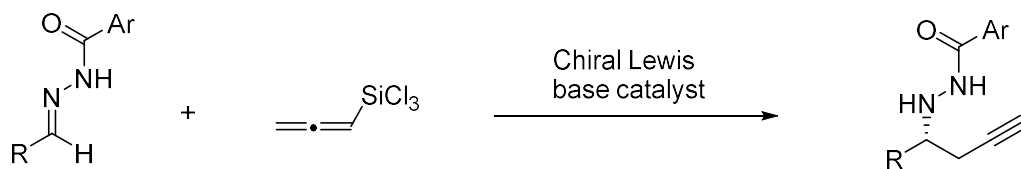
One approach utilized a silver-phosphine complex to catalyze the addition of allenylboronic acid pinacol ester to *N*-tosyl imines [83]. Another utilized a Cu-N-heterocyclic carbene complex to catalyze the addition of allenylboronic acid pinacol ester to *N*-phosphinoyl imines [84]. A third used a copper-phosphine complex to catalyze the addition of propargyl borolane to cyclic aldimines [85]. Other work explored three-reagent reactions consist of *N*-arylimines catalyzed by Rh₂(OAc)₄ and a chiral phosphoric acid [87], as well as *N*-phosphinoyl coupling reactions catalyzed by copper and a phosphine complex [88]. Last but not least, there was one organocatalytic method employing a glyoxylate-derived acylhydrazone catalyzed by (*S*)-BINOL that has also been published [90]. As shown in Scheme 9, when *N*-acylhydrazones is used as the substrate, propargylhydrazine is obtained. With the aforementioned benefits of hydrazine in

the last project, such a method became particularly interesting to us and served as an inspiration to this work.



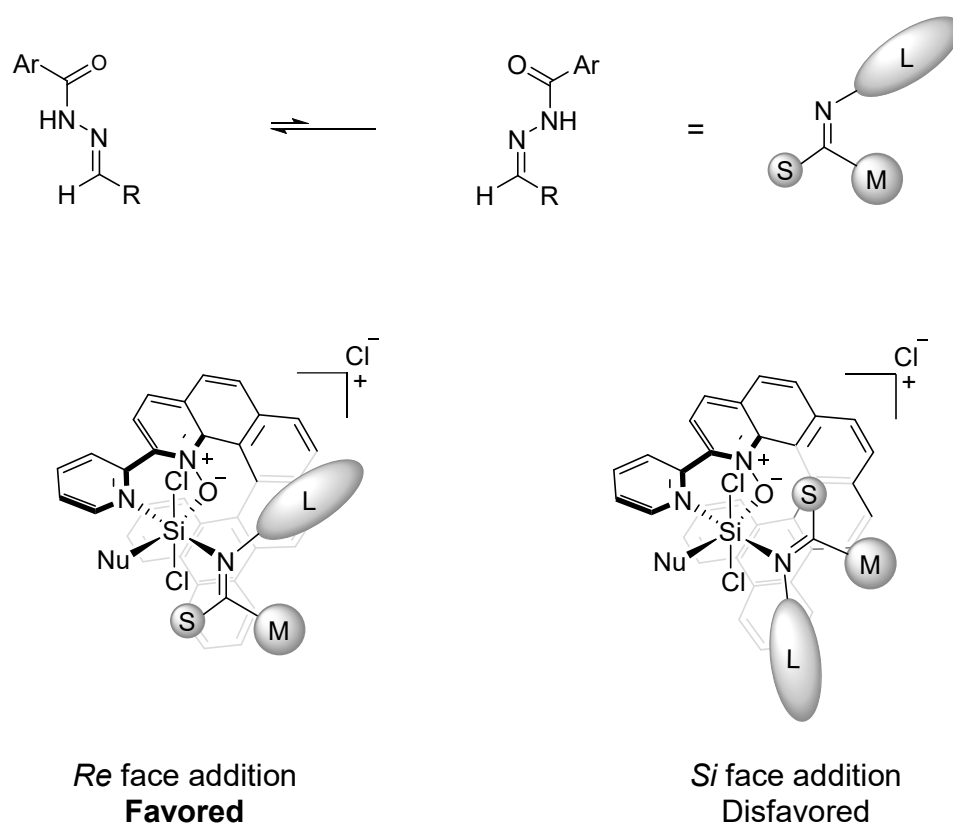
Scheme 9. Organocatalyst catalyst catalyzed propargylation of glyoxylate-derived acylhydrazone with allenylboronic acids [90].

While important discoveries had been made, the number of catalytic methods described in the literature that achieve high enantioselectivity was still somewhat limited as of that point. Considering this, we were interested in evaluating our previous observations that a helicene-derived 2,2'-bipyridine *N*-monoxide catalyst could efficiently catalyze the propargylation of *N*-acylhydrazones with allenyltrichlorosilane (Scheme 10; [77,80]).



Scheme 10. Preliminary experiment of chiral Lewis base-catalyzed propargylation of *N*-acylhydrazones with allenyltrichlorosilane [77,80].

The selectivity of this reaction is proposed to be as shown in Scheme 11, where reaction site is captured in the helicene catalyst's chiral pocket, favoring binding from one side of the electrophile than another.



Scheme 11. Purposed enantioselective intermediate complexes of the investigating catalysis.

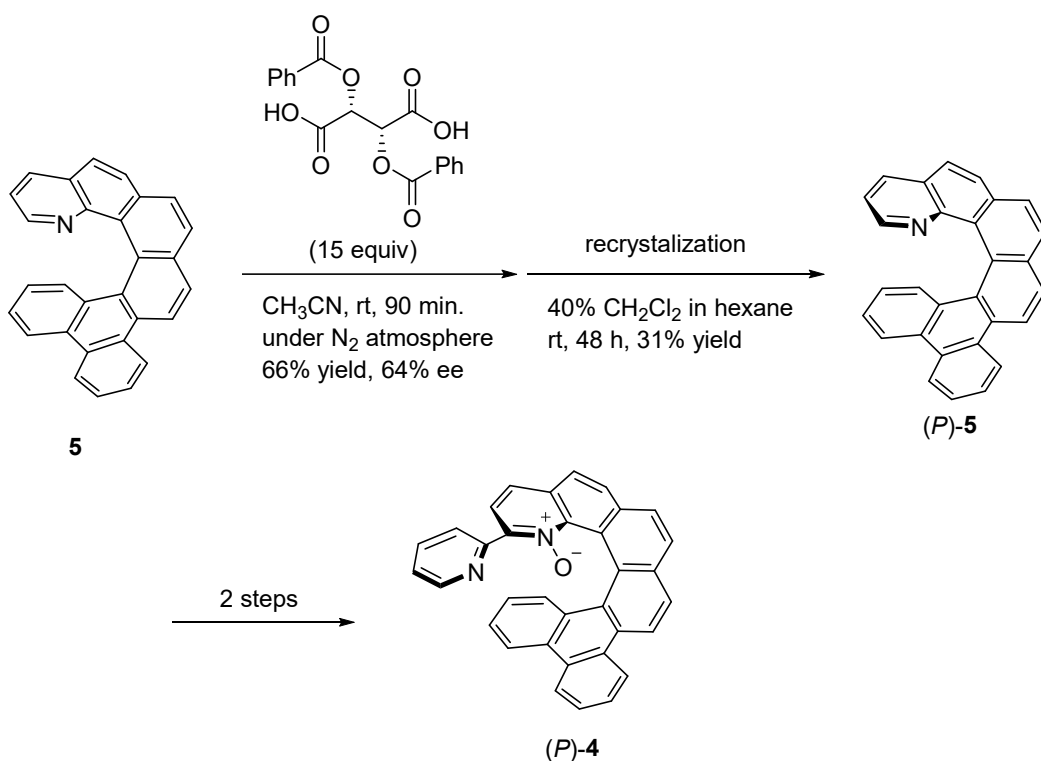
Like trichlorosilane used in our previous project, allenyltrichlorosilane appears as a liquid at room temperature that is readily available and produces non-toxic byproducts like NaCl and SiO₂ upon quenching with NaOH or NaHCO₃. The

hydrazone used, *N*-acylhydrazones, also served as a good starting material for being a C=N electrophile that is easy to handle and bench-stable [91,92].

2.2 Reaction Condition Optimization

2.2.1 Synthesis of Optically Pure Helicene Catalyst

Our research team had previously designed a modular strategy for synthesizing racemic 1-azahelicene derivatives. The enantiomers of these compounds can be separated by semi-preparative chiral high-performance liquid chromatography (HPLC) [76,78]. When preparing this catalyst in its optically pure form for this experiment, we also explored different diastereomeric salts for the resolution process. Through systematic evaluation of various optically pure acids, solvents, and crystallization environments, we determined that (-)-*O,O'*-dibenzoyl-L-tartaric acid in a 15-equivalent ratio with acetonitrile as solvent provided the optimal conditions for resolving helicene **5** via salt-mediated crystallization [93].



Scheme 12. Improved optical resolution process of helicene **5 with salt-mediated crystallization, with 2 more steps to get helicene catalyst (*p*)-**4** [77].**

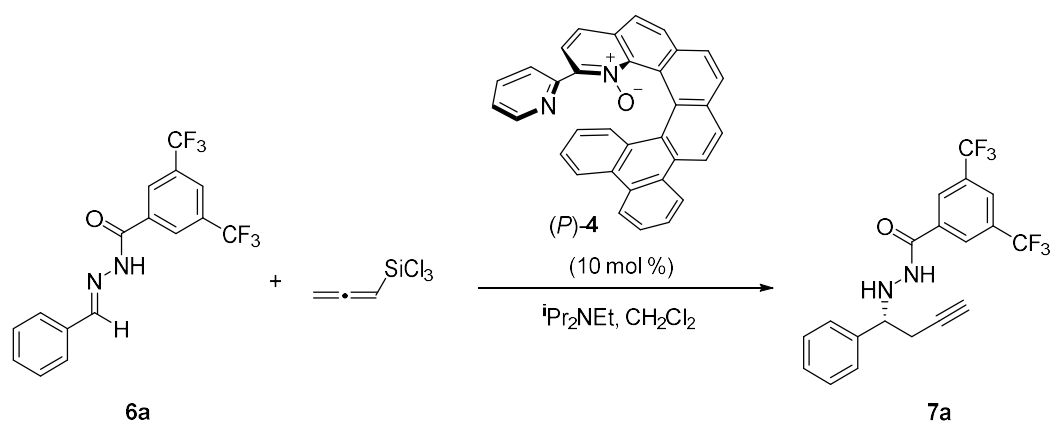
The original optimized procedure involved evaporating acetonitrile under an open-air fume hood to induce precipitation of the enantio-enriched salt. However, it was difficult to reproduce the result using this method during catalyst preparation, for which we speculated that the moisture absorption by acetonitrile during evaporation may be the reason of inconsistency. With that in mind, we first tried to perform the recrystallization under a positive atmosphere with N₂ environment, but

we could not avoid suppressing the evaporation of acetonitrile and selectivity and consistency did not improve. Fortunately, we discovered that simply allowing a room-temperature acetonitrile solution containing (-)-*O,O'*-dibenzoyl-L-tartaric acid and helicene **5** to stir vigorously under a N₂ environment for approximately 20 minutes will promote the precipitation of the enantio-enriched salt, which then led to an effective preparation of optically pure (*p*)-**5** (Scheme 12; [77]). We were pleased to resolve this issue since preparing enantio-enriched 1-aza-helicene type catalysts is known to be very challenging [94,95]. One study from Heller demonstrated a method to prepare enantio-enriched tetrahydro[6]helicenes with up to >99% yield and 64% ee through the enantioselective [2+2+2] cyclotrimerisation of alkynes. However, they can only get 20% yield without any enantioselectivity when applying the same method to the 1-aza[6]helicene counterpart [96].

2.2.2 Basic Reaction Parameters

As mentioned earlier, we had preliminary experiments that showed catalyst **4**'s efficiency when catalyzing enantioselective propargylation of *N*-acylhydrazones with allenyltrichlorosilane. In our observations, we found that the *N*-3,5-bis(trifluoromethyl)benzoylhydrazone (**6a**) is a superior substrate that was more

selective and gave better yield compared to the *N*-benzoylhydrazone counterpart. As the preliminary reaction with **6a** provided 53% yield and 78% ee (entry 1), we set it as the fundamental for the reaction condition optimization (Table 6).



| Entry | Method ^a | iPr ₂ NEt (equiv) | Temp (°C) | Time (h) | Yield (%) ^b | ee (%) |
|----------------|---------------------|------------------------------|-----------|----------|------------------------|------------------|
| 1 ^c | A | 5 | 0 | 12 | 53 ^d | 78 |
| 2 | A | 2 | 0 | 12 | 45 | 42 |
| 3 | A | 10 | 0 | 12 | 43 | 48 |
| 4 ^e | B | 5 | 0 | 20 | 24 | N/D ^f |
| 5 ^e | B | 5 | -40 | 20 | 13 | N/D |
| 6 ^e | B | 5 | -78 | 20 | trace | N/D |
| 7 | B | 5 | -78 | 20 | trace | - |
| 8 | B | 5 | -40 | 20 | 12 | 0 |
| 9 | B | 5 | 0 | 20 | 72 | 86 |

Table 6. Evaluation of the basic reaction parameters. a) **Method A:** neat allenyltrichlorosilane was added to a solution of acylhydrazone, catalyst, iPr₂NEt in CH₂Cl₂ at 0 °C. **Method B:** allenyltrichlorosilane was added as a

CH₂Cl₂ solution to a solution of acylhydrazone, catalyst, and ⁱPr₂NEt in CH₂Cl₂ at -78 °C. b) NMR yield was determined using 1, 1, 2, 2-tetrachloroethane as standard. c) obtained from previous work [77]. d) isolated yield. e) reactions ran without catalyst. f) ee not determined for checking background reactions.

We first tested different amounts of ⁱPr₂NEt for the reaction to see if that has any effect on reaction yield and selectivity. As shown in entries 2 and 3, lower or higher amount of ⁱPr₂NEt negatively affect the reaction outcome, giving 45% yield and 43% yield, respectively. The negative effect on selectivity was more significant, with 42% ee and 48% ee, respectively, compared to 78% ee from entry 1.

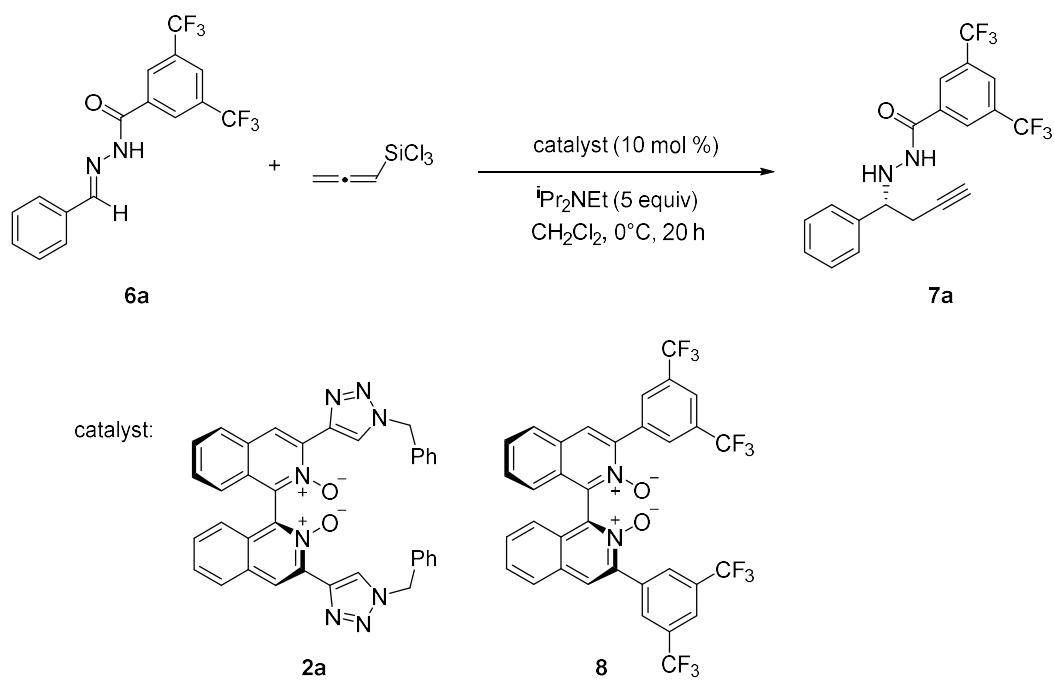
We then proceeded to set up a list of trials to check if there was any background reaction happening. We tested the reaction in 3 different temperatures, 0°C, -40°C and -78°C, without the catalyst (entry 4, 5, 6, respectively). To avoid having neat allenyltrichlorosilane from freezing in low temperature, we added it as a CH₂Cl₂ solution into a solution of *N*-acylhydrazone and ⁱPr₂NEt in CH₂Cl₂ at -78°C (Table 6, method B). In addition, we also let the reactions run longer (from 12 to 20 hours) to offset the presumable lower reactivity. The yields we got from entry 4, 5 and 6 were 24%, 13% and trace, respectively, showing a trend that indicates lower reaction temperature suppressing background reactions. This drives us to also try applying lower temperatures on the reactions that do use catalyst. Unfortunately,

we found that having catalyst did not improve the reactivity of the reactions in -78°C and -40°C, showing similar chemical yields (entry 7 vs. 6 and 8 vs. 5, respectively). However, we were delighted to find out that the catalytic reaction ran for 20 hours at 0°C using method B for allenyltrichlorosilane addition gave improved yield and ee (entry 9).

2.2.3 Evaluation of Biisoquinoline-Based Catalysts

Even though we noticed a clear advantage from method B over method A in Table 6, the reason for improved reactivity and selectivity remained unclear to us. It is worth noting that achieving substoichiometric enantioinduction remains a challenge in the chiral Lewis base promoted addition of chlorosilanes (LSiCl_3 , $\text{L}=\text{H}$, Cl , allyl, allenyl, propargyl, etc.) to acylhydrazones. The only other example we had was from Chapter 1, which 3,3'-Triazolyl biisoquinoline *N*, *N'*-dioxide derived catalyst being able to promote asymmetric reduction of acylhydrazones with HSiCl_3 using substoichiometric amount of catalyst [44,97]. To our knowledge, that was the second class of Lewis base catalysts, after catalyst **4**, capable of catalyzing enantioselective reduction of acylhydrazones with chlorosilanes. Therefore, we chose to compare it with catalyst **4** for the current reaction. Although catalyst **2a**

could catalyze the reaction with decent yield, its enantioselectivity was notably lacking compared to catalyst **4** (Table 7).



| Entry | Catalyst | Yield (%) | ee (%) |
|-------|-----------|-----------|--------|
| 1 | 2a | 63 | 12 |
| 2 | 8 | 44 | 26 |

Table 7. Evaluation of bisisoquinoline based catalysts with allenyltrichlorosilane added as a CH_2Cl_2 solution at -78°C .

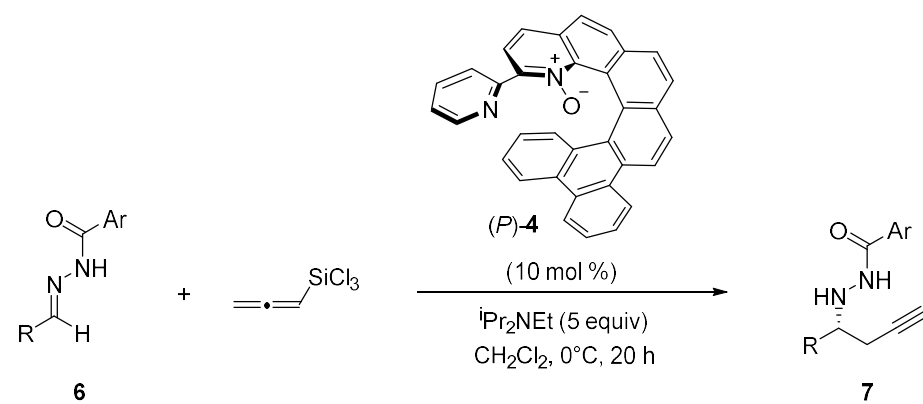
Recently, there was a new worth noting bisisoquinoline based catalyst reported by Malkov, *et al.* Their 3,3'-(3,5-bis(trifluoromethyl)phenyl)-bipyridine *N,N'*-dioxide

catalyst was able to effectively catalyze the addition of allenyltrichlorosilane to aldehydes despite of the considerably lower reactivity of allenyltrichlorosilane versus allyltrichlorosilane in Lewis base catalysis [92,98]. Thus, we chose to also evaluate our catalyst **8** [50], which is analogous to Malkov's catalyst, in this reaction (entry 2). While catalyst **8** falls short of **4** in both reactivity and selectivity, it did achieve better selectivity compared to **2a**, with a less impressive reactivity. Arguably, these observations emphasize the potential for 1-aza[6]helicene to serve as a chiral catalytic scaffold that complements the widely applicable axial-chiral motif.

2.3 Propargylation of *N*-Acylhydrazones

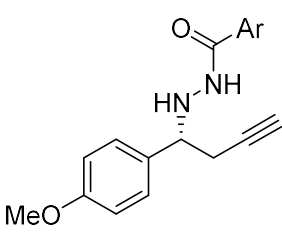
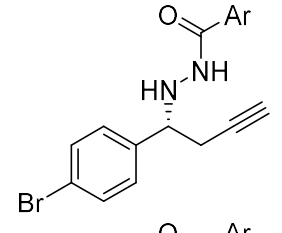
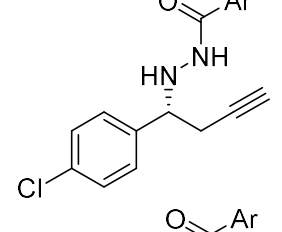
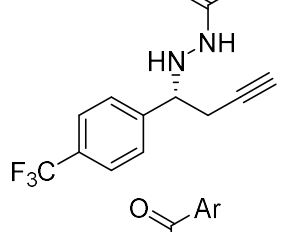
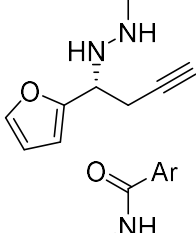
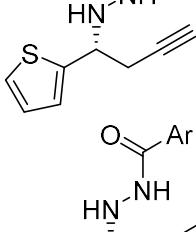
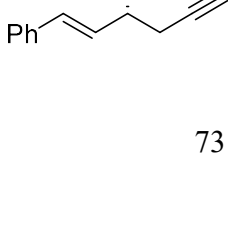
After establishing the fundamental reaction parameters with acylhydrazone **4a**, we then proceeded to assess the ability of the current catalytic system to selectively catalyze the propargylation of different *N*-acylhydrazones (Table 8). The first three substrates we tested were hydrazone **6b-d**. Consider how *ortho*-methyl substituted hydrazones are known to behave poorly and was showcased in Chapter 1's substrates scopes, we were surprised to see **7b** getting very promising reactivity and selectivity, affording 70% yield and 76% ee. Substrates **7c** and **7d** are structurally

similar to the model substrate **7a**. While **7c** was getting comparable yield of 73% and 76% ee, **7d**'s bearing *para*-methyl substitution yielded a lower chemical yield (45%) without significantly altering the enantioselectivity (76% ee). This finding led us to speculate that the reactivity of hydrazones in our catalytic system could be highly influenced by the electronic characteristics of the substrates. Therefore, we further tested this hypothesis with substrates that bare electronically different *para*-substitutions. The presence of an electron-donating methoxy group caused detrimental impact on both reactivity and enantioselectivity, resulting in a yield of 14% and 28% ee for product **7e**. Electron-withdrawing substitutions Br, Cl and CF₃ (**6f-h**), however, performed just as good as the model substrate and provided similar yield and ee. Heteroaromatic hydrazones with electron-rich properties proved to be unsuitable substrates for the current method. They yielded products **5i** and **5j** at 16% and 28% yields, respectively, with enantiomeric excess of 32 and 2. Somewhat unexpectedly, the hydrazone derived from cinnamaldehyde exhibited poor reactivity, resulting in product **5k** at a yield of 21% with 32% ee. The aliphatic substrate (**4l**) produced only trace amount of product, with the crude reaction mixture exhibiting significant impurities in TLC and ¹H NMR analysis. Since this did not happen to any other entries tested prior to this substrate, we speculated that it is possible that **4l** underwent tautomerization to its corresponding nucleophilic enamine in the presence of ⁱPr₂NEt and caused background reactions with allenyltrichlorosilane.



Ar = 3,5-(CF₃)₂Ph

| Entry ^a | Hydrazine ^b | Yield (%) ^c | ee (%) |
|--------------------|------------------------|------------------------|--------|
| 1 | 7a | 72 (68 ^d) | 86 |
| 2 | 7b | 70 | 76 |
| 3 | 7c | 73 | 82 |
| 4 | 7d | 45 | 76 |

| | | | | |
|----|-----------|---|----|----|
| 5 | 7e |  | 14 | 28 |
| 6 | 7f |  | 63 | 74 |
| 7 | 7g |  | 65 | 78 |
| 8 | 7h |  | 74 | 78 |
| 9 | 7i |  | 16 | 32 |
| 10 | 7j |  | 28 | 2 |
| 11 | 7k |  | 21 | 32 |

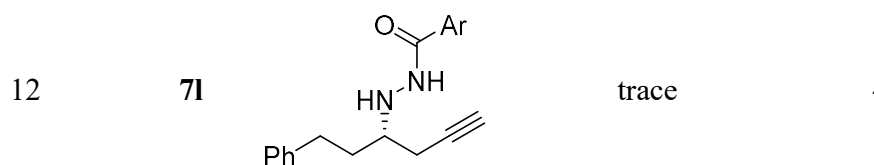


Table 8. Propargylation of various acylhydrazones in 0.1 mmol scale with allenyltrichlorosilane and catalyst (*P*)-4 under optimized reaction parameters. a) all entries used method B from Table 6 for allenyltrichlorosilane addition. b) the absolute stereochemistry of 7a was determined in previous work and others were assigned by analogy. c) yields were determined by ^1H NMR using 1,1,2,2-tetrachloroethane as standard. d) isolated yield.

2.4 Conclusion

In this work, we demonstrated that catalyst **2**, derived from helicene-based 2,2'-bipyridine *N*-monoxide, exhibits potential as an efficient asymmetric catalyst for propargylation reactions with allenyltrichlorosilane on various acylhydrazones. The flexibility of our catalyst's synthesis procedure means we can easily access a good variety of helicene-derived 2,2'-bipyridine *N*-monoxides that have different steric and electronic properties. This opens the possibility of identifying catalysts that outperform the one highlighted here.

2.5 Experimental Section

2.5.1 General Information

All reactions were carried out in oven- or flame-dried glassware under an atmosphere of dry argon or nitrogen unless otherwise noted. Except as otherwise indicated, all reactions were magnetically stirred and monitored by analytical thin-layer chromatography using EMD Millipore pre-coated silica gel plates with F₂₅₄ indicator. Visualization was accomplished by UV light (254 nm), with a combination of potassium permanganate, *p*-anisaldehyde, and/or cerium molybdate solution as an indicator. Flash column chromatography was performed according to the method of Still [49] using silica gel 60 (mesh 230-400) supplied by SiliCycle[®] Inc. Isolated yields refer to chromatographically and spectroscopically pure compounds, unless otherwise stated.

Commercial grade reagents and solvents were purchased from Sigma-Aldrich, Alfa-Aesar, Acros, Fisher, TCI, and VWR, and were used as received without further purification except as indicated below. THF and Et₂O were freshly distilled over sodium/benzophenone under an atmosphere of dry nitrogen prior to use. CH₃CN, CH₂Cl₂, and toluene were freshly distilled over CaH₂ under an atmosphere

of dry nitrogen prior to use. *N,N*-Diisopropylethylamine and triethylamine were distilled over KOH under an atmosphere of dry nitrogen, stored over NaOH in a Schlenk flask, and used from there. Trichlorosilane (Sigma-Aldrich) was freshly distilled over CaH₂ under an atmosphere of dry nitrogen prior to use.

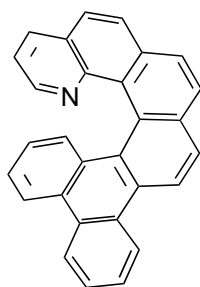
Allenyltrichlorosilane was prepared according to the reported procedure [92] and either freshly distilled over CaH₂ under an atmosphere of dry nitrogen prior to use as neat (Method A) or distilled over CaH₂ under an atmosphere of dry nitrogen, stored as a CH₂Cl₂ solution (1.5 M) in a Schlenk flask, and used from there (Method B). Catalysts **2**, **2a**, and **8** were prepared according to our published procedures (vide infra), stored as a CH₂Cl₂ solution (0.05 M) in a Schlenk flask, and used from there (Method B).

All ¹H NMR and ¹³C NMR spectra were obtained using a Bruker 400 Ultrashield or an Oxford AS400 Spectrometer (¹H 400 MHz, ¹³C 100 MHz) at ambient temperature in CDCl₃ purchased from Cambridge Isotope Laboratories, Inc. Chemical shifts in ¹H NMR spectra are reported in parts per million (ppm) respective to tetramethylsilane (δ 0.00 ppm) unless otherwise noted. The proton spectra are reported as follows δ (multiplicity, coupling constant *J*, number of

protons). Multiplicities are indicated by s (singlet), d (doublet), t (triplet), q (quartet), m (multiplet), and br (broad). Chemical shifts in ^{13}C NMR spectra are reported in ppm relative to CDCl_3 (δ 77.0 ppm). All ^{13}C NMR spectra were recorded with complete proton decoupling. HRMS data were obtained at the USF Mass Spec and Peptide Core Facility in the Department of Chemistry at the University of South Florida. Optical rotations were measured using a Jasco P2000 Polarimeter at 589 nm and were reported as $[\alpha]_D^{25}$, where C is reported in g/100 mL.

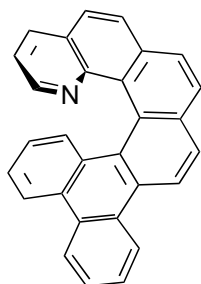
2.5.2 Experimental Procedures

(±)-11,12-Benzo-1-aza[6]helicene (5):



The title compound was prepared according to our published procedures [76,78].

(P)-11,12-Benzo-1-aza[6]helicene (5):



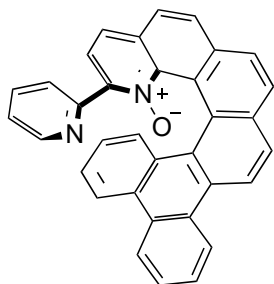
The diastereomeric salt-mediated optical resolution of racemic **5**. A round bottom flask was charged with (\pm)-11,12-benzo-1-aza[6]helicene (500 mg, 1.32 mmol) and a magnetic stir bar, flushed with nitrogen, and sealed by a septum with a nitrogen-filled balloon. To this was added freshly distilled CH₃CN (60 mL), and then the resulting suspension was sonicated for 30 min. to make solid chunks into fine powders. The suspension of fine powders was heated by a heat gun to completely dissolve all solids, and then the resulting clear solution was stirred at room temperature for 15 min. to cool down. To this stirring solution was added a solution of (–)-*O,O'*-dibenzoyl-L-tartaric acid monohydrate (7.45 g, 19.80 mmol) in CH₃CN (14 mL) in a stream by a syringe. The resulting clear bright yellow solution was stirred at room temperature under an atmosphere of nitrogen for 90 min. The resulting precipitate was filtered and washed with CH₃CN cooled to 0 °C to give bright yellow solid (493 mg). The filtrates were combined and condensed *in vacuo* to yield bright yellow solid (7.45 g). The precipitated solid (493 mg) was dissolved in CH₂Cl₂ (20 mL) and washed with aqueous 1 M NaOH solution (20 mL) to

remove tartaric acid. The aqueous layer was back-extracted once with CH₂Cl₂ (20 mL) and combined CH₂Cl₂ layers were washed with brine, dried over Na₂SO₄, filtered, concentrated *in vacuo* to afford enantio-enriched **5** (164 mg, 33% or 66% theoretical yield, 64% ee in (*P*)-enantiomer).

In the following procedure we crystallized 64% ee sample twice to get optically pure **5**. In our hands, samples with <80% ee usually precipitate small clear crystals (mostly racemic), but on the other hand, samples with >80% ee form relatively large yellow prisms (optically pure).

Enantio-enriched **5** (194 mg, 65% ee) was dissolved in a minimum amount of 40% CH₂Cl₂ in hexanes with gentle heating in a round bottom flask. The mouth of the flask was covered loosely with aluminum foil, and left in the fume hood for overnight, at which point, small clear crystals formed at the bottom of the flask. The mother liquor was decanted into another round bottom flask, condensed *in vacuo* to provide **5** (111 mg, 84% ee). The resulting 84% ee sample was recrystallized in the same manner to afford optically pure yellow prisms (61 mg, 31% after two crystallizations), which was used without further purification in the subsequent step.

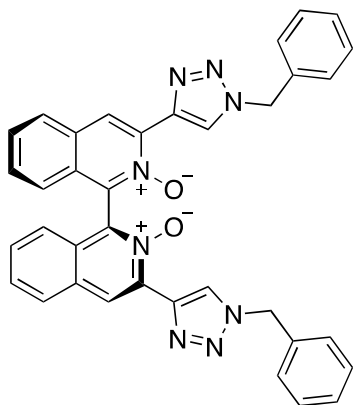
(P)-Helicene-derived 2,2'-bipyridine *N*-monoxide (4):



The title compound was prepared according to our published procedures [77].

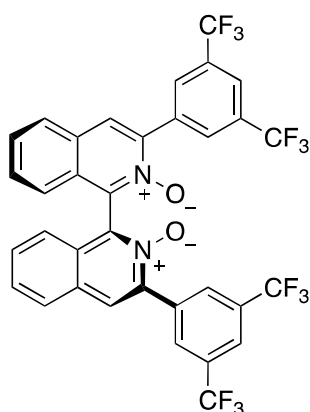
(S)-3,3'-Bis-(1-benzyl-1*H*-1,2,3-triazole-4-yl)-1,1'-biisoquinoline *N*, *N*'-dioxide

(2a):



The title compound was prepared according to our published procedures [44].

(S)-3,3'-Bis[3,5-bis(trifluoromethyl)phenyl]-1,1'-biisoquinoline *N,N'*-dioxide
(8).



The title compound was prepared according to our published procedures [50].

General Procedure for the Preparation of *N*-Acylhydrazones (6a-l).

A round bottom flask was charged with 3,5-bis(trifluoromethyl)benzoylhydrazine (500 mg, 1.84 mmol) and a magnetic stir bar, flushed with nitrogen, and then sealed by a septum with a nitrogen-filled balloon. To this was added successively commercial anhydrous MeOH (4.6 mL) and aldehyde (1.84 mmol). The resulting solution was stirred overnight at room temperature. The precipitate was filtered, washed with MeOH cooled to 0 °C, and dried further on the filter funnel for a few min. The solid was transferred to a round bottom flask, to which freshly distilled toluene was added and condensed *in vacuo* three times to remove residual MeOH

(61%-96% yields for **6a-k**). The resulting *N*-acylhydrazone was checked for any residual MeOH by ^1H NMR in CDCl_3 and then used in the propargylation reaction without further purification. Hydrocinnamaldehyde-derived *N*-acylhydrazone **7l** did not precipitate under the reaction condition. As such, the reaction mixture was condensed *in vacuo*, and purified by a flash chromatography on silica using 15% EtOAc in hexanes as eluent to afford a white solid (356 mg, 50%). All *N*-acylhydrazones (**6a-l**) produced broad uncharacterizable ^1H NMR spectra presumably due to expected rotamers, and thus were used in the propargylation reaction without further characterization.

Racemic Homopropargylic Hydrazide (7a-k)

Racemic products **7a-k** used for the chiral HPLC analysis were prepared from **6a-k** by following the reported procedure [91].

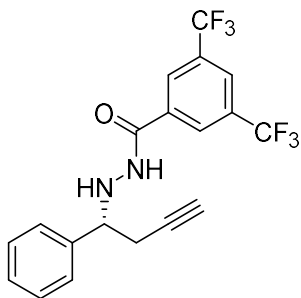
General Procedure for the Enantioselective Catalytic Propargylation (Method A).

The propargylation reaction was performed according to our published procedure [77].

General Procedure for the Enantioselective Catalytic Propargylation (Method B).

A test tube was charged with a magnetic stir bar, flame-dried *in vacuo*, and cooled to room temperature under an atmosphere of nitrogen. To this was added acylhydrazone (0.1 mmol), a solution of (*P*)-**4** in CH₂Cl₂ (0.05 M, 200 mL), and ¹Pr₂NEt (87 mL, 0.5 mmol). The resulting heterogeneous mixture was cooled to -78 °C, treated with a solution of allenyltrichlorosilane in CH₂Cl₂ (1.5 M, 100 mL) drop-by-drop through the sidewall of the test tube, and stirred at the same temperature for a further 30 min. The reaction test tube was transferred to the isopropanol bath at 0 °C and kept therein for 20 h. The reaction mixture was cooled back to -78 °C, quenched with 50% Et₃N in MeOH (400 mL), allowed to warm up to room temperature, and washed with saturated aqueous NaHCO₃ solution (1 mL). The aqueous layer was extracted with CH₂Cl₂ (1 mL) three times, and the combined organic layers were dried over Na₂SO₄, filtered, and concentrated *in vacuo* to provide the crude reaction mixture. ¹H NMR yield was determined with the crude reaction mixture by using 1,1,2,2-tetrachloroethane as an internal standard. Some portions of the crude reaction mixture were purified by preparative TLC for characterization and chiral HPLC analysis.

(*R*)-*N'*-(1-Phenylbut-3-ynyl)-3,5-bis(trifluoromethyl)benzohydrazide (7a**):**



The general procedure was followed with **4a** (36 mg, 0.1 mmol) to give the title compound in 72% NMR yield. The crude reaction mixture was purified by a flash chromatography on silica using 7% EtOAc in hexanes as eluent to afford a white solid (27 mg, 68%). All spectral data were identical to the literature values [77].

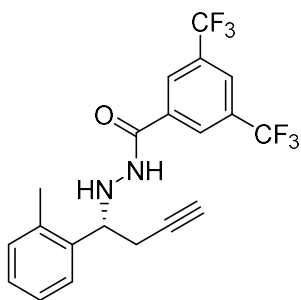
^1H NMR (400 MHz, CDCl_3) δ 8.08 (s, 2H), 7.99 (s, 1H), 7.80 (br s, 1H), 7.43-7.34 (m, 5H), 5.47 (br s, 1H), 4.34 (t, $J = 6.0$ Hz, 1H), 2.73-2.61 (m, 2H), 2.14, (s, 1H).

^{13}C NMR (100 MHz, CDCl_3) δ 164.4, 139.8, 134.9, 132.4 (q, $^2J_{\text{C-F}} = 33.8$ Hz), 128.8, 128.5, 127.5, 127.3 (d, $^3J_{\text{C-F}} = 3.0$ Hz, *ortho* CH-Ar), 125.4 (t, $^3J_{\text{C-F}} = 3.5$ Hz, *para* CH-Ar), 122.8 (q, $^1J_{\text{C-F}} = 271.3$ Hz), 80.7, 71.2, 63.2, 25.8.

The (*R*)-absolute stereochemistry was assigned by HPLC analysis [77]. er = 93:7; t_{R} (*R*) 13.57 min; (*S*) 17.00 min, (Daicel Chiralcel[®] OJ-H with an OJ-H guard column, hexane/2-propanol = 85/15, 0.5 mL/min).

$[\alpha]_{\text{D}}^{21} = -2.9$ (c = 0.13, CH_2Cl_2).

(R)-N'-[1-(2-methylphenyl)but-3-ynyl]-3,5-bis(trifluoromethyl)benzohydrazide
(7b):



The general procedure was followed with **6b** (37 mg, 0.1 mmol) to give the title compound in 70% NMR yield.

^1H NMR (400 MHz, CDCl_3) δ 8.10 (s, 2H), 8.00 (s, 1H), 7.77 (d, $J = 5.6$ Hz, 1H), 7.55 (d, $J = 7.2$ Hz, 1H), 7.29-7.17 (m, 3H), 5.42 (d, $J = 6$ Hz, 1H), 4.67 (t, $J = 6.4$ Hz, 1H), 2.71-2.57 (m, 2H), 2.37 (s, 3H), 2.14 (t, $J = 2.4$ Hz, 1H).

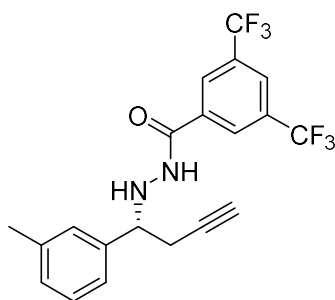
^{13}C NMR (100 MHz, CDCl_3) δ 164.4, 137.9, 136.5, 134.9, 132.4 (q, $^2J_{\text{C-F}} = 33.8$ Hz), 130.8, 128.0, 127.3 (d, $^3J_{\text{C-F}} = 2.9$ Hz, *ortho* CH-Ar), 126.6, 126.0, 125.4 (m, $^3J_{\text{C-F}} = 3.8$ Hz, *para* CH-Ar), 122.8 (q, $^1J_{\text{C-F}} = 271.2$ Hz), 81.1, 70.9, 29.7, 25.2, 19.3.

HRMS (ESI): Exact mass calculated for $\text{C}_{20}\text{H}_{17}\text{F}_6\text{N}_2\text{O}$ $[\text{M}+\text{H}]^+$ expected: 415.1240, found: 415.1223.

The (*R*)-absolute stereochemistry was assigned by analogy. er = 88:12; HPLC analysis: t_R (*R*) 9.92 min; (*S*) 11.44 min, (Daicel Chiralcel® OD-H with an OD-H guard column, hexane/2-propanol = 85/15, 0.5 mL/min).

$[\alpha]_D^{21} = -12.7$ (c = 0.17, CH₂Cl₂).

(*R*)-*N*'-[1-(3-methylphenyl)but-3-ynyl]-3,5-bis(trifluoromethyl)benzohydrazide (7c):



The general procedure was followed with **6c** (37 mg, 0.1 mmol) to give the title compound in 73% NMR yield.

¹H NMR (400 MHz, CDCl₃) δ 8.07 (s, 2H), 7.99 (s, 1H), 7.71 (br s, 1H), 7.29-7.21 (m, 3H), 7.15 (d, $J = 7.3$ Hz, 1H), 5.47 (d, $J = 5.6$ Hz, 1H), 4.30 (br s, 1H), 2.73-2.59 (m, 2H), 2.36 (s, 3H), 2.15 (t, $J = 2.4$ Hz, 1H).

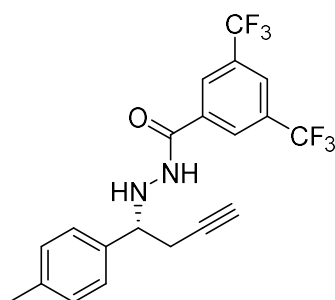
^{13}C NMR (100 MHz, CDCl_3) δ 164.4, 139.8, 138.6, 135.0, 132.4 (q, $^2J_{\text{C-F}} = 33.8$ Hz), 129.3, 128.8, 128.2, 127.3 (d, $^3J_{\text{C-F}} = 2.9$ Hz, *ortho* CH-Ar), 125.4 (m, $^3J_{\text{C-F}} = 3.6$ Hz, *para* CH-Ar), 124.5, 122.8 (q, $^1J_{\text{C-F}} = 271.6$ Hz), 80.9, 71.1, 63.3, 25.8, 21.4.

HRMS (ESI): Exact mass calculated for $\text{C}_{20}\text{H}_{17}\text{F}_6\text{N}_2\text{O}$ $[\text{M}+\text{H}]^+$ expected: 415.1240, found: 415.1229.

The (*R*)-absolute stereochemistry was assigned by analogy. er = 88:12; HPLC analysis: t_{R} (*S*) 9.40 min; (*R*) 10.71 min, (Daicel Chiralcel[®] OD-H with an OD-H guard column, hexane/2-propanol = 85/15, 0.5 mL/min).

$[\alpha]_{\text{D}}^{21} = -9.1$ (c = 0.08, CH_2Cl_2).

(*R*)-*N'*-[1-(4-methylphenyl)but-3-ynyl]-3,5-bis(trifluoromethyl)benzohydrazide (7d):



The general procedure was followed with **6d** (37 mg, 0.1 mmol) to give the title compound in 45% NMR yield.

^1H NMR (400 MHz, CDCl_3) δ 8.06 (s, 2H), 7.99 (s, 1H), 7.66 (d, $J = 4.0$ Hz, 1H), 7.31 (d, $J = 8.0$ Hz, 2H), 7.19 (d, $J = 8.0$ Hz, 2H), 5.45 (d, $J = 5.6$ Hz, 1H), 4.32 (t, $J = 6.0$ Hz, 1H), 2.72-2.59 (m, 2H), 2.36 (s, 3H), 2.15 (t, $J = 2.8$ Hz, 1H).

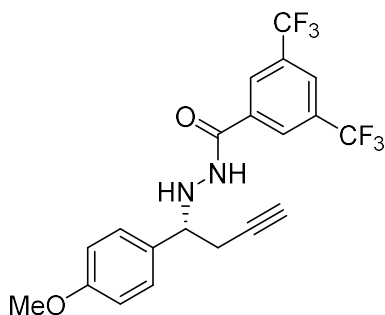
^{13}C NMR (100 MHz, CDCl_3) δ 164.3, 138.3, 136.8, 134.9, 132.3 (q, $^2J_{\text{C-F}} = 33.7$ Hz), 129.5, 127.4, 127.2 (d, $^3J_{\text{C-F}} = 2.6$ Hz, *ortho* CH-Ar), 125.3 (m, $^3J_{\text{C-F}} = 3.7$ Hz, *para* CH-Ar), 122.8 (q, $^1J_{\text{C-F}} = 271.0$ Hz), 80.9, 71.1, 62.9, 25.9, 21.1.

HRMS (ESI): Exact mass calculated for $\text{C}_{20}\text{H}_{17}\text{F}_6\text{N}_2\text{O}$ $[\text{M}+\text{H}]^+$ expected: 415.1240, found: 415.1217.

The (*R*)-absolute stereochemistry was assigned by analogy. er = 88:12; HPLC analysis: t_{R} (*S*) 8.99 min; (*R*) 10.87 min, (Daicel Chiralcel[®] OD-H with an OD-H guard column, hexane/2-propanol = 85/15, 0.5 mL/min).

$[\alpha]_{\text{D}}^{21} = -29.7$ (c = 0.07, CH_2Cl_2).

(*R*)-*N'*-[1-(4-methoxyphenyl)but-3-ynyl]-3,5-bis(trifluoromethyl)benzohydrazide (7e):



The general procedure was followed with **6e** (36 mg, 0.1 mmol) to give the title compound in 14% NMR yield.

^1H NMR (400 MHz, CDCl_3) δ 8.08 (s, 2H), 7.99 (s, 1H), 7.69 (br s, 1H), 7.34 (d, J = 8.6 Hz, 2H), 6.91 (d, J = 8.6 Hz, 2H), 5.42 (d, J = 5.6 Hz, 1H), 4.30 (t, J = 6.4 Hz, 1H), 3.81 (s, 3H), 2.72-2.58 (m, 2H), 2.14 (t, J = 2.4 Hz, 1H).

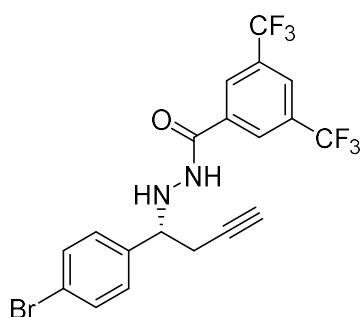
^{13}C NMR (100 MHz, CDCl_3) δ 164.4, 159.7, 135.0, 132.4 (q, $^2J_{\text{C-F}}$ = 33.8 Hz), 131.8, 128.6, 127.3 (d, $^3J_{\text{C-F}}$ = 2.9 Hz, *ortho* CH-Ar), 125.4 (m, $^3J_{\text{C-F}}$ = 3.6 Hz, *para* CH-Ar), 122.8 (q, $^1J_{\text{C-F}}$ = 271.5 Hz), 114.2, 80.9, 71.1, 62.7, 55.3, 25.9.

HRMS (ESI): Exact mass calculated for $\text{C}_{20}\text{H}_{16}\text{F}_6\text{N}_2\text{O}_2\text{Na}$ $[\text{M}+\text{Na}]^+$ expected: 453.1008, found: 453.1005.

The (*R*)-absolute stereochemistry was assigned by analogy. er = 64:36; HPLC analysis: t_R (*S*) 12.31 min; (*R*) 20.43 min, (Daicel Chiralcel® OD-H with an OD-H guard column, hexane/2-propanol = 85/15, 0.5 mL/min).

$[\alpha]_D^{21} = -7.2$ ($c = 0.07$, CH_2Cl_2).

(*R*)-*N'*-[1-(4-bromophenyl)but-3-ynyl]-3,5-bis(trifluoromethyl)benzohydrazide (7f**):**



The general procedure was followed with **6f** (44 mg, 0.1 mmol) to give the title compound in 63% NMR yield.

^1H NMR (400 MHz, CDCl_3) δ 8.10 (s, 2H), 8.01 (s, 1H), 7.68 (br s, 1H), 7.51 (d, $J = 8.3$ Hz, 2H), 7.32 (d, $J = 8.3$ Hz, 2H), 5.40 (d, $J = 5.2$ Hz, 1H), 4.32 (t, $J = 6.0$ Hz, 1H), 2.70-2.57 (m, 2H), 2.14 (t, $J = 2.6$ Hz, 1H).

^{13}C NMR (100 MHz, CDCl_3) δ 164.6, 138.9, 134.7, 132.5 (q, $^2J_{\text{C-F}} = 33.7$ Hz), 132.0, 129.2, 127.2 (d, $^3J_{\text{C-F}} = 2.9$ Hz, *ortho* CH-Ar), 125.5 (m, $^3J_{\text{C-F}} = 3.7$ Hz, *para* CH-Ar), 122.8 (q, $^1J_{\text{C-F}} = 271.1$ Hz), 122.4, 80.2, 71.5, 62.6, 25.8.

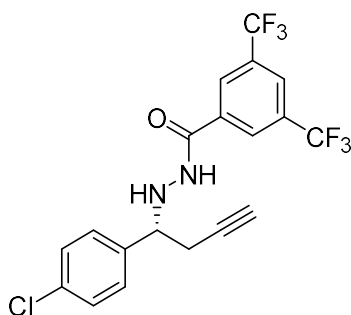
HRMS (ESI): Exact mass calculated for $\text{C}_{19}\text{H}_{14}\text{BrF}_6\text{N}_2\text{O}$ $[\text{M}+\text{H}]^+$ expected:

479.0188, found: 479.0157.

The (*R*)-absolute stereochemistry was assigned by analogy. er = 87:13; HPLC analysis: t_{R} (*S*) 24.07 min; (*R*) 36.49 min, (Daicel Chiralpak[®] AS-H with an AS-H guard column, hexane/2-propanol = 85/15, 0.5 mL/min).

$[\alpha]_{\text{D}_{21}}^{\text{D}} = -13.5$ (c = 0.13, CH_2Cl_2).

(*R*)-*N*'-[1-(4-chlorophenyl)but-3-ynyl]-3,5-bis(trifluoromethyl)benzohydrazide (7g):



The general procedure was followed with **6g** (40 mg, 0.1 mmol) to give the title compound in 65% NMR yield.

^1H NMR (400 MHz, CDCl_3) δ 8.09 (s, 2H), 8.01 (s, 1H), 7.66 (br s, 1H), 7.39-7.34 (m, 4H), 5.40 (d, $J = 5.3$ Hz, 1H), 4.33 (t, $J = 6.6$ Hz, 1H), 2.70-2.57 (m, 2H), 2.14 (t, $J = 2.6$ Hz, 1H).

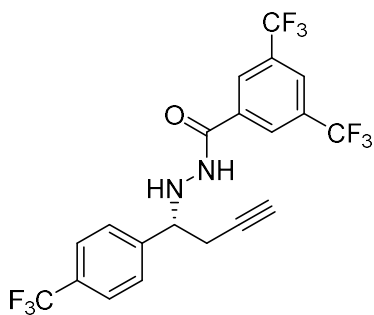
^{13}C NMR (100 MHz, CDCl_3) δ 164.6, 138.4, 134.7, 134.3, 132.5 (q, $^2J_{\text{C-F}} = 34.0$ Hz), 129.1, 128.9, 127.2 (d, $^3J_{\text{C-F}} = 3.0$ Hz, *ortho* CH-Ar), 125.5 (m, $^3J_{\text{C-F}} = 3.6$ Hz, *para* CH-Ar), 122.8 (q, $^1J_{\text{C-F}} = 271.5$ Hz), 80.2, 71.5, 62.6, 25.9.

HRMS (ESI): Exact mass calculated for $\text{C}_{19}\text{H}_{14}\text{ClF}_6\text{N}_2\text{O}$ $[\text{M}+\text{H}]^+$ expected: 435.0693, found: 435.0667.

The (*R*)-absolute stereochemistry was assigned by analogy. er = 89:11; HPLC analysis: t_{R} (*S*) 23.00 min; (*R*) 34.20 min, (Daicel Chiralpak[®] AS-H with an AS-H guard column, hexane/2-propanol = 85/15, 0.5 mL/min).

$[\alpha]_{\text{D}}^{21} = -37.3$ (c = 0.07, CH_2Cl_2).

(*R*)-*N'*-[1-[4-(trifluoromethyl)phenyl]but-3-ynyl]-3,5-bis(trifluoromethyl)benzohydrazide (7h**):**



The general procedure was followed with **6h** (36 mg, 0.1 mmol) to give the title compound in 74% NMR yield.

^1H NMR (400 MHz, CDCl_3) δ 8.09 (s, 2H), 8.01 (s, 1H), 7.69 (br s, 1H), 7.65 (d, J = 8 Hz, 2H), 7.58 (d, J = 8 Hz, 2H), 5.42 (dd, J = 4.4, 2 Hz, 1H), 4.43 (t, J = 5.6 Hz, 1H), 2.73-2.60 (m, 2H), 2.16 (t, J = 2.8 Hz, 1H).

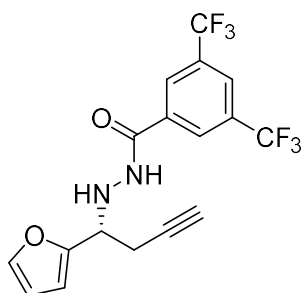
^{13}C NMR (100 MHz, CDCl_3) δ 164.8, 143.9, 134.6, 132.5 (q, $^2J_{\text{C-F}}$ = 34.0 Hz), 130.8 (q, $^2J_{\text{C-F}}$ = 32.7 Hz), 127.9, 127.2 (q, $^3J_{\text{C-F}}$ = 2.9 Hz, *ortho* CH-Ar), 125.8 (q, $^3J_{\text{C-F}}$ = 3.7 Hz), 125.6 (m, $^3J_{\text{C-F}}$ = 3.3 Hz, *para* CH-Ar), 124.0 (q, $^1J_{\text{C-F}}$ = 270.6 Hz), 122.7 (q, $^1J_{\text{C-F}}$ = 271.5 Hz), 79.9, 71.7, 62.8, 25.8.

HRMS (ESI): Exact mass calculated for $\text{C}_{20}\text{H}_{14}\text{F}_9\text{N}_2\text{O}$ $[\text{M}+\text{H}]^+$ expected: 469.0957, found: 469.0956.

The (*R*)-absolute stereochemistry was assigned by analogy. er = 89:11; HPLC analysis: t_R (*S*) 16.11 min; (*R*) 19.76 min, (Daicel Chiralpak® AS-H with an AS-H guard column, hexane/2-propanol = 85/15, 0.5 mL/min).

$[\alpha]_D^{21} = -10.2$ (c = 0.13, CH₂Cl₂).

(*R*)-*N'*-[1-(2-furan)but-3-ynyl]-3,5-bis(trifluoromethyl)benzohydrazide (7i**):**



The general procedure was followed with **6i** (30 mg, 0.1 mmol) to give the title compound in 16% NMR yield.

¹H NMR (400 MHz, CDCl₃) δ 8.15 (s, 2H), 8.02 (s, 1H), 7.83 (d, J = 6.8 Hz, 1H), 7.42 (s, 1H), 6.37 (d, J = 0.8 Hz, 2H), 5.47 (dd, J = 6, 3.2 Hz, 1H), 4.43 (td, J = 6.4, 3.2 Hz, 1H), 2.85-2.73 (m, 2H), 2.15 (t, J = 2.4 Hz, 1H).

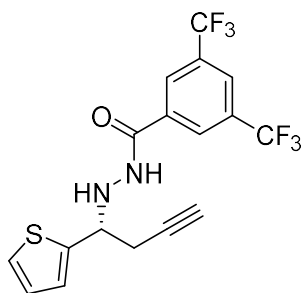
^{13}C NMR (100 MHz, CDCl_3) δ 164.5, 152.4, 142.7, 134.8, 132.5 (q, $^2J_{\text{C-F}} = 34.0$ Hz), 127.3 (br s), 125.5 (m, $^3J_{\text{C-F}} = 3.1$ Hz, *para* CH-Ar), 122.8 (q, $^1J_{\text{C-F}} = 270.9$ Hz), 110.5, 108.3, 80.2, 71.3, 56.9, 22.8.

HRMS (ESI): Exact mass calculated for $\text{C}_{17}\text{H}_{12}\text{F}_6\text{N}_2\text{O}_2\text{Na}$ $[\text{M}+\text{Na}]^+$ expected: 413.0695, found: 413.0694.

The (*R*)-absolute stereochemistry was assigned by analogy. er = 66:34; HPLC analysis: t_{R} (*R*) 13.27 min; (*S*) 15.92 min, (Daicel Chiralcel[®] OJ-H with an OJ-H guard column, hexane/2-propanol = 85/15, 0.5 mL/min).

$[\alpha]_{\text{D}_{21}} = 25.7$ (c = 0.03, CH_2Cl_2).

(*R*)-*N*'-[1-(2-thiophene)but-3-ynyl]-3,5-bis(trifluoromethyl)benzohydrazide (7j):



The general procedure was followed with **6j** (31 mg, 0.1 mmol) to give the title compound in 28% NMR yield.

^1H NMR (400 MHz, CDCl_3) δ 8.11 (s, 2H), 8.01 (s, 1H), 7.73 (d, $J = 6.8$ Hz, 1H), 7.32 (d, $J = 5.2$ Hz, 1H), 7.08 (d, $J = 3.2$ Hz, 1H), 7.00 (dd, $J = 4.8, 3.6$ Hz, 1H), 5.52 (dd, $J = 6.6, 2.2$ Hz, 1H), 4.68 (td, $J = 6.6, 2$ Hz, 1H), 2.80-2.69 (m, 2H), 2.19 (t, $J = 2.4$ Hz, 1H).

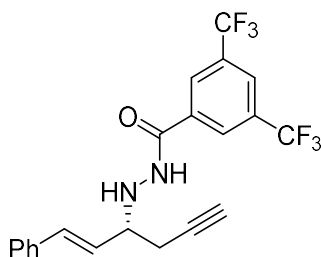
^{13}C NMR (100 MHz, CDCl_3) δ 164.6, 143.1, 134.8, 132.5 (q, $^2J_{\text{C-F}} = 33.7$ Hz), 127.3 (br s), 126.9, 126.2, 125.5 (br s), 122.8 (q, $^1J_{\text{C-F}} = 271.5$ Hz), 80.1, 71.7, 58.9, 26.6, (two signals overlap).

HRMS (ESI): Exact mass calculated for $\text{C}_{17}\text{H}_{12}\text{F}_6\text{N}_2\text{OSNa}$ $[\text{M}+\text{Na}]^+$ expected: 429.0467, found: 429.0462.

The (*R*)-absolute stereochemistry was assigned by analogy. er = 51:49; HPLC analysis: t_{R} (*S*) 30.08 min; (*R*) 38.52 min, (Daicel Chiralpak[®] AS-H with an AS-H guard column, hexane/2-propanol = 85/15, 0.5 mL/min).

$[\alpha]_{\text{D}_{21}}^{\text{D}} = \text{N/D}$.

(R)-N'-[(1E)-1-phenylhex-1-en-5-ynyl]-3,5-bis(trifluoromethyl)benzohydrazide (7k):



The general procedure was followed with **6k** (39 mg, 0.1 mmol) to give the title compound in 21% NMR yield.

^1H NMR (400 MHz, CDCl_3) δ 8.17 (s, 2H), 8.00 (s, 1H), 7.86 (d, $J = 5.2$ Hz, 1H), 7.38 (d, $J = 7.2$ Hz, 2H), 7.32 (t, $J = 7.6$ Hz, 2H), 7.28-7.26 (m, 1H), 6.65 (d, $J = 16$ Hz, 1H), 6.19 (dd, $J = 15.6, 8.4$ Hz, 1H), 5.25 (br s, 1H), 3.90 (br q, $J = 6$, 1H), 2.64-2.52 (m, 2H), 2.16 (t, $J = 2.4$, 1H).

^{13}C NMR (100 MHz, CDCl_3) δ , 164.5, 136.1, 134.9, 134.4, 132.5 (q, $^2J_{\text{C-F}} = 33.9$ Hz), 128.7, 128.2, 127.6, 127.3 (d, $^3J_{\text{C-F}} = 3.4$ Hz, *ortho* CH-Ar), 126.9, 125.4 (m, $^3J_{\text{C-F}} = 3.7$ Hz, *para* CH-Ar), 122.8 (q, $^1J_{\text{C-F}} = 271.3$ Hz), 80.4, 71.3, 61.6, 24.1.

HRMS (ESI): Exact mass calculated for $\text{C}_{21}\text{H}_{16}\text{F}_6\text{N}_2\text{ONa}$ $[\text{M}+\text{Na}]^+$ expected: 449.1059, found: 449.1057.

The (*R*)-absolute stereochemistry was assigned by analogy. er = 66:34; HPLC analysis: t_R (*S*) 10.41 min; (*R*) 13.15 min, (Daicel Chiralcel® OD-H with an OD-H guard column, hexane/2-propanol = 85/15, 0.5 mL/min).

$[\alpha]_{21}^D = -2.4$ (c = 0.07, CH₂Cl₂).

Chapter 3

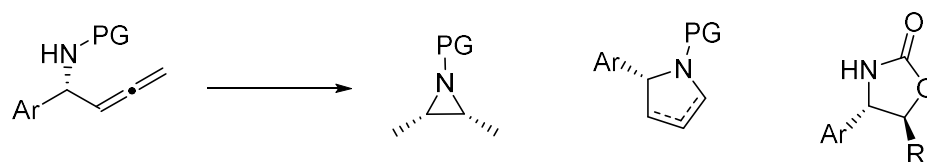
Asymmetric Allenylation of *N*-Acylhydrazones with Propargyltrichlorosilane Catalyzed by Helical Chiral 2,2'-Bipyridine *N*-Monoxide

3.1 Introduction

3.1.1 Allenes and α -allenylamines

Allenes are becoming increasingly important in modern synthetic methodologies, serving as the basis of many widely adopted transformations because of their distinctive chemical characteristics [99,100]. The higher reactivity of allenic compounds, as opposed to their alkenyl and alkynyl counterparts, enables easy control on selectivity under mild reaction conditions [101]. Their importance in organic synthesis has generated significant interest in developing the asymmetric synthesis of chiral compounds containing an allenyl group [102–104]. Among these chiral compounds, α -allenylamines were particularly interesting for being precursors of many bioactive molecules and can serve as pivots for synthesizing selections of heterocycles (Scheme 13; [102]), while bearing highly versatile allene functionality [99,100,105]. However, the synthetic pathways for obtaining optically

pure allenic amines or their ketone derivatives remain lacking compared to their corresponding allylic analog [102].



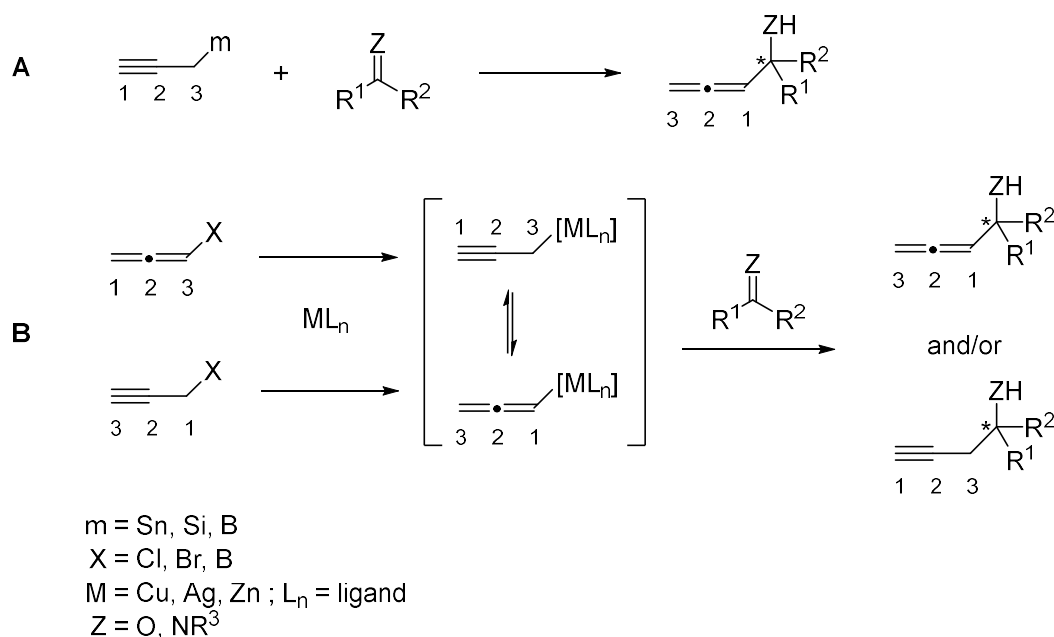
PG = protecting group

Scheme 13. Examples of diverse heterocycles synthesized from allenic amines [102].

3.1.2 Enantioselective Allenylation of Imines

The enantioselective allenylation reactions have been an attractive topic for gaining direct access to optically pure allenic molecules. Like the propargylation reactions mentioned in Chapter 2, it also poses the challenge of needing both enantioselectivity and regioselectivity controls [106,107]. These reactions are often categorized into two types of mechanisms. It can be either a direct addition between the organometallic reagent and the electrophile (Scheme 14A; [106]) or involve transition-metal before the nucleophilic addition (Scheme 14B; [106]). Although these two pathways can be distinguished from each other by tracing oxidatively different carbon 1 and 3 from starting materials to products (Scheme 14, **A** vs. **B**;

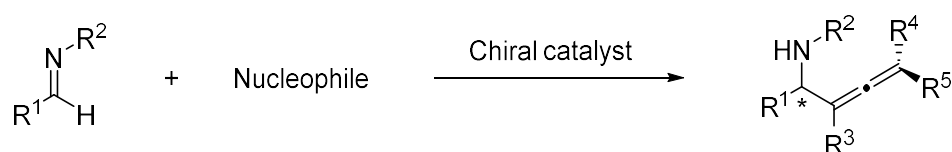
[106]), detailed mechanisms remain elusive, making regioselectivity a challenging task.



Scheme 14. Regioselectivity of propargylation and allenylation addition reactions. A: direct addition. B: transition-metal catalyzed isomerization followed by addition [106].

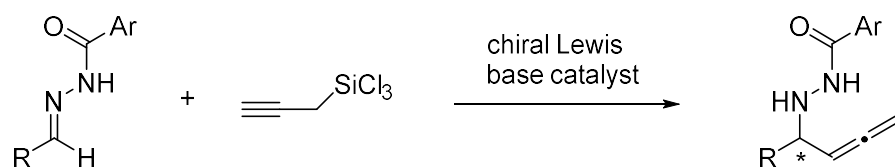
With the recent boom in asymmetric catalysis, chiral catalysts that can provide not only enantioselectivity but also regioselectivity are possible. Therefore, catalytic approaches for allenylation additions became a good option for solving those said challenges. Among those targeted molecules, α -allenylamines are particularly attractive and asymmetric methods that can give direct access to these chiral amines

are highly sought-after. So far, there have been many examples of catalytic enantioselective allenylation reported proving the potential of this approach (Scheme 15; [108–117]).



Scheme 15. Catalytic enantioselective allenylation of imines [108–117].

By utilizing *N*-acylhydrazones instead of imines in the asymmetric allenylation reaction, it will generate chiral α -allenyl hydrazines (Scheme 16). Enantio-enriched chiral hydrazines not only act as pivotal synthetic precursors, but they can also be readily converted into the corresponding α -allenylamines through N-N bond cleavage [16,97,118].



Scheme 16. Lewis base catalyzed allenylation of acylhydrazones with propargyltrichlorosilane.

At the time of writing, however, the scope of catalytic methods that enable access to this set of chiral amines has been limited. Considering this, we became interested in exploring propargyltrichlorosilane as the allenylation reagent for the allenylation of acylhydrazones under chiral Lewis base catalysis conditions. The set of acylhydrazones used in this work were also presented in Chapter 2's study and are tried and proven bench-stabled molecules that are easy to access.

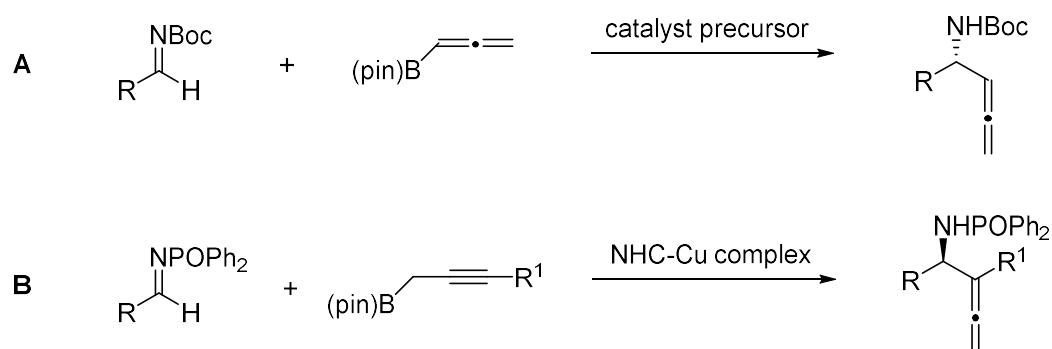
Propargyltrichlorosilane, also like the allenyltrichlorosilane counterparts, upon quenching with aqueous NaOH or NaHCO₃ solutions only generates innocuous NaCl and SiO₂ as byproducts.

3.2 Reaction Condition Optimization

3.2.1 Synthesis of Propargyltrichlorosilane

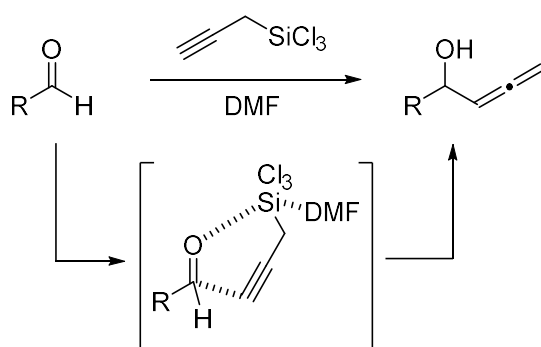
As described in Jarvo's review, isomerization of the metal/metalloid organometallic reagents in the allenylation reactions has always been an issue [106]. It is worth mentioning that in 2014, Hoveyda, *et al.* reported a few catalytic methods that attempted to address this shortcoming. Their group was able to achieve impressive results with an in-situ-generated boron-based catalyst (Scheme 17A; [111]), a copper complex formed by N-heterocyclic carbene and copper(I)

chloride (Scheme 17B; [112]). Despite their breakthrough on this topic, it remains a significant challenge to the date of writing.



Scheme 17. Hoveyda’s catalytic approaches for allenylation of aldimines. A: using *in situ*-generated boron-based catalyst [111]. B: using copper complex formed by N-heterocyclic carbene (NHC) and CuCl [112].

Inspired by Kobayashi’s work, our approach began with the selective synthesis of the trichlorosilane-based nucleophile [91,118–120]. Their group showcased the first selective formation of propargyltrichlorosilanes from propargyl halides, which proceeded to react with aldehydes and underwent S_E2' addition to afford allenic alcohols (Scheme 18; [119]).

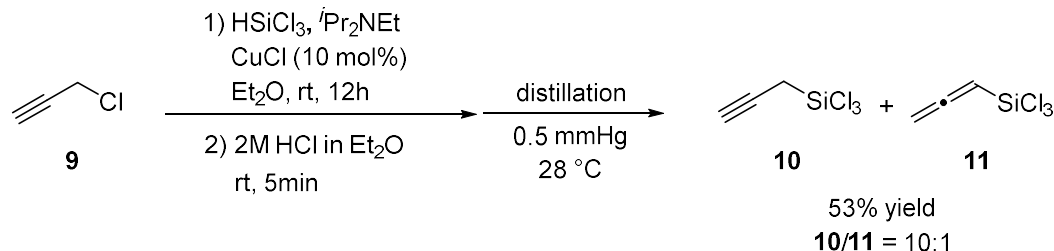


Scheme 18. Regioselective synthesis of allenic alcohol from aldehyde and propargyltrichlorosilane [119].

When preparing the propargyltrichlorosilane, they noticed significant isomerization during distillation which changed the ratio of propargyl- and allenyltrichlorosilane from 6:1 to 1:2. Therefore, they used the crude solution for the allenylation to avoid the formation of allenyltrichlorosilane. Subsequently, in 2006, they enhanced this nonstereoselective method of preparing propargyltrichlorosilane and included *N*-acylhydrazones in their substrate scope, resulting in the regioselective production of racemic α -allenic hydrazines [91,120]. These studies, although highlighted the isomerization issue in forming propargyltrichlorosilane, but also proved its capability in regioselective allenylation additions [91,98,120,121].

In our attempts, we chose $i\text{Pr}_2\text{NEt}$ as the amine since multiple reports indicated that Et_3N will result in a lower ratio of **10/11** (Scheme 19). We then proceeded to follow Kobayashi's procedure and were able to reproduce the result at the scale of 2 mmol of propargyl chloride [91]. However, we did not successfully reach the

same level of selectivity when increasing the scale to anything greater than 10 mmol, for which we still do not have a clear answer. Moreover, we observed that **10** can further isomerize to **11** after distillation during our preliminary investigation. This unexpected isomerization occurred during the storage without any solvent presented but with small amount of $i\text{Pr}_2\text{NEt}$ accompanied, which were carried out from the reaction. Based on these observations, we hypothesized that $i\text{Pr}_2\text{NEt}$ may be the reason of the metallotropic rearrangement during distillation, in addition to the increased temperature caused by vaporization. To test how $i\text{Pr}_2\text{NEt}$ affects the isomerization occurred during distillation, we added HCl to neutralize the remaining $i\text{Pr}_2\text{NEt}$ before distilling the crude mixture (Scheme 19).

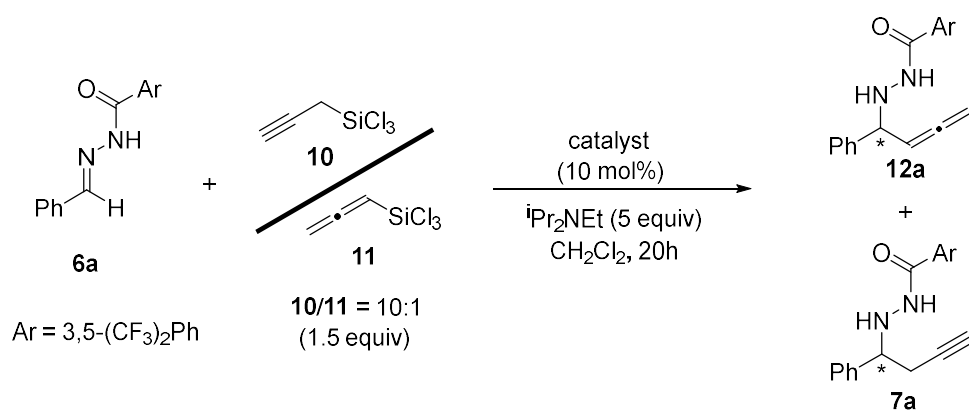


Scheme 19. Regioselective synthesis of propargyltrichlorosilane.

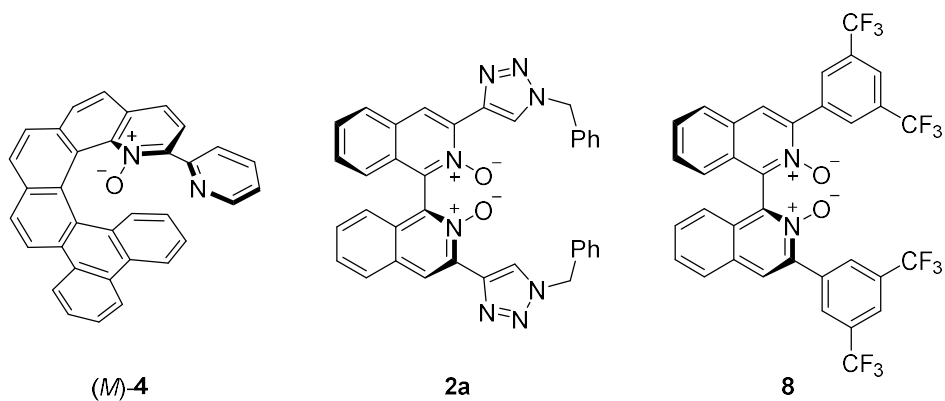
We were pleased to discover that not only did we significantly suppress the isomerization, but we also prevented **10** from further isomerizing to **11** during storage in the absence of $i\text{Pr}_2\text{NEt}$.

3.2.2 Evaluation of Lewis Base Catalysts

Based on the performance of the model reaction from the propargylation of acylhydrazones (Chapter 2, Table 8) and Kobayashi's work, we set our basic reaction parameters accordingly [91,119,120]. We chose substrate **6a** as the model substrate, a mixture of allenyl- and propargyltrichlorosilane as the organometallic nucleophile, $i\text{Pr}_2\text{NEt}$ as the amine base, dichloromethane as the solvent, and decided to run the reaction at 0 °C for 20 hours with a selection of catalysts (Table 9, entries 1-3). Regarding the catalysts, our team has pioneered various categories of Lewis-base catalysts [44,77,97]. These catalyst types synergize well with each other on various hydrocarbon trichlorosilanes. For instance, the helicene-based catalyst **4** outperforms others when handling allenyltrichlorosilane in Chapter 2; the triazole-containing catalyst **2a** is uniquely effective with HSiCl_3 as shown in Chapter 1; catalyst **8** exhibits significantly higher enantioselectivity compared to others for allyltrichlorosilane [50]. It is worth mentioning that all three catalysts used in this evaluation are the ones with the best overall performance in each of their respective categories, based on our previous studies.



catalyst:



| Entry | Catalyst | Temp (°C) | 12a Yield (%) ^a | 7a Yield (%) ^a | 12a er ^b |
|-------|----------|-----------|-----------------------------------|----------------------------------|----------------------------|
| 1 | 4 | 0 | 59 | 5 | 79:21 |
| 2 | 2a | 0 | 53 | 4 | 49:51 |
| 3 | 8 | 0 | 60 | 6 | 43:57 |
| 4 | 4 | -20 | 57 | 3 | 75:25 |
| 5 | 4 | -40 | 30 | 0 | 58:42 |
| 6 | None | 0 | 34 | 3 | N/D ^c |
| 7 | None | -20 | 33 | Trace | N/D ^c |
| 8 | None | -40 | 28 | 0 | N/D ^c |

Table 9. Evaluation of the Lewis base catalysts in allenylation of *N*-acylhydrazones with propargyltrichlorosilane. All entries were carried out with 0.1 mmol of acylhydrazones. a) yields were determined by ¹H NMR using 1,1,2,2-tetrachloroethane as standard. b) enantiomeric ratio determined by HPLC on a chiral stationary phase. c) not determined.

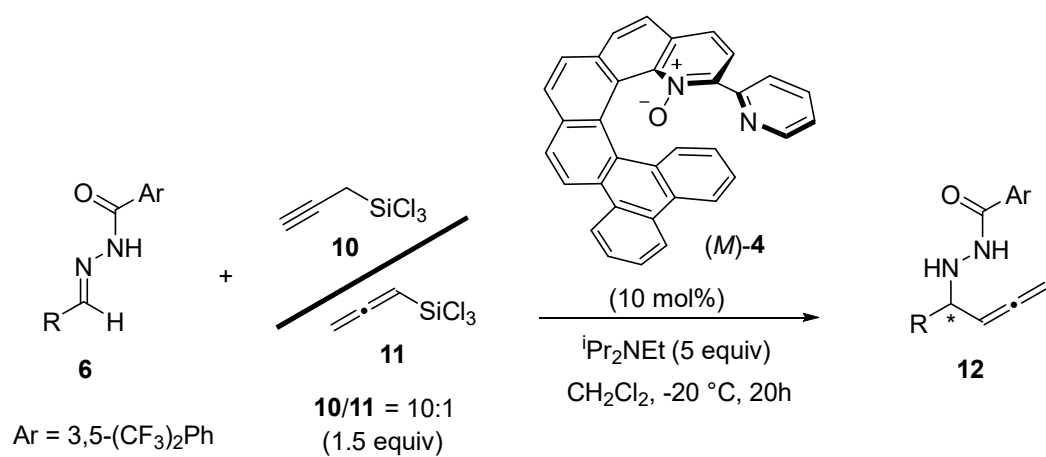
To our delight, helicene derived catalyst **4** effectively catalyzed the allenylation in terms of reactivity and enantioselectivity, affording the corresponding α -allenylamine **12a** in 59% yield and 79:21 enantiomeric ratio (entry 1).

Biisoquinoline-derived catalysts **2a** and **8**, however, provided comparable reactivity versus **4** with 53% and 60% yield, respectively, but almost did not catalyze the reaction enantioselectively (entries 2 and 3). Subsequently, we proceeded to assess the effectiveness of catalyst **4** at lower temperatures. Its reactivity and enantioselectivity at -20°C were found to be nearly the same as those at 0°C (entry 4) but lower the temperature to -40°C adversely affected both the chemical yield and the enantiomeric ratio (entry 5). We also tested the background reactions without any catalyst at 0°C, -20°C and -40°C (entries 6-8). The chemical yield of **12a** appeared to be very similar to entry 5, suggesting that catalyst **4** did not catalyze the reaction very well at -40°C. It is worth noting that we only observed minimal amount of propargylic product **7a** produced in all entries (0-6% yield), which was speculated to be distinctively coming from the allenyltrichlorosilane presented in the propargyltrichlorosilane solution.

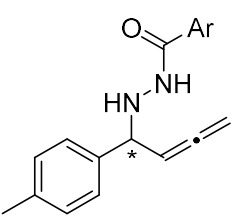
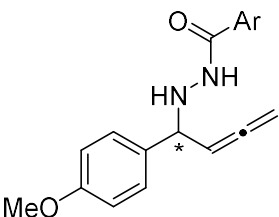
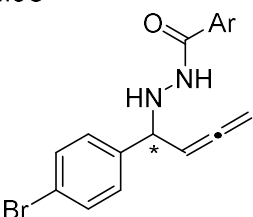
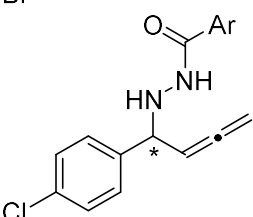
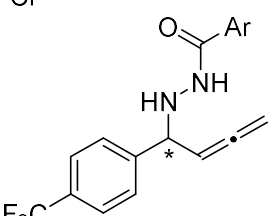
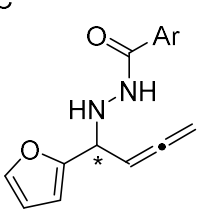
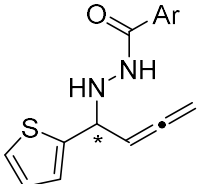
3.3 Allenylation of *N*-Acylhydrazones

Considering the lower yield of the undesired homopropargylic amine **7a** when running model reactions in lower temperatures, we proceeded to evaluate the capability of catalyst (*M*)-**4** to selectively catalyze the allenylation of various *N*-acylhydrazones at -20°C (Table 10). To our delight, sterically difficult *ortho*-methyl substituted **6b** was tolerated well in this catalytic system, affording similar yield and enantiomeric ratio compared to model substrate. The *meta*- and *para*-methyl substituted substrates, which are considered structurally similar to model substrate **6a**, perform better on enantioselectivity while affording yields within the same range as **6a** (**6c**, **d**). We then tested the effect of electronically different *para*-substitutions on benzene and found that they provided very close results to the model substrate in terms of reactivity and enantioselectivity, regardless of being electron-withdrawing or donating (**12e-h**). The furan-derived **6i** exhibited significantly greater enantioselectivity but lower reactivity compared to the model substrate. In contrast, the thiophen-derived substrate **6j** showed distinct behavior from its furan counterpart, yielding **12j** in only 26% yield with a 56:44 enantiomeric ratio. The cinnamaldehyde derived **6k** and the aliphatic substrate **6l** performed poorly on reactivity, giving 39% yield and 22% yield, respectively.

While **6k** also did not form **12k** enantioselectively at all, **6l** was a little bit better, giving **12l** with 63:38 er.



| Entry | Hydrazine | Yield ^b (%) | er |
|----------------|------------|------------------------|-------|
| 1 ^a | 12a | 57 (50 ^c) | 75:25 |
| 2 | 12b | 63 | 78:22 |
| 3 | 12c | 76 | 83:17 |

| | | | | |
|----------------|------------|---|----|--------------------|
| 4 | 12d |  | 60 | 83:17 |
| 5 | 12e |  | 65 | 71:29 |
| 6 ^a | 12f |  | 59 | 72:28 |
| 7 ^a | 12g |  | 57 | 74:26 |
| 8 ^a | 12h |  | 62 | 70:30 ^d |
| 9 | 12i |  | 41 | 81:19 |
| 10 | 12j |  | 26 | 56:44 |

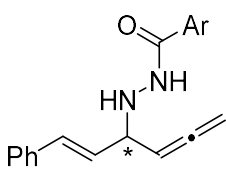
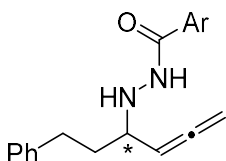
| | | | | |
|----|------------|---|-----------------------|-------|
| 11 | 12k |  | 39 (33 ^c) | 51:49 |
| 12 | 12l |  | 22 (19 ^c) | 62:38 |

Table 10. Allenylation of various acylhydrazones in 0.1 mmol scale with propargyltrichlorosilane and catalyst (*M*)-4 under optimized reaction parameters. a) 2-3% of propargylic product formed. b) yields were determined by ¹H NMR using 1,1,2,2-tetrachloroethane as standard. c) isolated yield. d) an estimated value as enantiomers were not fully separated at the baseline by chiral HPLC; see Supporting Information for details.

It is worth noting that among all the entries, there were only four out of the twelve substrates produced undesired propargylic products (**6a**, **6f-h**). These results also demonstrated that catalyst (*M*)-4 can effectively induce enantioselectivity in the allenylation of a good variety of acylhydrazones while maintaining the regioselectivity of the addition reactions.

3.4 Conclusion

In this work, we showcased a regiospecific asymmetric allenylation reaction using propargyltrichlorosilane under a helicene-derived Lewis base catalytic system. At the time of writing, this study marks the first catalytic enantioselective allenylation of *N*-acylhydrazones. The findings presented here indicate promising prospects for the continued advancement of asymmetric Lewis base catalysis with propargyltrichlorosilane.

3.5 Experimental Section

3.5.1 General Information

All reactions were carried out in oven- or flame-dried glassware under an atmosphere of dry argon or nitrogen unless otherwise noted. Except as otherwise indicated, all reactions were magnetically stirred and monitored by analytical thin-layer chromatography using EMD Millipore pre-coated silica gel plates with F₂₅₄ indicator. Visualization was accomplished by UV light (254 nm), with combination of potassium permanganate, *p*-anisaldehyde, and/or cerium molybdate solution as an indicator. Flash column chromatography was performed according to the method of Still [49] using silica gel 60 (mesh 230-400) supplied by SiliCycle® Inc. Isolated yields refer to chromatographically and spectroscopically pure compounds, unless otherwise stated.

Commercial grade reagents and solvents were purchased from Sigma-Aldrich, Alfa-Aesar, Acros, Fisher, TCI, and VWR, and were used as received without further purification except as indicated below. THF and Et₂O were freshly distilled over sodium/benzophenone under an atmosphere of dry nitrogen prior to use. CH₃CN, CH₂Cl₂, and toluene were freshly distilled over CaH₂ under an atmosphere

of dry nitrogen prior to use. *N,N*-Diisopropylethylamine and triethylamine were distilled over KOH under an atmosphere of dry nitrogen, stored over NaOH in a Schlenk flask, and used from there. Propargyl chloride (Sigma-Aldrich) was fractionally distilled over P₂O₅ under an atmosphere of dry nitrogen prior to use. Trichlorosilane (Sigma-Aldrich) was freshly distilled over CaH₂ under an atmosphere of dry nitrogen prior to use. Propargyltrichlorosilane was prepared according to the reported procedure [91] with some modifications (*vide infra*) and then distilled under reduced pressure, stored as a CH₂Cl₂ solution (1.5 M) in a Schlenk flask, and used from there. Catalysts **4**, **2a**, and **8** were prepared according to our published procedures [44,50,76–78], stored as a CH₂Cl₂ solution (0.05 M) in a Schlenk flask, and used from there.

All ¹H NMR and ¹³C NMR spectra were obtained using a Bruker 400 Ultrashield or an Oxford AS400 Spectrometer (¹H 400 MHz, ¹³C 100 MHz) at ambient temperature in CDCl₃ purchased from Cambridge Isotope Laboratories, Inc. Chemical shifts in ¹H NMR spectra are reported in parts per million (ppm) respective to tetramethylsilane (δ 0.00 ppm) unless otherwise noted. The proton spectra are reported as follows δ (multiplicity, coupling constant *J*, number of protons). Multiplicities are indicated by s (singlet), d (doublet), t (triplet), q (quartet), m (multiplet), and br (broad). Chemical shifts in ¹³C NMR spectra are

reported in ppm respective to CDCl₃ (δ 77.0 ppm). All ¹³C NMR spectra were recorded with complete proton decoupling. HRMS data were obtained at USF Mass Spec and Peptide Core Facility in the Department of Chemistry at University of South Florida. Optical rotations were measured using a Jasco P2000 Polarimeter at 589 nm and were reported as $[\alpha]_D^{T\text{ }^\circ\text{C}}$, where C is reported in g/100 mL.

3.5.2 Experimental Procedure

General Procedure for the Preparation of *N*-Acylhydrazones (6a-l).

A round bottom flask was charged with 3,5-bis(trifluoromethyl)benzoylhydrazine (500 mg, 1.84 mmol) and a magnetic stir bar, flushed with nitrogen, and then sealed by a septum with a nitrogen-filled balloon. To this was added successively commercial anhydrous MeOH (4.6 mL) and aldehyde (1.84 mmol). The resulting solution was stirred overnight at room temperature. The precipitate was filtered, washed with MeOH cooled to 0 °C, and dried further on the filter funnel for a few min. The solid was transferred to a round bottom flask, to which freshly distilled toluene was added and condensed *in vacuo* three times to remove residual MeOH (61%-96% yields for **6a-k**). The resulting *N*-acylhydrazone was checked for any residual MeOH by ¹H NMR in CDCl₃ and then used in the allenylation reaction

without further purification. Hydrocinnamaldehyde-derived *N*-acylhydrazone **6l** did not precipitate under the reaction condition. As such, the reaction mixture was condensed *in vacuo*, and purified by a flash chromatography on silica using 15% EtOAc in hexanes as eluent to afford a white solid (356 mg, 50%). All *N*-acylhydrazones (**6a-l**) produced broad uncharacterizable ¹H NMR spectra presumably due to expected rotamers, and thus were used in the propargylation reaction without further characterization.

Propargyltrichlorosilane (10)

We basically followed the procedure reported by Kobayashi *et al.* [91]. While we fully reproduced the reported result (propargyltrichlorosilane : allenyltrichlorosilane > 49 : 1 in the crude reaction mixture) at the scale of 2.0 mmol of propargyl chloride, we always got the ratio of propargyltrichlorosilane : allenyltrichlorosilane = 15 – 11 : 1 in the crude reaction mixture in a preparative scale (> 10 mmol) as detailed below.

A round-bottom flask was charged with a magnetic stir bar, flame-dried *in vacuo*, and cooled to room temperature under an atmosphere of nitrogen. This was charged with CuCl (342 mg, 3.46 mmol) inside the dry box, sealed with a septum, and taken out of the dry box. To this was added freshly distilled Et₂O (69 mL), ⁱPr₂NEt (12.10

mL, 69.26 mmol), propargyl chloride (2.5 mL, 34.63 mmol) under an atmosphere of nitrogen. The resulting heterogeneous reaction mixture was treated dropwise with HSiCl_3 (7.7 mL, 76.19 mmol), and then stirred for 12 h at ambient temperature. (At this point, a small aliquot of the reaction mixture was removed by a gas-tight syringe and diluted with anhydrous CDCl_3 in a flame-dried NMR tube for ^1H NMR analysis. The ratio of propargyltrichlorosilane : allenyltrichlorosilane was found to be ~11 : 1.) A commercial solution of HCl in Et_2O (2.0 M, 28.6 mL) was added to the reaction mixture and stirred for 5 min. to precipitate residual $^i\text{Pr}_2\text{NEt}$ as a salt, at which point ^1H NMR of another small aliquot of the reaction mixture was taken to confirm that no $^i\text{Pr}_2\text{NEt}$ remained in the reaction mixture. The reaction mixture was filtered via a short pad of oven-dried ($140\text{ }^\circ\text{C}$, 12 h) Celite® using a Schlenk filter tube to remove all solids. The resulting clear orange-brown solution was distilled in an oil bath at $28\text{ }^\circ\text{C}$, first at 150 mmHg to remove all volatiles, and then at 0.5 mmHg to take out propargyltrichlorosilane that was collected in a round bottom flask cooled in a liquid nitrogen (3.2 g, 53% yield, propargyltrichlorosilane : allenyltrichlorosilane = 10 : 1). We stored the distilled silane mixture as a CH_2Cl_2 solution (1.5 M) in a Schlenk flask in a regular freezer ($-20\text{ }^\circ\text{C}$) and the ratio remained unchanged when we took again ^1H NMR of this solution after 18 days.

It is worthy of mention that the distillation of the crude silane mixture (~13 : 1) containing $i\text{Pr}_2\text{NEt}$ not only significantly promoted the isomerization of propargyltrichlorosilane to allenyltrichlorosilane (~6 : 1) but also could not remove $i\text{Pr}_2\text{NEt}$. The ratio of distilled propargyltrichlorosilane : allenyltrichlorosilane (~6 : 1) contaminated with $i\text{Pr}_2\text{NEt}$ became 4.5 : 1 after only 2 days in the freezer.

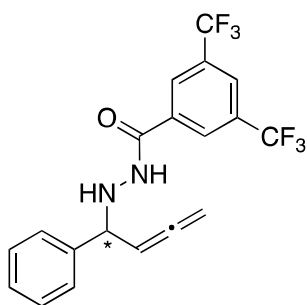
Racemic Allenic Hydrazides (12a-l) for the Chiral HPLC Analysis.

Racemic products **12a-h**, **12j** and **12l** were prepared from **6a-h,6j** and **6l** by following the reported procedure [91], which employs the supernatant solution of *in situ* prepared propargyltrichlorosilane in Et_2O . *N*-3,5-bis(trifluoromethyl)benzoylhydrazones are found to be relatively unreactive substrates for this procedure, affording the products in 7 – 13% yields. Hydrazides **12i** and **12k** formed only in trace amounts by this procedure and thus were prepared by using a CH_2Cl_2 solution of propargyltrichlorosilane (1.5 M) instead of the supernatant Et_2O solution, yielding in 31% and 32%, respectively (not optimized).

General Procedure for the Enantioselective Catalytic Allenylation.

A test tube was charged with a magnetic stir bar, flame-dried *in vacuo*, and cooled to room temperature under an atmosphere of nitrogen. To this was added acylhydrazone (0.1 mmol), a solution of (*M*)-**4** in CH₂Cl₂ (0.05 M, 200 mL), and ⁱPr₂N⁺Et⁻ (87 mL, 0.5 mmol). The resulting heterogeneous mixture was cooled to –78 °C, treated with a solution of propargyltrichlorosilane in CH₂Cl₂ (1.5 M, 100 mL) drop-by-drop through the sidewall of the test tube. The reaction test tube was transferred to the isopropanol bath at –20 °C and kept therein for 20 h. The reaction mixture was cooled back to –78 °C, quenched with 50% Et₃N in MeOH (400 mL), allowed to warm up to room temperature, and washed with saturated aqueous NaHCO₃ solution (1 mL). The aqueous layer was extracted with CH₂Cl₂ (1 mL) three times, and the combined organic layers were dried over Na₂SO₄, filtered, and concentrated *in vacuo* to provide the crude reaction mixture. ¹H NMR yield was determined with the crude reaction mixture by using 1,1,2,2-tetrachloroethane as an internal standard. Some portions of the crude reaction mixture were purified by preparative TLC for characterization and chiral HPLC analysis.

(-)-*N'*-(1-phenylbuta-2,3-dien-1-yl)-3,5-bis(trifluoromethyl)benzohydrazide
(12a)



The general procedure was followed with **6a** (36 mg, 0.1 mmol) to give the title compound and corresponding homopropargylic hydrazide **7a** [122] in 57% and 3% NMR yields, respectively. The crude reaction mixture was purified by preparative TLC using 10% EtOAc in toluene as eluent to afford a white solid (20 mg, 50%).

^1H NMR (400 MHz, CDCl_3) δ 8.08 (s, 2H), 8.01 (s, 1H), 7.53 (d, $J = 7.2$ Hz, 1H), 7.45 (d, $J = 7.2$ Hz, 2H), 7.40 (t, $J = 7.5$ Hz, 2H), 7.36 (d, $J = 7.0$ Hz, 1H), 5.41 (q, $J = 7.0$ Hz, 1H), 5.24-5.21 (m, 1H), 4.91 (dd, $J = 6.6, 2.0$ Hz, 2H), 4.77-4.75 (m, 1H).

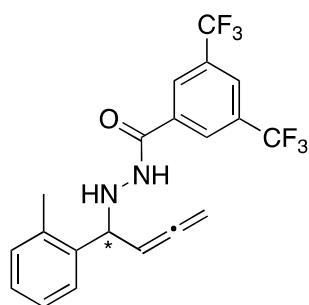
^{13}C NMR (100 MHz, CDCl_3) δ 208.5, 164.5, 139.9, 135.1, 132.4 (q, $^2J_{\text{C-F}} = 33.8$ Hz), 128.8, 128.3, 127.8, 127.2 (br s), 125.4 (t, $^3J_{\text{C-F}} = 3.5$ Hz), 122.8 (q, $^1J_{\text{C-F}} = 271.4$ Hz), 91.8, 77.3, 63.8.

HRMS (ESI): Exact mass calculated for C₁₉H₁₅F₆N₂O [M+H]⁺ expected: 401.1083, found: 401.1073.

er = 75:25; *t*_R (+) 17.87 min; (–) 23.12 min, (Daicel Chiralcel[®] OJ-H with an OJ-H guard column, hexane/2-propanol = 90/10, 0.5 mL/min).

[α]^D₂₂ = –72.8 (c = 0.33, CHCl₃).

(–)-*N'*-(1-(*o*-tolyl)buta-2,3-dien-1-yl)-3,5-bis(trifluoromethyl)benzohydrazide (12b)



The general procedure was followed with **6b** (37 mg, 0.1 mmol) to give the title compound in 63% NMR yield. Only trace amount of the corresponding homopropargylic hydrazide [122] was seen in ¹H NMR of the crude reaction mixture.

^1H NMR (400 MHz, CDCl_3) δ 8.11 (s, 2H), 8.02 (s, 1H), 7.63 (br s, 1H), 7.55 (d, J = 7.2 Hz, 1H), 7.28-7.19 (m, 3H), 5.34 (q, J = 7.0 Hz, 1H), 5.18 (br s, 1H), 5.03 (d, J = 7.1 Hz, 1H), 4.89 (d, J = 6.4 Hz, 2H), 2.41 (s, 3H).

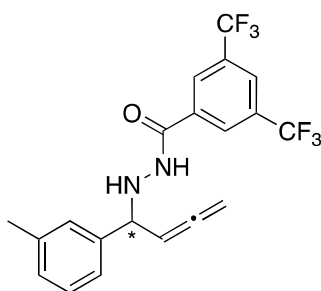
^{13}C NMR (100 MHz, CDCl_3) δ 208.8, 164.5, 137.8, 136.6, 135.1, 132.5 (q, $^2J_{\text{C-F}}$ = 33.8 Hz), 130.9, 127.9, 127.2 (br s), 126.7, 126.5, 125.4 (m), 122.8 (q, $^1J_{\text{C-F}}$ = 270.9 Hz), 91.5, 77.2, 60.1, 19.3.

HRMS (ESI): Exact mass calculated for $\text{C}_{20}\text{H}_{17}\text{F}_6\text{N}_2\text{O}$ $[\text{M}+\text{H}]^+$ expected: 415.1240, found: 415.1224.

er = 78:22; HPLC analysis: t_{R} (+) 10.12 min; (–) 12.49 min, (Daicel Chiralcel[®] OD-H with an OD-H guard column, hexane/2-propanol = 85/15, 0.5 mL/min).

$[\alpha]_{\text{D}_{21}}^{\text{D}} = -15.2$ (c = 0.27, CHCl_3).

(-)-*N'*-(1-(*m*-tolyl)buta-2,3-dien-1-yl)-3,5-bis(trifluoromethyl)benzohydrazide
(12c)



The general procedure was followed with **6c** (37 mg, 0.1 mmol) to give the title compound in 76% NMR yield. Only trace amount of the corresponding homopropargylic hydrazide [122] was seen in ^1H NMR of the crude reaction mixture.

^1H NMR (400 MHz, CDCl_3) δ 8.08 (s, 2H), 8.01 (s, 1H), 7.53 (d, $J = 6.6$ Hz, 1H), 7.31-7.23 (m, 3H), 7.16 (d, $J = 7.1$ Hz, 1H), 5.40 (q, $J = 7.0$ Hz, 1H), 5.22 (d, $J = 4.8$ Hz, 1H), 4.91 (dd, $J = 6.6, 1.8$ Hz, 2H), 4.71 (d, $J = 5.4$ Hz, 1H), 2.38 (s, 3H).

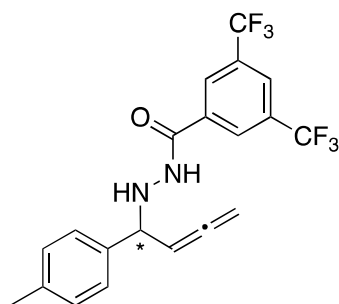
^{13}C NMR (100 MHz, CDCl_3) δ 208.5, 164.5, 139.8, 138.6, 135.1, 132.4 (q, $^2J_{\text{C-F}} = 33.8$ Hz), 129.1, 128.7, 128.5, 127.2 (br s), 125.4 (m), 124.8, 122.8 (q, $^1J_{\text{C-F}} = 271.5$ Hz), 91.8, 77.2, 63.8, 21.4.

HRMS (ESI): Exact mass calculated for $\text{C}_{20}\text{H}_{17}\text{F}_6\text{N}_2\text{O}$ $[\text{M}+\text{H}]^+$ expected: 415.1240, found: 415.1220.

er = 83:17; HPLC analysis: t_R (–) 36.75 min; (+) 46.25 min, (Daicel Chiralpak® AS-H with an AS-H guard column, hexane/2-propanol = 95/5, 0.5 mL/min).

$[\alpha]_D^{22} = -13.7$ ($c = 0.67$, CHCl_3).

(–)-*N'*-(1-(*p*-tolyl)buta-2,3-dien-1-yl)-3,5-bis(trifluoromethyl)benzohydrazide (12d)



The general procedure was followed with **6d** (37 mg, 0.1 mmol) to give the title compound in 60% NMR yield. Only trace amount of the corresponding homopropargylic hydrazide [122] was seen in ^1H NMR of the crude reaction mixture.

^1H NMR (400 MHz, CDCl_3) δ 8.07 (s, 2H), 8.01 (s, 1H), 7.51 (d, $J = 4.6$ Hz, 1H), 7.33 (d, $J = 8.0$ Hz, 2H), 7.20 (d, $J = 7.9$ Hz, 2H), 5.39 (q, $J = 6.9$ Hz, 1H), 5.20 (d, $J = 3.6$ Hz, 1H), 4.90 (dd, $J = 6.6, 1.8$ Hz, 2H), 4.72 (d, $J = 6.32$ Hz, 1H), 2.37 (s, 3H).

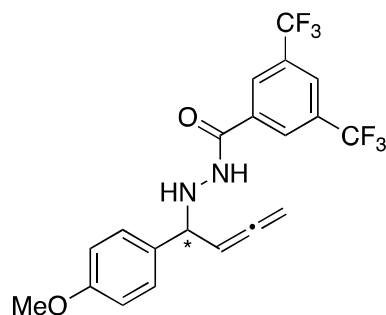
^{13}C NMR (100 MHz, CDCl_3) δ 208.4, 164.5, 138.2, 136.9, 135.2, 132.4 (q, $^2J_{\text{C-F}} = 33.7$ Hz), 129.5, 127.7, 127.3 (br s), 125.3 (m), 122.8 (q, $^1J_{\text{C-F}} = 271.4$ Hz), 91.9, 77.2, 63.5, 21.1.

HRMS (ESI): Exact mass calculated for $\text{C}_{20}\text{H}_{17}\text{F}_6\text{N}_2\text{O}$ $[\text{M}+\text{H}]^+$ expected: 415.1240, found: 415.1232.

er = 83:17; HPLC analysis: t_{R} (–) 10.00 min; (+) 11.23 min, (Daicel Chiralcel[®] OD-H with an OD-H guard column, hexane/2-propanol = 85/15, 0.5 mL/min).

$[\alpha]_{\text{D}}^{22} = -9.5$ ($c = 0.53$, CHCl_3).

(–)-*N'*-(1-(4-methoxyphenyl)buta-2,3-dien-1-yl)-3,5-bis(trifluoromethyl)benzohydrazide (12e)



The general procedure was followed with **6e** (39 mg, 0.1 mmol) to give the title compound in 65% NMR yield. Only trace amount of the corresponding

homopropargylic hydrazide [122] was seen in ^1H NMR of the crude reaction mixture.

^1H NMR (400 MHz, CDCl_3) δ 8.09 (s, 2H), 8.01 (s, 1H), 7.57 (br s, 1H), 7.36 (d, J = 8.5 Hz, 2H), 6.92 (d, J = 8.6 Hz, 2H), 5.39 (q, J = 6.8 Hz, 1H), 5.19 (br s, 1H), 4.90 (dd, J = 6.5, 1.7 Hz, 2H), 4.71 (d, J = 6.6 Hz, 1H), 3.82 (s, 3H).

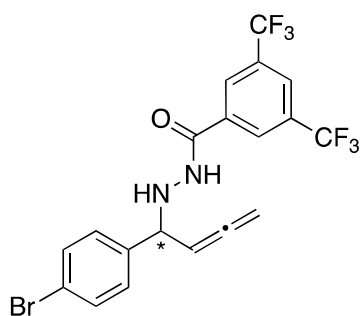
^{13}C NMR (100 MHz, CDCl_3) δ 208.4, 164.4, 159.7, 135.1, 132.4 (q, $^2J_{\text{C-F}}$ = 34.0 Hz), 131.9, 129.0, 127.2 (br s), 125.4 (m), 122.8 (q, $^1J_{\text{C-F}}$ = 271.4 Hz), 114.2, 92.0, 77.2, 63.1, 55.3.

HRMS (ESI): Exact mass calculated for $\text{C}_{20}\text{H}_{17}\text{F}_6\text{N}_2\text{O}_2$ $[\text{M}+\text{H}]^+$ expected: 431.1189, found: 431.1195.

er = 71:29; HPLC analysis: t_{R} (–) 15.03 min; (+) 20.92 min, (Daicel Chiralcel[®] OD-H with an OD-H guard column, hexane/2-propanol = 85/15, 0.5 mL/min).

$[\alpha]_{\text{D}}^{22} = -16.6$ (c = 0.40, CHCl_3).

(-)-*N'*-(1-(4-bromophenyl)buta-2,3-dien-1-yl)-3,5-bis(trifluoromethyl)benzohydrazide (**12f**).



The general procedure was followed with **6f** (44 mg, 0.1 mmol) to give the title compound and corresponding homopropargylic hydrazide **7f** [122] in 59% and 2% NMR yields, respectively.

^1H NMR (400 MHz, CDCl_3) δ 8.10 (s, 2H), 8.03 (s, 1H), 7.57 (d, $J = 4.0$ Hz, 1H), 7.52 (d, $J = 8.3$ Hz, 2H), 7.32 (d, $J = 8.3$ Hz, 2H), 5.34 (q, $J = 6.9$ Hz, 1H), 5.19 (br s, 1H), 4.91 (dd, $J = 6.6, 2.0$ Hz, 2H), 4.72 (d, $J = 6.7$ Hz, 1H).

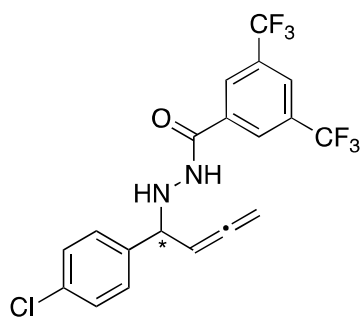
^{13}C NMR (100 MHz, CDCl_3) δ 208.5, 164.6, 139.0, 134.9, 132.5 (q, $^2J_{\text{C-F}} = 33.8$ Hz), 132.0, 129.5, 127.2 (br s), 125.5 (m), 122.8 (q, $^1J_{\text{C-F}} = 272.0$ Hz), 122.3, 91.5, 77.6, 63.2.

HRMS (ESI): Exact mass calculated for $\text{C}_{19}\text{H}_{14}\text{BrF}_6\text{N}_2\text{O}$ $[\text{M}+\text{H}]^+$ expected: 479.0188, found: 479.0192.

er = 72:28; HPLC analysis: t_R (–) 21.29 min; (+) 29.20 min, (Daicel Chiralpak® AS-H with an AS-H guard column, hexane/2-propanol = 85/15, 0.5 mL/min).

$[\alpha]_D^{22} = -81.1$ ($c = 0.27$, CHCl_3).

(–)-*N'*-(1-(4-chlorophenyl)buta-2,3-dien-1-yl)-3,5-bis(trifluoromethyl)benzohydrazide (12g).



The general procedure was followed with **6g** (40 mg, 0.1 mmol) to give the title compound and corresponding homopropargylic hydrazide **7g** [122] in 57% and 3% NMR yields, respectively.

^1H NMR (400 MHz, CDCl_3) δ 8.10 (s, 2H), 8.03 (s, 1H), 7.59 (br s, 1H), 7.40-7.35 (m, 4H), 5.35 (q, $J = 6.8$ Hz, 1H), 5.19 (br s, 1H), 4.91 (d, $J = 6.6$ Hz, 2H), 4.74 (d, $J = 6.9$ Hz, 1H).

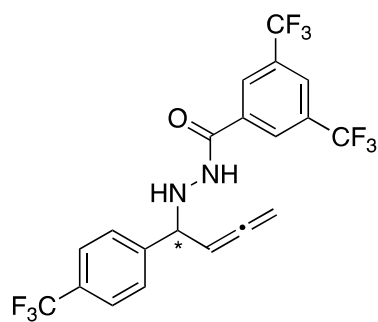
^{13}C NMR (100 MHz, CDCl_3) δ 208.5, 164.6, 138.5, 134.9, 134.2, 132.5 (q, $^2J_{\text{C-F}} = 34.0$ Hz), 129.1, 129.0, 127.2 (br s), 125.5 (m), 122.8 (q, $^1J_{\text{C-F}} = 271.5$ Hz), 91.6, 77.6, 63.1.

HRMS (ESI): Exact mass calculated for $\text{C}_{19}\text{H}_{14}\text{ClF}_6\text{N}_2\text{O}$ $[\text{M}+\text{H}]^+$ expected: 435.0693, found: 435.0683.

er = 74:26; HPLC analysis: t_{R} (–) 20.84 min; (+) 27.56 min, (Daicel Chiralpak[®] AS-H with an AS-H guard column, hexane/2-propanol = 85/15, 0.5 mL/min).

$[\alpha]_{\text{D}}^{22} = -78.5$ (c = 0.27, CHCl_3).

(–)-3,5-bis(trifluoromethyl)-*N'*-(1-(4-(trifluoromethyl)phenyl)buta-2,3-dien-1-yl)benzohydrazide (12h).



The general procedure was followed with **6h** (43 mg, 0.1 mmol) to give the title compound and corresponding homopropargylic hydrazide **7h** [122] in 62% and 3% NMR yields, respectively.

^1H NMR (400 MHz, CDCl_3) δ 8.10 (s, 2H), 8.03 (s, 1H), 7.65 (d, $J = 8.2$ Hz, 2H), 7.58-7.56 (m, 3H), 5.37 (q, $J = 6.9$ Hz, 1H), 5.21 (d, $J = 3.8$ Hz, 1H), 4.92 (dd, $J = 6.6, 1.9$ Hz, 2H), 4.83 (d, $J = 6.9$ Hz, 1H).

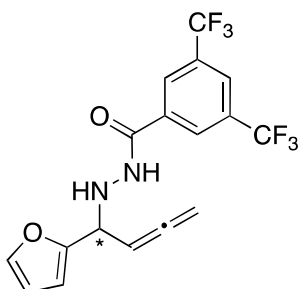
^{13}C NMR (100 MHz, CDCl_3) δ 208.6, 164.8, 144.1, 134.8, 132.5 (q, $^2J_{\text{C-F}} = 33.7$ Hz), 130.6 (q, $^2J_{\text{C-F}} = 32.7$ Hz), 128.1, 127.2 (br s), 125.8 (br s), 125.6 (m), 124.0 (q, $^1J_{\text{C-F}} = 270.0$ Hz), 122.8 (q, $^1J_{\text{C-F}} = 271.4$ Hz), 91.4, 77.7, 63.4.

HRMS (ESI): Exact mass calculated for $\text{C}_{20}\text{H}_{14}\text{F}_9\text{N}_2\text{O}$ $[\text{M}+\text{H}]^+$ expected: 469.0957, found: 469.0970.

The er was estimated to be 70:30 as enantiomers were not fully separated at the base line.; HPLC analysis: t_{R} (–) 37.21 min; (+) 45.36 min, (Daicel Chiralpak[®] AS-H with an AS-H guard column, hexane/2-propanol = 95/5, 0.5 mL/min).

$[\alpha]_{\text{D}}^{22} = -78.0$ (c = 0.27, CHCl_3).

(-)-*N'*-(1-(furan-2-yl)buta-2,3-dien-1-yl)-3,5-bis(trifluoromethyl)benzohydrazide (**12i**).



The general procedure was followed with **6i** (35 mg, 0.1 mmol) to give the title compound in 41% NMR yield.

^1H NMR (400 MHz, CDCl_3) δ 8.15 (s, 2H), 8.03 (s, 1H), 7.81 (br s, 1H), 7.42 (s, 1H), 6.35 (dd, $J = 9.2, 1.6$ Hz, 2H), 5.45 (q, $J = 7.2$ Hz, 1H), 5.3 (br s, 1H), 4.91 (br d, $J = 6.8$ Hz, 2H), 4.84 (br d, $J = 5.2$ Hz, 1H).

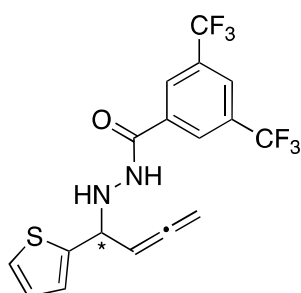
^{13}C NMR (100 MHz, CDCl_3) δ 209.2, 164.5, 152.5, 142.7, 135.0, 132.5 (q, $^2J_{\text{C-F}} = 33.8$ Hz), 127.3 (br s), 125.5 (m), 122.8 (q, $^1J_{\text{C-F}} = 271.3$ Hz), 110.4, 108.1, 88.7, 77.5, 57.6.

HRMS (ESI): Exact mass calculated for $\text{C}_{17}\text{H}_{13}\text{F}_6\text{N}_2\text{O}_2$ $[\text{M}+\text{H}]^+$ expected: 391.0876, found: 391.0873.

er = 81:19; HPLC analysis: t_R (+) 10.72 min; (–) 12.37 min, (Daicel Chiralcel[®] OD-H with an OD-H guard column, hexane/2-propanol = 85/15, 0.5 mL/min).

$[\alpha]_{22}^D = -12.0$ ($c = 0.53$, CHCl_3).

(-)-*N'*-(1-(thiophen-2-yl)buta-2,3-dien-1-yl)-3,5-bis(trifluoromethyl)benzohydrazide (12j).



The general procedure was followed with **6j** (37 mg, 0.1 mmol) to give the title compound in 26% NMR yield. Only trace amount of the corresponding homopropargylic hydrazide [122] was seen in ^1H NMR of the crude reaction mixture.

^1H NMR (400 MHz, CDCl_3) δ 8.12 (s, 2H), 8.03 (s, 1H), 7.67 (br s, 1H), 7.32 (d, $J = 4.5$ Hz, 1H), 7.08 (d, $J = 3.1$ Hz, 1H), 7.01 (dd, $J = 4.9, 3.6$ Hz, 1H), 5.43 (q, $J = 7.0$ Hz, 1H), 5.3 (br s, 1H), 5.06 (d, $J = 6.3$ Hz, 1H), 4.93 (dd, $J = 6.6, 1.5$ Hz, 2H).

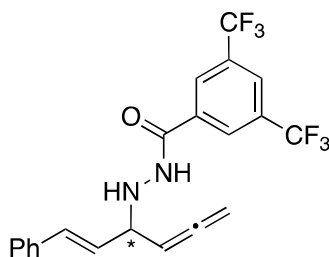
^{13}C NMR (100 MHz, CDCl_3) δ 208.5, 164.6, 143.3, 134.9, 132.5 (q, $^2J_{\text{C-F}} = 33.8$ Hz), 127.2 (br s), 126.9, 125.9, 125.6, 125.5 (m), 122.8 (q, $^1J_{\text{C-F}} = 271.2$ Hz), 91.7, 77.7, 59.5.

HRMS (ESI): Exact mass calculated for C₁₇H₁₃F₆N₂OS [M+H]⁺ expected:
407.0647, found: 407.0657.

er = 56:44; HPLC analysis: *t*_R (–) 11.41 min; (+) 13.23 min, (Daicel Chiralcel®
OD-H with an OD-H guard column, hexane/2-propanol = 85/15, 0.5 mL/min).

[α]^D₂₂ = –10.8 (c = 0.20, CHCl₃).

(–)-(E)-N'-(1-phenylhexa-1,4,5-trien-3-yl)-3,5-bis(trifluoromethyl)benzohydrazide (12k).



The general procedure was followed with **6k** (39 mg, 0.1 mmol) to give the title compound in 39% NMR yield. The crude reaction mixture was purified by preparative TLC using 10% EtOAc in toluene as eluent to afford a white solid (14 mg, 33%).

¹H NMR (400 MHz, CDCl₃) δ 8.16 (s, 2H), 8.01 (s, 1H), 7.83 (br s, 1H), 7.38 (d, *J* = 7.2 Hz, 2H), 7.31 (t, *J* = 7.2 Hz, 2H), 7.27-7.25 (m, 1H), 6.64 (d, *J* = 16.0 Hz,

1H), 6.19 (dd, $J = 15.6, 8.4$ Hz, 1H), 5.30 (q, $J = 6.8$ Hz, 1H), 5.13 (br s, 1H), 4.94-4.86 (m, 2H), 4.31 (br s, 1H).

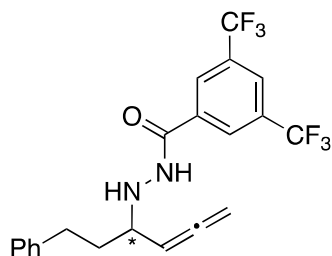
^{13}C NMR (100 MHz, CDCl_3) δ 208.9, 164.5, 136.2, 135.1, 133.6, 132.5 (q, $^2J_{\text{C-F}} = 33.8$ Hz), 128.7, 128.1, 127.6, 127.2 (br s), 126.6, 125.4 (m), 122.8 (q, $^1J_{\text{C-F}} = 271.3$ Hz), 90.4, 77.3, 62.4.

HRMS (ESI): Exact mass calculated for $\text{C}_{21}\text{H}_{17}\text{F}_6\text{N}_2\text{O}$ $[\text{M}+\text{H}]^+$ expected: 427.1240, found: 427.1229.

er = 51:49; HPLC analysis: t_{R} (+) 10.88 min; (–) 13.40 min, (Daicel Chiralcel[®] OD-H with an OD-H guard column, hexane/2-propanol = 85/15, 0.5 mL/min).

$[\alpha]_{\text{D}}^{22} = -17.9$ ($c = 0.67$, CHCl_3).

(–)-*N'*-(1-phenylhexa-4,5-dien-3-yl)-3,5-bis(trifluoromethyl)benzohydrazide (12l)



The general procedure was followed with **6l** (39 mg, 0.1 mmol) to give the title compound in 22% NMR yield. The crude reaction mixture was purified by preparative TLC using 10% EtOAc in toluene as eluent to afford a white solid (8 mg, 19%).

^1H NMR (400 MHz, CDCl_3) δ 8.14 (s, 2H), 8.03 (s, 1H), 7.50 (br s, 1H), 7.32-7.18 (m, 5H), 5.15 (q, $J = 7.6$ Hz, 1H), 4.99 (br s, 1H), 4.88-4.78 (m, 2H), 3.60 (br d, $J = 6.5$ Hz, 1H), 2.86-2.69 (m, 2H), 2.03-1.83 (m, 2H).

^{13}C NMR (100 MHz, CDCl_3) δ 209.3, 164.2, 141.5, 135.1, 132.5 (q, $^2J_{\text{C-F}} = 33.9$ Hz), 128.5, 128.4, 127.2 (br s), 126.1, 125.3 (m), 122.8 (q, $^1J_{\text{C-F}} = 271.2$ Hz), 91.0, 76.3, 60.3, 35.0, 32.0.

HRMS (ESI): Exact mass calculated for $\text{C}_{21}\text{H}_{19}\text{F}_6\text{N}_2\text{O}$ $[\text{M}+\text{H}]^+$ expected: 429.1396, found: 429.1393.

er = 62:38; HPLC analysis: t_{R} (–) 10.03 min; (+) 13.69 min, (Daicel Chiralcel[®] OD-H with an OD-H guard column, hexane/2-propanol = 85/15, 0.5 mL/min).

$[\alpha]_{\text{D}_{21}} = -21.5$ (c = 0.53, CHCl_3).

References

1. Bernstein, J.; Losee, K.A.; Smith, C.I.; Rubin, B. A NOVEL RESOLUTION OF 1-PHENYL-2-PROPYLHYDRAZINE. *J Am Chem Soc* **1959**, *81*, 4433–4433, doi:10.1021/ja01525a083.
2. Cheon, H.G.; Kim, S.-S.; Kim, K.-R.; Rhee, S.-D.; Yang, S.-D.; Ahn, J.H.; Park, S.-D.; Lee, J.M.; Jung, W.H.; Lee, H.S.; et al. Inhibition of Dipeptidyl Peptidase IV by Novel Inhibitors with Pyrazolidine Scaffold. *Biochem Pharmacol* **2005**, *70*, 22–29, doi:10.1016/j.bcp.2005.04.004.
3. Gould, E.; Lebl, T.; Slawin, A.M.Z.; Reid, M.; Davies, T.; Smith, A.D. The Development of Highly Active Acyclic Chiral Hydrazides for Asymmetric Iminium Ion Organocatalysis. *Org Biomol Chem* **2013**, *11*, 7877, doi:10.1039/c3ob41719k.
4. Bold, G.; Fässler, A.; Capraro, H.-G.; Cozens, R.; Klimkait, T.; Lazdins, J.; Mestan, J.; Poncioni, B.; Rösel, J.; Stover, D.; et al. New Aza-Dipeptide Analogues as Potent and Orally Absorbed HIV-1 Protease Inhibitors: Candidates for Clinical Development. *J Med Chem* **1998**, *41*, 3387–3401, doi:10.1021/jm970873c.
5. Chen, Z.-P.; Hu, S.-B.; Chen, M.-W.; Zhou, Y.-G. Synthesis of Chiral Fluorinated Hydrazines via Pd-Catalyzed Asymmetric Hydrogenation. *Org Lett* **2016**, *18*, 2676–2679, doi:10.1021/acs.orglett.6b01118.
6. Chen, Z.-P.; Hu, S.-B.; Zhou, J.; Zhou, Y.-G. Synthesis of Chiral Trifluoromethyl-Substituted Hydrazines via Pd-Catalyzed Asymmetric Hydrogenation and Reductive Amination. *ACS Catal* **2015**, *5*, 6086–6089, doi:10.1021/acscatal.5b01641.

7. Xie, J.-H.; Zhu, S.-F.; Zhou, Q.-L. Transition Metal-Catalyzed Enantioselective Hydrogenation of Enamines and Imines. *Chem Rev* **2011**, *111*, 1713–1760, doi:10.1021/cr100218m.
8. Abdine, R.A.A.; Hedouin, G.; Colobert, F.; Wencel-Delord, J. Metal-Catalyzed Asymmetric Hydrogenation of C=N Bonds. *ACS Catal* **2021**, *11*, 215–247, doi:10.1021/acscatal.0c03353.
9. Yoshikawa, N.; Tan, L.; McWilliams, J.C.; Ramasamy, D.; Sheppard, R. Catalytic Enantioselective Hydrogenation of *N*-Alkoxy carbonyl Hydrazones: A Practical Synthesis of Chiral Hydrazines. *Org Lett* **2010**, *12*, 276–279, doi:10.1021/ol902602c.
10. Burk, M.J.; Feaster, J.E. Enantioselective Hydrogenation of the C:N Group: A Catalytic Asymmetric Reductive Amination Procedure. *J Am Chem Soc* **1992**, *114*, 6266–6267, doi:10.1021/ja00041a067.
11. Burk, M.J.; Martinez, J.P.; Feaster, J.E.; Cosford, N. Catalytic Asymmetric Reductive Amination of Ketones via Highly Enantioselective Hydrogenation of the C=N Double Bond. *Tetrahedron* **1994**, *50*, 4399–4428, doi:10.1016/S0040-4020(01)89375-3.
12. Fan, D.; Hu, Y.; Jiang, F.; Zhang, Z.; Zhang, W. Rhodium-Catalyzed Chemo- and Enantioselective Hydrogenation of Alkynyl-Aryl Hydrazones. *Adv Synth Catal* **2018**, *360*, 2228–2232, doi:10.1002/adsc.201800243.
13. Wang, Y.-Q.; Lu, S.-M.; Zhou, Y.-G. Highly Enantioselective Pd-Catalyzed Asymmetric Hydrogenation of Activated Imines. *J Org Chem* **2007**, *72*, 3729–3734, doi:10.1021/jo0700878.

14. Chen, Z.-P.; Chen, M.-W.; Shi, L.; Yu, C.-B.; Zhou, Y.-G. Pd-Catalyzed Asymmetric Hydrogenation of Fluorinated Aromatic Pyrazol-5-Ols via Capture of Active Tautomers. *Chem Sci* **2015**, *6*, 3415–3419, doi:10.1039/C5SC00835B.
15. Chang, M.; Liu, S.; Huang, K.; Zhang, X. Direct Catalytic Asymmetric Reductive Amination of Simple Aromatic Ketones. *Org Lett* **2013**, *15*, 4354–4357, doi:10.1021/ol401851c.
16. Schuster, C.H.; Dropinski, J.F.; Shevlin, M.; Li, H.; Chen, S. Ruthenium-Catalyzed Enantioselective Hydrogenation of Hydrazones. *Org Lett* **2020**, *22*, 7562–7566, doi:10.1021/acs.orglett.0c02756.
17. Li, B.; Liu, D.; Hu, Y.; Chen, J.; Zhang, Z.; Zhang, W. Nickel-Catalyzed Asymmetric Hydrogenation of Hydrazones. *European J Org Chem* **2021**, *2021*, 3421–3425, doi:10.1002/ejoc.202100642.
18. Yang, P.; Zhang, C.; Ma, Y.; Zhang, C.; Li, A.; Tang, B.; Zhou, J.S. Nickel-Catalyzed N-Alkylation of Acylhydrazines and Arylamines Using Alcohols and Enantioselective Examples. *Angewandte Chemie International Edition* **2017**, *56*, 14702–14706, doi:10.1002/anie.201708949.
19. Yang, P.; Lim, L.H.; Chuanprasit, P.; Hirao, H.; Zhou, J. (Steve) Nickel-Catalyzed Enantioselective Reductive Amination of Ketones with Both Arylamines and Benzhydrazide. *Angewandte Chemie International Edition* **2016**, *55*, 12083–12087, doi:10.1002/anie.201606821.

20. Xu, H.; Yang, P.; Chuanprasit, P.; Hirao, H.; Zhou, J. (Steve) Nickel-Catalyzed Asymmetric Transfer Hydrogenation of Hydrazones and Other Ketimines. *Angewandte Chemie* **2015**, *127*, 5201–5205, doi:10.1002/ange.201501018.
21. Hu, Y.; Zhang, Z.; Zhang, J.; Liu, Y.; Gridnev, I.D.; Zhang, W. Cobalt-Catalyzed Asymmetric Hydrogenation of C=N Bonds Enabled by Assisted Coordination and Nonbonding Interactions. *Angewandte Chemie International Edition* **2019**, *58*, 15767–15771, doi:10.1002/anie.201909928.
22. Wang, T.; Di, X.; Wang, C.; Zhou, L.; Sun, J. Reductive Hydrazination with Trichlorosilane: A Method for the Preparation of 1,1-Disubstituted Hydrazines. *Org Lett* **2016**, *18*, 1900–1903, doi:10.1021/acs.orglett.6b00675.
23. Iwasaki, F.; Matsumura, K.; Onomura, O. Preparation of Amino Esters or Hydrazines from Imino Esters or Hydrazones 2001.
24. Chen, W.; Tan, C.; Wang, H.; Ye, X. The Development of Organocatalytic Asymmetric Reduction of Carbonyls and Imines Using Silicon Hydrides. *European J Org Chem* **2021**, *2021*, 3091–3112, doi:10.1002/ejoc.202100394.
25. Rossi, S.; Benaglia, M.; Massolo, E.; Raimondi, L. Organocatalytic Strategies for Enantioselective Metal-Free Reductions. *Catal Sci Technol* **2014**, *4*, 2708–2723, doi:10.1039/C4CY00033A.

26. Iwasaki, F.; Onomura, O.; Mishima, K.; Kanematsu, T.; Maki, T.; Matsumura, Y. First Chemo- and Stereoselective Reduction of Imines Using Trichlorosilane Activated with N-Formylpyrrolidine Derivatives. *Tetrahedron Lett* **2001**, *42*, 2525–2527, doi:10.1016/S0040-4039(01)00219-2.
27. Malkov, A. V.; Vranková, K.; Stončius, S.; Kočovský, P. Asymmetric Reduction of Imines with Trichlorosilane, Catalyzed by Sigamide, an Amino Acid-Derived Formamide: Scope and Limitations [†]. *J Org Chem* **2009**, *74*, 5839–5849, doi:10.1021/jo900561h.
28. Malkov, A. V.; Mariani, A.; MacDougall, K.N.; Kocovský, P. Role of Noncovalent Interactions in the Enantioselective Reduction of Aromatic Ketimines with Trichlorosilane. *Org Lett* **2004**, *6*, 2253–2256, doi:10.1021/ol049213+.
29. Malkov, A. V.; Stončius, S.; MacDougall, K.N.; Mariani, A.; McGeoch, G.D.; Kočovský, P. Formamides Derived from N-Methyl Amino Acids Serve as New Chiral Organocatalysts in the Enantioselective Reduction of Aromatic Ketimines with Trichlorosilane. *Tetrahedron* **2006**, *62*, 264–284, doi:10.1016/j.tet.2005.08.117.
30. Kočovský, P.; Malkov, A. V. *Lewis Base Catalysis in Organic Synthesis*; Vedejs, E., Denmark, S.E., Eds.; 1st ed.; Wiley: Weinheim, Germany, 2016; Vol. 3; ISBN 9783527336180.
31. Jones, S.; Warner, C.J.A. Trichlorosilane Mediated Asymmetric Reductions of the C=N Bond. *Org Biomol Chem* **2012**, *10*, 2189, doi:10.1039/c2ob06854k.

32. Guizzetti, S.; Benaglia, M. Trichlorosilane-Mediated Stereoselective Reduction of C=N Bonds. *European J Org Chem* **2010**, 2010, 5529–5541, doi:10.1002/ejoc.201000728.
33. Žeimytė, S.; Stončius, S. Chiral Bipyridine-Annulated Bicyclo[3.3.1]Nonane N-Oxide Organocatalysts for Stereoselective Allylation and Hydrosilylation Reactions. *Tetrahedron* **2021**, 78, doi:10.1016/j.tet.2020.131831.
34. Wrzeszcz, Z.; Siedlecka, R. Heteroaromatic N-Oxides in Asymmetric Catalysis: A Review. *Molecules* **2020**, 25, 330, doi:10.3390/molecules25020330.
35. Dong, M.; Wang, J.; Wu, S.; Zhao, Y.; Ma, Y.; Xing, Y.; Cao, F.; Li, L.; Li, Z.; Zhu, H. Catalytic Mechanism Study on the 1,2- and 1,4-Transfer Hydrogenation of Ketimines and β -Enamino Esters Catalyzed by Axially Chiral Biscarboline-Based Alcohols. *Adv Synth Catal* **2019**, 361, 4602–4610, doi:10.1002/adsc.201900665.
36. Xing, Y.; Wu, S.; Dong, M.; Wang, J.; Liu, L.; Zhu, H. Synthesis and Application of Axially Chiral Biscarbolines with Functional N-O and Sulfone for 1,2-Transfer Hydrogenations of Ketimines. *Tetrahedron* **2019**, 75, 130495, doi:10.1016/j.tet.2019.130495.
37. Pei, Y.-N.; Deng, Y.; Li, J.-L.; Liu, L.; Zhu, H.-J. New Chiral Biscarboline N,N'-Dioxide Derivatives as Catalyst in Enantioselective Reduction of Ketoimines with Trichlorosilane. *Tetrahedron Lett* **2014**, 55, 2948–2952, doi:10.1016/j.tetlet.2014.03.100.

38. Pan, W.; Deng, Y.; He, J.-B.; Bai, B.; Zhu, H.-J. Highly Efficient Asymmetric-Axle-Supported N–O Amides in Enantioselective Hydrosilylation of Ketimines with Trichlorosilane. *Tetrahedron* **2013**, *69*, 7253–7257, doi:10.1016/j.tet.2013.06.081.
39. Warner, C.J.A.; Berry, S.S.; Jones, S. Evaluation of Bifunctional Chiral Phosphine Oxide Catalysts for the Asymmetric Hydrosilylation of Ketimines. *Tetrahedron* **2019**, *75*, 130733, doi:10.1016/j.tet.2019.130733.
40. Warner, C.J.A.; Reeder, A.T.; Jones, S. P-Chiral Phosphine Oxide Catalysed Reduction of Prochiral Ketimines Using Trichlorosilane. *Tetrahedron Asymmetry* **2016**, *27*, 136–141, doi:10.1016/j.tetasy.2016.01.001.
41. Cauteruccio, S.; Dova, D.; Benaglia, M.; Genoni, A.; Orlandi, M.; Licandro, E. Synthesis, Characterisation, and Organocatalytic Activity of Chiral Tetrathiahelicene Diphosphine Oxides. *European J Org Chem* **2014**, *2014*, 2694–2702, doi:10.1002/ejoc.201301912.
42. Pei, D.; Wang, Z.; Wei, S.; Zhang, Y.; Sun, J. S-Chiral Sulfinamides as Highly Enantioselective Organocatalysts. *Org Lett* **2006**, *8*, 5913–5915, doi:10.1021/ol062633+.
43. Pei, D.; Zhang, Y.; Wei, S.; Wang, M.; Sun, J. Rationally-Designed S-Chiral Bissulfinamides as Highly Enantioselective Organocatalysts for Reduction of Ketimines. *Adv Synth Catal* **2008**, *350*, 619–623, doi:10.1002/adsc.200700504.

44. Sun, S.; Reep, C.; Zhang, C.; Captain, B.; Peverati, R.; Takenaka, N. Design and Synthesis of 3,3'-Triazolyl Biisoquinoline N,N'-Dioxides via Hiyama Cross-Coupling of 4-Trimethylsilyl-1,2,3-Triazoles. *Tetrahedron Lett* **2021**, *81*, 153338, doi:10.1016/j.tetlet.2021.153338.
45. Parmar, D.; Sugiono, E.; Raja, S.; Rueping, M. Complete Field Guide to Asymmetric BINOL-Phosphate Derived Brønsted Acid and Metal Catalysis: History and Classification by Mode of Activation; Brønsted Acidity, Hydrogen Bonding, Ion Pairing, and Metal Phosphates. *Chem Rev* **2014**, *114*, 9047–9153, doi:10.1021/cr5001496.
46. Xu, C.; Reep, C.; Jarvis, J.; Naumann, B.; Captain, B.; Takenaka, N. Asymmetric Catalytic Ketimine Mannich Reactions and Related Transformations. *Catalysts* **2021**, *11*, 712–759, doi:10.3390/catal11060712.
47. Sugiura, M.; Sato, N.; Kotani, S.; Nakajima, M. Lewis Base-Catalyzed Conjugate Reduction and Reductive Aldol Reaction of α,β -Unsaturated Ketones Using Trichlorosilane. *Chemical Communications* **2008**, 4309–4311, doi:10.1039/b807529h.
48. Lu, T.; Porterfield, M.A.; Wheeler, S.E. Explaining the Disparate Stereoselectivities of *N*-Oxide Catalyzed Allylations and Propargylations of Aldehydes. *Org Lett* **2012**, *14*, 5310–5313, doi:10.1021/ol302493d.
49. Still, W.C.; Kahn, M.; Mitra, A. Rapid Chromatographic Technique for Preparative Separations with Moderate Resolution. *J Org Chem* **1978**, *43*, 2923–2925, doi:10.1021/jo00408a041.

50. Reep, C.; Morgante, P.; Peverati, R.; Takenaka, N. Axial-Chiral Biisoquinoline *N*, *N'*-Dioxides Bearing Polar Aromatic C-H Bonds as Catalysts in Sakurai-Hosomi-Denmark Allylation. *Org Lett* **2018**, *20*, 5757–5761, doi:10.1021/acs.orglett.8b02457.
51. Wang, Y.; Xu, J.-K.; Gu, Y.; Tian, S.-K. Catalytic Stereospecific Allylation of Protected Hydrazines with Enantioenriched Primary Allylic Amines. *Organic Chemistry Frontiers* **2014**, *1*, 812, doi:10.1039/C4QO00155A.
52. Shao, Y.; Gan, Z.; Epifanovsky, E.; Gilbert, A.T.B.; Wormit, M.; Kussmann, J.; Lange, A.W.; Behn, A.; Deng, J.; Feng, X.; et al. Advances in Molecular Quantum Chemistry Contained in the Q-Chem 4 Program Package. *Mol Phys* **2015**, *113*, 184–215, doi:10.1080/00268976.2014.952696.
53. Grimme, S.; Brandenburg, J.G.; Bannwarth, C.; Hansen, A. Consistent Structures and Interactions by Density Functional Theory with Small Atomic Orbital Basis Sets. *J Chem Phys* **2015**, *143*, 054107, doi:10.1063/1.4927476.
54. Barone, V.; Cossi, M. Quantum Calculation of Molecular Energies and Energy Gradients in Solution by a Conductor Solvent Model. *J Phys Chem A* **1998**, *102*, 1995–2001, doi:10.1021/jp9716997.
55. Truong, T.N.; Stefanovich, E. V. A New Method for Incorporating Solvent Effect into the Classical, Ab Initio Molecular Orbital and Density Functional Theory Frameworks for Arbitrary Shape Cavity. *Chem Phys Lett* **1995**, *240*, 253–260, doi:10.1016/0009-2614(95)00541-B.
56. Morgante, P.; Peverati, R. CLB18: A New Structural Database with Unusual Carbon–Carbon Long Bonds. *Chem Phys Lett* **2021**, *765*, 138281, doi:10.1016/j.cplett.2020.138281.

57. Morgante, P.; Peverati, R. Statistically Representative Databases for Density Functional Theory *via* Data Science. *Physical Chemistry Chemical Physics* **2019**, *21*, 19092–19103, doi:10.1039/C9CP03211H.
58. *Comprehensive Asymmetric Catalysis I–III*; Jacobsen, E.N., Pfaltz, A., Yamamoto, H., Eds.; 1st ed.; Springer Berlin Heidelberg: Berlin, Heidelberg, 1999; Vol. 1–3; ISBN 978-3-642-63651-6.
59. Schreyer, L.; Properzi, R.; List, B. IDPi Catalysis. *Angewandte Chemie International Edition* **2019**, *58*, 12761–12777, doi:10.1002/anie.201900932.
60. Huang, Y.; Hayashi, T. Chiral Diene Ligands in Asymmetric Catalysis. *Chem Rev* **2022**, *122*, 14346–14404, doi:10.1021/acs.chemrev.2c00218.
61. Genzink, M.J.; Kidd, J.B.; Swords, W.B.; Yoon, T.P. Chiral Photocatalyst Structures in Asymmetric Photochemical Synthesis. *Chem Rev* **2022**, *122*, 1654–1716, doi:10.1021/acs.chemrev.1c00467.
62. *Helicenes*; Crassous, J., Stará, I.G., Starý, I., Eds.; Wiley, 2022; ISBN 9783527348107.
63. Tsurusaki, A.; Kamikawa, K. Multiple Helicenes Featuring Synthetic Approaches and Molecular Structures. *Chem Lett* **2021**, *50*, 1913–1932, doi:10.1246/cl.210409.
64. Meisenheimer, J.; Witte, K. Reduction von 2-Nitronaphtalin. *Berichte der deutschen chemischen Gesellschaft* **1903**, *36*, 4153–4164, doi:10.1002/cber.19030360481.

65. Newman, M.S.; Lednicer, D. The Synthesis and Resolution of Hexahelicene¹. *J Am Chem Soc* **1956**, *78*, 4765–4770, doi:10.1021/ja01599a060.
66. Wynberg, H.; Groen, M.B. Synthesis, Resolution, and Optical Rotatory Dispersion of a Hexa- and a Heptaheterohelicene. *J Am Chem Soc* **1968**, *90*, 5339–5341, doi:10.1021/ja01021a088.
67. Dhbaibi, K.; Favereau, L.; Crassous, J. Enantioenriched Helicenes and Helicenoids Containing Main-Group Elements (B, Si, N, P). *Chem Rev* **2019**, *119*, 8846–8953, doi:10.1021/acs.chemrev.9b00033.
68. Shen, Y.; Chen, C.-F. Helicenes: Synthesis and Applications. *Chem Rev* **2012**, *112*, 1463–1535, doi:10.1021/cr200087r.
69. Hasan, M.; Borovkov, V. Helicene-Based Chiral Auxiliaries and Chirogenesis. *Symmetry (Basel)* **2017**, *10*, 10–58, doi:10.3390/sym10010010.
70. Narcis, M.J.; Takenaka, N. Helical-Chiral Small Molecules in Asymmetric Catalysis. *European J Org Chem* **2014**, *2014*, 21–34, doi:10.1002/ejoc.201301045.
71. Gingras, M. One Hundred Years of Helicene Chemistry. Part 3: Applications and Properties of Carbohelicenes. *Chem. Soc. Rev.* **2013**, *42*, 1051–1095, doi:10.1039/C2CS35134J.
72. Aillard, P.; Voituriez, A.; Marinetti, A. Helicene-like Chiral Auxiliaries in Asymmetric Catalysis. *Dalton Trans.* **2014**, *43*, 15263–15278, doi:10.1039/C4DT01935K.

73. Saleh, N.; Shen, C.; Crassous, J. Helicene-Based Transition Metal Complexes: Synthesis, Properties and Applications. *Chem Sci* **2014**, *5*, 3680–3694, doi:10.1039/C4SC01404A.
74. Morgante, P.; Captain, B.; Chouinard, C.D.; Peverati, R.; Takenaka, N. Synthesis of Electrophilic N-Heterocyclic Carbenes Based on Azahelicene. *Tetrahedron Lett* **2020**, *61*, 152143, doi:10.1016/j.tetlet.2020.152143.
75. Míšek, J.; Teplý, F.; Stará, I.G.; Tichý, M.; Šaman, D.; Císařová, I.; Vojtíšek, P.; Starý, I. A Straightforward Route to Helically Chiral N-Heteroaromatic Compounds: Practical Synthesis of Racemic 1,14-Diaza[5]Helicene and Optically Pure 1- and 2-Aza[6]Helicenes. *Angewandte Chemie International Edition* **2008**, *47*, 3188–3191, doi:10.1002/anie.200705463.
76. Takenaka, N.; Sarangthem, R.S.; Captain, B. Helical Chiral Pyridine *N*-Oxides: A New Family of Asymmetric Catalysts. *Angewandte Chemie International Edition* **2008**, *47*, 9708–9710, doi:10.1002/anie.200803338.
77. Chen, J.; Captain, B.; Takenaka, N. Helical Chiral 2,2'-Bipyridine *N*-Monoxides as Catalysts in the Enantioselective Propargylation of Aldehydes with Allenyltrichlorosilane. *Org Lett* **2011**, *13*, 1654–1657, doi:10.1021/ol200102c.
78. Takenaka, N.; Chen, J.; Captain, B.; Sarangthem, R.S.; Chandrakumar, A. Helical Chiral 2-Aminopyridinium Ions: A New Class of Hydrogen Bond Donor Catalysts. *J Am Chem Soc* **2010**, *132*, 4536–4537, doi:10.1021/ja100539c.

79. Narcis, M.J.; Sprague, D.J.; Captain, B.; Takenaka, N. Enantio- and Periselective Nitroalkene Diels–Alder Reaction. *Org Biomol Chem* **2012**, *10*, 9134–9136, doi:10.1039/c2ob26674a.
80. Peng, Z.; Takenaka, N. Applications of Helical-Chiral Pyridines as Organocatalysts in Asymmetric Synthesis. *The Chemical Record* **2013**, *13*, 28–42, doi:10.1002/tcr.201200010.
81. Ding, C.-H.; Hou, X.-L. Catalytic Asymmetric Propargylation. *Chem Rev* **2011**, *111*, 1914–1937, doi:10.1021/cr100284m.
82. Kagoshima, H.; Uzawa, T.; Akiyama, T. Catalytic, Enantioselective Propargyl- and Allenylation Reactions of α -Imino Ester. *Chem Lett* **2002**, *31*, 298–299, doi:10.1246/cl.2002.298.
83. Wisniewska, H.M.; Jarvo, E.R. Enantioselective Silver-Catalyzed Propargylation of Imines. *Chem Sci* **2011**, *2*, 807–810, doi:10.1039/c0sc00613k.
84. Vieira, E.M.; Haeffner, F.; Snapper, M.L.; Hoveyda, A.H. A Robust, Efficient, and Highly Enantioselective Method for Synthesis of Homopropargyl Amines. *Angewandte Chemie International Edition* **2012**, *51*, 6618–6621, doi:10.1002/anie.201202694.
85. Fandrick, D.R.; Hart, C.A.; Okafor, I.S.; Mercadante, M.A.; Sanyal, S.; Masters, J.T.; Sarvestani, M.; Fandrick, K.R.; Stockdill, J.L.; Grinberg, N.; et al. Copper-Catalyzed Asymmetric Propargylation of Cyclic Aldimines. *Org Lett* **2016**, *18*, 6192–6195, doi:10.1021/acs.orglett.6b03253.

86. Smith, M.W.; Zhou, Z.; Gao, A.X.; Shimbayashi, T.; Snyder, S.A. A 7-Step Formal Asymmetric Total Synthesis of Strictamine via an Asymmetric Propargylation and Metal-Mediated Cyclization. *Org Lett* **2017**, *19*, 1004–1007, doi:10.1021/acs.orglett.6b03839.
87. Yu, S.; Hua, R.; Fu, X.; Liu, G.; Zhang, D.; Jia, S.; Qiu, H.; Hu, W. Asymmetric Multicomponent Reactions for Efficient Construction of Homopropargyl Amine Carboxylic Esters. *Org Lett* **2019**, *21*, 5737–5741, doi:10.1021/acs.orglett.9b02139.
88. Manna, S.; Dherbassy, Q.; Perry, G.J.P.; Procter, D.J. Enantio- and Diastereoselective Synthesis of Homopropargyl Amines by Copper-Catalyzed Coupling of Imines, 1,3-Enynes, and Diborons. *Angewandte Chemie International Edition* **2020**, *59*, 4879–4882, doi:10.1002/anie.201915191.
89. Cowper, N.G.W.; Hesse, M.J.; Chan, K.M.; Reisman, S.E. A Copper-Catalyzed Asymmetric Oxime Propargylation Enables the Synthesis of the Gliovirin Tetrahydro-1,2-Oxazine Core. *Chem Sci* **2020**, *11*, 11897–11901, doi:10.1039/D0SC04802J.
90. Jonker, S.J.T.; Diner, C.; Schulz, G.; Iwamoto, H.; Eriksson, L.; Szabó, K.J. Catalytic Asymmetric Propargyl- and Allylboration of Hydrazonoesters: A Metal-Free Approach to Sterically Encumbered Chiral α -Amino Acid Derivatives. *Chemical Communications* **2018**, *54*, 12852–12855, doi:10.1039/C8CC07908K.

91. Schneider, U.; Sugiura, M.; Kobayashi, S. Highly Selective Preparation of Allenic and Homopropargylic Hydrazides through Regiospecific Addition of Propargyltrichlorosilane and Allenyltrichlorosilane to Various Types of *N*-Acyldiazones. *Adv Synth Catal* **2006**, *348*, 323–329, doi:10.1002/adsc.200505379.
92. Vaganov, V.Yu.; Fukazawa, Y.; Kondratyev, N.S.; Shipilovskikh, S.A.; Wheeler, S.E.; Rubtsov, A.E.; Malkov, A. V. Optimization of Catalyst Structure for Asymmetric Propargylation of Aldehydes with Allenyltrichlorosilane. *Adv Synth Catal* **2020**, *362*, 5467–5474, doi:10.1002/adsc.202000936.
93. Peng, Z. Development of Helical Chiral Catalysts and Their Application in Asymmetric Catalysis. Ph.D. Thesis, University of Miami: Miami, FL, USA, 2014.
94. Wang, Y.; Wu, Z.-G.; Shi, F. Advances in Catalytic Enantioselective Synthesis of Chiral Helicenes and Helicenoids. *Chem Catalysis* **2022**, *2*, 3077–3111, doi:10.1016/j.checat.2022.10.011.
95. Liu, W.; Qin, T.; Xie, W.; Yang, X. Catalytic Enantioselective Synthesis of Helicenes. *Chemistry – A European Journal* **2022**, *28*, doi:10.1002/chem.202202369.
96. Heller, B.; Hapke, M.; Fischer, C.; Andronova, A.; Starý, I.; Stará, I.G. Chiral Cobalt^I and Nickel⁰ Complexes in the Synthesis of Nonracemic Helicenes through the Enantioselective [2 + 2 + 2] Cyclootrimerisation of Alkynes. *J Organomet Chem* **2013**, *723*, 98–102, doi:10.1016/j.jorganchem.2012.07.005.

97. Sun, S.; Xu, C.; Jarvis, J.; Nader, P.; Naumann, B.; Soliven, A.; Peverati, R.; Takenaka, N. Evaluation of 3,3'-Triazolyl Biisoquinoline N,N'-Dioxide Catalysts for Asymmetric Hydrosilylation of Hydrazones with Trichlorosilane. *Catalysts* **2021**, *11*, 1103, doi:10.3390/catal11091103.
98. Nakajima, M.; Saito, M.; Hashimoto, S. Selective Synthesis of Optically Active Allenic and Homopropargylic Alcohols from Propargyl Chloride. *Tetrahedron Asymmetry* **2002**, *13*, 2449–2452, doi:10.1016/S0957-4166(02)00640-7.
99. Ma, S. Some Typical Advances in the Synthetic Applications of Allenes. *Chem Rev* **2005**, *105*, 2829–2872, doi:10.1021/cr020024j.
100. Hoffmann-Röder, A.; Krause, N. Synthesis and Properties of Allenic Natural Products and Pharmaceuticals. *Angewandte Chemie International Edition* **2004**, *43*, 1196–1216, doi:10.1002/anie.200300628.
101. Yu, S.; Ma, S. Allenes in Catalytic Asymmetric Synthesis and Natural Product Syntheses. *Angewandte Chemie International Edition* **2012**, *51*, 3074–3112, doi:10.1002/anie.201101460.
102. Glatz, F.; Petrone, D.A.; Carreira, E.M. Ir-Catalyzed Enantioconvergent Synthesis of Diversely Protected Allenylic Amines Employing Ammonia Surrogates. *Angewandte Chemie International Edition* **2020**, *59*, 16404–16408, doi:10.1002/anie.202005599.
103. Petrone, D.A.; Isomura, M.; Franzoni, I.; Rössler, S.L.; Carreira, E.M. Allenylic Carbonates in Enantioselective Iridium-Catalyzed Alkylations. *J Am Chem Soc* **2018**, *140*, 4697–4704, doi:10.1021/jacs.8b01416.

104. Li, Q.; Fu, C.; Ma, S. Palladium-Catalyzed Asymmetric Amination of Allenyl Phosphates: Enantioselective Synthesis of Allenes with an Additional Unsaturated Unit. *Angewandte Chemie International Edition* **2014**, *53*, 6511–6514, doi:10.1002/anie.201402647.
105. Nugent, T.C.; El-Shazly, M. Chiral Amine Synthesis – Recent Developments and Trends for Enamide Reduction, Reductive Amination, and Imine Reduction. *Adv Synth Catal* **2010**, *352*, 753–819, doi:10.1002/adsc.200900719.
106. Wisniewska, H.M.; Jarvo, E.R. Enantioselective Propargylation and Allenylation Reactions of Ketones and Imines. *J Org Chem* **2013**, *78*, 11629–11636, doi:10.1021/jo4019107.
107. Thaima, T.; Zamani, F.; Hyland, C.; Pyne, S. Allenylation and Propargylation Reactions of Ketones, Aldehydes, Imines, and Iminium Ions Using Organoboronates and Related Derivatives. *Synthesis (Stuttg)* **2017**, *49*, 1461–1480, doi:10.1055/s-0036-1588397.
108. Zhong, F.; Yue, W.-J.; Yin, X.-H.; Zhang, H.-M.; Yin, L. Copper(I)-Catalyzed Asymmetric Synthesis of α -Allenylamines and β -Lactams through Regioselective Mannich-Type Reactions. *ACS Catal* **2022**, *12*, 9181–9189, doi:10.1021/acscatal.2c01399.
109. Kondo, M.; Omori, M.; Hatanaka, T.; Funahashi, Y.; Nakamura, S. Catalytic Enantioselective Reaction of Allenylnitriles with Imines Using Chiral Bis(Imidazoline)s Palladium(II) Pincer Complexes. *Angewandte Chemie International Edition* **2017**, *56*, 8677–8680, doi:10.1002/anie.201702429.

110. Sieber, J.D.; Angeles-Dunham, V. V.; Chennamadhavuni, D.; Fandrick, D.R.; Haddad, N.; Grinberg, N.; Kurouski, D.; Lee, H.; Song, J.J.; Yee, N.K.; et al. Rhodium-Catalyzed Asymmetric Allenylation of Sulfonylimines and Application to the Stereospecific Allylic Allenylation. *Adv Synth Catal* **2016**, *358*, 3062–3068, doi:10.1002/adsc.201600686.
111. Wu, H.; Haeffner, F.; Hoveyda, A.H. An Efficient, Practical, and Enantioselective Method for Synthesis of Homoallenylamides Catalyzed by an Aminoalcohol-Derived, Boron-Based Catalyst. *J Am Chem Soc* **2014**, *136*, 3780–3783, doi:10.1021/ja500374p.
112. Mszar, N.W.; Haeffner, F.; Hoveyda, A.H. NHC–Cu-Catalyzed Addition of Propargylboron Reagents to Phosphinoylimines. Enantioselective Synthesis of Trimethylsilyl-Substituted Homoallenylamides and Application to the Synthesis of *S* -(-)-Cyclooridin. *J Am Chem Soc* **2014**, *136*, 3362–3365, doi:10.1021/ja500373s.
113. Mbofana, C.T.; Miller, S.J. Diastereo- and Enantioselective Addition of Anilide-Functionalized Allenates to *N*-Acyylimines Catalyzed by a Pyridylalanine-Based Peptide. *J Am Chem Soc* **2014**, *136*, 3285–3292, doi:10.1021/ja412996f.
114. Hashimoto, T.; Sakata, K.; Tamakuni, F.; Dutton, M.J.; Maruoka, K. Phase-Transfer-Catalysed Asymmetric Synthesis of Tetrasubstituted Allenes. *Nat Chem* **2013**, *5*, 240–244, doi:10.1038/nchem.1567.
115. Huang, Y.; Chakrabarti, A.; Morita, N.; Schneider, U.; Kobayashi, S. A Catalytic Asymmetric Borono Variant of Hosomi–Sakurai Reactions with *N,O*-Aminals. *Angewandte Chemie International Edition* **2011**, *50*, 11121–11124, doi:10.1002/anie.201105182.

116. Cowen, B.J.; Saunders, L.B.; Miller, S.J. Pyridylalanine (Pal)-Peptide Catalyzed Enantioselective Allenolate Additions to *N*-Acyl Imines. *J Am Chem Soc* **2009**, *131*, 6105–6107, doi:10.1021/ja901279m.
117. Kagoshima, H.; Uzawa, T.; Akiyama, T. Catalytic, Enantioselective Propargyl- and Allenylation Reactions of α -Imino Ester. *Chem Lett* **2002**, *31*, 298–299, doi:10.1246/cl.2002.298.
118. Hirabayashi, R.; Ogawa, C.; Sugiura, M.; Kobayashi, S. Highly Stereoselective Synthesis of Homoallylic Amines Based on Addition of Allyltrichlorosilanes to Benzoylhydrazones. *J Am Chem Soc* **2001**, *123*, 9493–9499, doi:10.1021/ja011125m.
119. Kobayashi, S.; Nishio, K. Selective Formation of Propargylsilanes and Allenylsilanes and Their Reactions with Aldehydes for the Preparation of Homopropargylic and Allenic Alcohols. *J Am Chem Soc* **1995**, *117*, 6392–6393, doi:10.1021/ja00128a043.
120. Schneider, U.; Sugiura, M.; Kobayashi, S. Highly Selective Formation of Propargyl- and Allenyltrichlorosilanes and Their Regiospecific Addition to Various Types of Aldehydes: Preparation of Both Allenic and Homopropargylic Alcohols. *Tetrahedron* **2006**, *62*, 496–502, doi:10.1016/j.tet.2005.08.114.
121. Iseki, K.; Kuroki, Y.; Kobayashi, Y. Asymmetric Allenylation of Aliphatic Aldehydes Catalyzed by a Chiral Formamide. *Tetrahedron Asymmetry* **1998**, *9*, 2889–2894, doi:10.1016/S0957-4166(98)00290-0.

122. Xu, C.; Nader, P.; Xavier, J.; Captain, B.; Takenaka, N. Evaluation of Helicene-Derived 2,2'-Bipyridine N-Monoxide Catalyst for the Enantioselective Propargylation of N-Acylhydrazones with Allenyltrichlorosilane. *Tetrahedron* **2023**, *141*, 133496, doi:10.1016/j.tet.2023.133496.